WEATHER RESISTIVE BARRIERS IN STUCCO CLADDING SYSTEMS

Jian Zhang

A Thesis in the

Department of

Building, Civil and Environmental Engineering

Presented in Partial Fulfillment of the Requirements

For the Degree of Master of Applied Science (Building Engineering) at

Concordia University

Montreal, Quebec, Canada

June 2003

Your file Votre référence
ISBN: 0-612-83860-9
Our file Notre référence
ISBN: 0-612-83860-9

ABSTRACT

WEATHER RESISTIVE BARRIERS IN STUCCO CLADDING SYSTEMS

Jian Zhang

Recent moisture related building envelope failures in wood frame walls with stucco cladding provided a reason for a question if adjacent components such as wood-based sheathing board or stucco layer could affect the field performance of water resistive barriers (WRB).

This thesis either selected or developed a few experimental techniques for laboratory testing of WRB with the view to their use for evaluating the material performance. In particular, test methods such as air permeance test, modified inverted cup test, and water absorption test were used to examine the effects from WRB surroundings on air and water transmission through the materials.

Theoretically, WRB resistance to water transmission changes when chemicals e.g. surfactants or wood extracts are dissolved in the water. Yet, the measured moisture transmission did not indicate significant effects when wood extracts were dissolved in water or deposited on WRB surfaces. Neither four-month outdoor weathering nor laboratory mechanical stretching showed a significant effect in WRB performance when measured with typical test methods. This is because in most cases vapour transmission is a dominant phase of the transport.

On the other hand, when employing more discrimination test methods, the interaction of bentonite particles with the wood extract deposits was evidently found to alter the water transport rate.

Although this study did not address explicitly the durability of different WRB products, it showed the significance of an interactive weathering mechanism that could affect the long-term performance of some WRB products. By enhanced understanding of the interactions with the adjacent components of the wall, this study will assist in improved design of stucco cladding systems.

ACKNOWLEDGEMENTS

I would like to express my sincere gratitude to my supervisors, **Dr. M. Bomberg** and **Dr. F. Haghighat**, for their thorough guidance, constant support, and encouragement throughout this research.

Financial assistance from the Exterior Moisture Control Consortium, including Canada Mortgage and Housing Corporation (CMHC), Concordia University, Du Pont Inc., Fortiber Corporation, Hal Industries, Homeowner Protection Office, DMO Associates, and Louisiana Pacific Corporation, are gratefully acknowledged. Meanwhile, provisions of financial supports from the EJLB foundation, the Power Corporation of Canada Graduate Fellowship, and the Concordia University Partial Tuition Scholarship for International Student are appreciated as well.

Many thanks are also due to my friends and the technicians in Concordia University for their helpful advice during the study period.

Finally, I would like to express my appreciation to my parents for their love, patience, understanding, and encouragement.

TABLE OF CONTENTS

LIST OF FIGURES

CHAPTER 4

CHAPTER 5

CHAPTER 6

APPENDIX C

APPENDIX D

APPENDIX E

APPENDIX F

APPENDIX G

APPENDIX H

APPENDIX I

LIST OF TABLES

CHAPTER 2

CHAPTER 3

CHAPTER 4

CHAPTER 5

CHAPTER 6

LIST OF SYMBOLS

Symbol	Parameter	Unit
A	normal cross-sectional area of the material	(m^2)
A_w	water absorption coefficient	($kg/m^2 \cdot s^{0.5}$)
C	airflow coefficient	(--)
C_v	calibration constant of the viscometer	(mm^2/s^2)
D	mean pore diameter	(m)
D_w	material specific liquid diffusion coefficient	(m^2/s)
F	correction factor of the Fisher Tensiomat	(--)
N	number of the setup	(--)
P	air permeance of the material	($L/s \cdot m^2 \cdot Pa$)
Q	volumetric airflow rate through the material	(L/s)
Q_{ti}	total air leakage rate through the material and the test apparatus	(L/s)
Q_{ei}	extraneous air leakage rate through the test apparatus	(L/s)
R	airflow resistance of the material	($Pa \cdot m^2 \cdot s/L$)
S	absolute value of surface tension	(N/m)

Symbol	Parameter	Unit
T	duration of contact	(s)
W_c	the saturated volumetric moisture content of the material	(kg/m^3)
average effect of a factor	average of the effects of a factor from its two result series	(--)
d	difference between effects of a factor from its two series of results	(--)
e	material thickness	(m)
factor(+)	test result obtained at the high setting for a given factor	(--)
factor(−)	test result obtained at the low setting for a given factor	(--)
m_w	mass of absorbed water	(kg/m^2)
n	air pressure exponent,	(--)
p	apparent value (Dial reading of the Fisher Tensiomat)	(--)
q	volumetric airflow rate calculated from Equation 2.3	(L/s)
t	mean flow time	(s)
Δp	pressure difference across the material	(Pa)
α	dimensionless constant	(--)

η	dynamic viscosity of air	(Pa·s)
κ_i	intrinsic permeability of the material	(m^2)
ν	kinematic viscosity	(mm^2/s)

CHAPTER 1 INTRODUCTION

1.1 General

Moisture is one of the most important environmental factors impacting the durability and performance of building envelope, especially in cold climates. The structural integrity of components of building envelope can be reduced by mechanical, chemical and biological degradation induced by uncontrolled moisture accumulation. It is estimated that 80% envelope damage is related to moisture problems (Bomberg *et. al.*, 1993).

Recent surveys on some failed buildings in Vancouver of British Columbia showed that among all types of cladding walls, which have experienced moisture orientated performance failures, stucco systems are in the majority. Serving as a critical environmental control element and taking on crucial functions of environmental control in the stucco cladding systems, weather resistive barriers (WRB), or sheathing membranes as they are called by National Building Code, are often suspected to be responsible for the failures. Some people assumed that the performance and the durability of WRB may be significantly influenced by their surroundings. These issues are examined in the following thesis.

1.2 Rain penetration control strategies

Wood frame walls have received substantial attention on their design because they are not only popular wall structure of low-rise resident buildings but also susceptible to moisture. Among various moisture sources, rain penetration is the main consideration of designing

building envelopes. Based on the understanding for various moisture transfer mechanisms, the guideline of moisture management is postulated as to minimize moisture ingress into systems, maximize drainage, and keep moisture accumulation in a safe level (Maref *et. al.*, 2002). The following moisture management strategies have been used in design of building envelopes:

- Face sealed wall (or barrier wall) method - This system requires a water-impermeable layer located on the exterior face of the enclosure assembly. Rainwater is not allowed to enter the wall. Therefore all the rain penetration control is fulfilled by the exterior surface.
- Mass wall (moisture storage) system - This wall is required to provide enough moisture storage to absorb penetrated rainwater through the exterior surface. Meanwhile, it should allow removal of the absorbed moisture by evaporation, so that the moisture accumulation can be controlled within a safe level.
- Screened wall approach - It acknowledges that some rainwater can penetrate its exterior cladding, which mainly serves as the first line of defence by shedding rain. Also, this approach provides one or several other complementary mechanisms, such as capillary break, water barrier and ventilated space, to resist further inward movement of the water and to increase the drying capacity of the wall.

1.3 Stucco cladding systems and WRB functions

Widely used stucco cladding wall in the regions with cold climate is the system, which utilizes the screened wall approach to control rain penetration. As shown in Figure 1.1, it consists of, from outside to inside, stucco layer, self-furring lath, WRB, wood sheathing

and wood studs with insulation between.

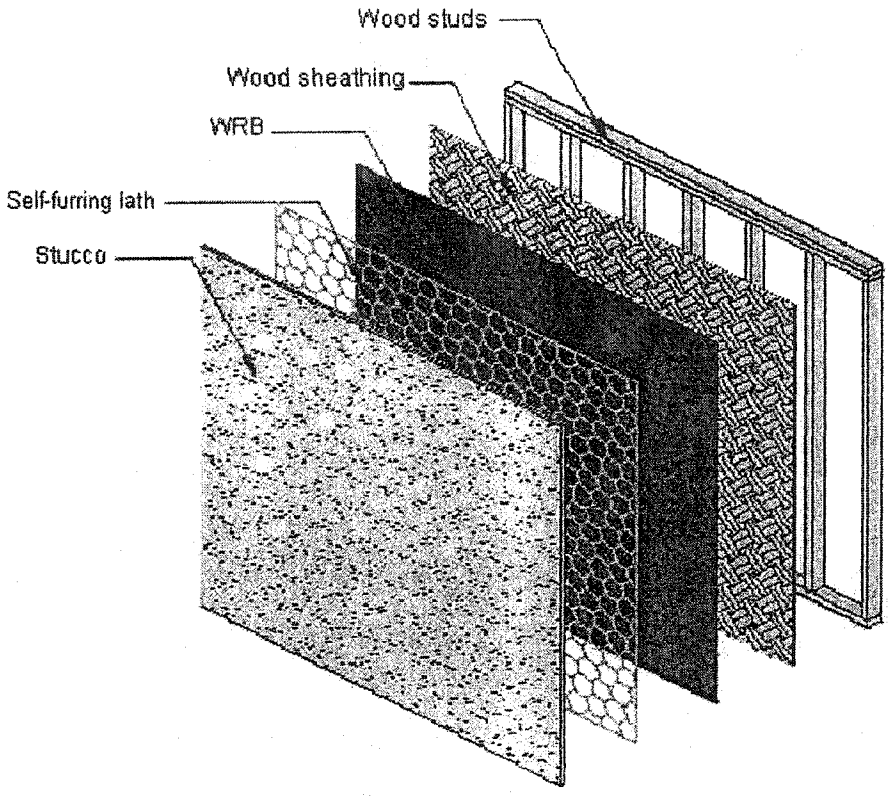

Figure 1.1 Composition of stucco cladding wall (Bomberg *et. al.*, 2002)

In some designs, a certain width of cavity is applied between the stucco and the WRB to provide one or a few functions, such as capillary break, drainage approach, drying by ventilation, and reduction of airflow driven moisture movement. While the diversity on the design between the stucco and WRB exists corresponding to the variation of environmental conditions, the stucco cladding system commonly employs the screened wall approach as its moisture control strategy, where the action of shedding rainwater is fulfilled by the exterior stucco layer as the first line of defence, and the second protection by WRB. Therefore WRB are required to have the following three main functions (Bomberg *et. al.*, 2003a):

- Restricting rainwater, which penetrates the exterior cladding, from reaching moisture sensitive components of walls.
- Permitting outward diffusion of water vapour that may accumulate inside the wall cavities, while being capable of reducing vapour flow inwards when the reverse thermal gradient causes its diffusion into the wall cavity.
- Controlling the flow of air through the assemblies

WRB performance depends not only on their characteristics as manufactured but also on some factors, such as, installation methods, and ambient conditions during construction and service life. Surveys on the stucco cladding walls, which failed in moisture control, have shown some problems of WRB performance, such as missing of material section, improper installation, material degradation or reduction of water resistance due to surfactants or chemical interaction presence.

1.4 Research objectives

To obtain more understanding on WRB performance, find out WRB responsibilities for the building moisture problems and the methods to avoid the problems through adequate design of stucco cladding systems, an Exterior Moisture Control (EMC) Consortium, including Canada Mortgage and Housing Corporation (CMHC), Concordia University, Du Pont Inc., Fortiber Corporation, Hal Industries, Homeowner Protection Office, DMO Associates, and Louisiana Pacific Corporation, was formed to support four academic researches. This thesis is one of them and its objectives are to:

- review the present knowledge of laboratory testing on moisture and air transmission through WRB,

- develop and select appropriate experimental techniques for characterizing WRB performance,
- investigate influences of outdoor weathering and mechanical stress on the performance of WRB, and
- investigate influences of leached chemicals from WRB adjacent components on the performance of WRB.

1.5 Thesis organization

This thesis consists of seven chapters. Following this chapter, Chapter 2 contains a brief review on WRB classification, researches on WRB, and existing test methods for characterizing WRB. Chapter 3 presents the selected experimental tools for examining WRB properties and their results. In succession, these tools are used to investigate effects of various factors on WRB. Chapter 4 presents the investigation on the effects of mechanical stress and outdoor weathering. Chapter 5 presents the investigation on the effects of wood extracts. Chapter 6 introduces an interactive weathering mechanism and evaluate its influences. Finally, Chapter 7 summarizes the findings of the study and gives recommendations for future research.

CHAPTER 2 LITERATURE REVIEW

2.1 Classification of WRB

Since original building paper was brought to control air leakage through building envelopes, various kinds of WRB products have been introduced in the market. Inevitably, the products are different because of their respective manufacturing techniques as well as raw materials. It is necessary to classify the various products for characterizing them, understanding their mechanisms, and analyzing the potential factors, which may cause the material to poorly perform.

To this end, the EMC Consortium proposed to classify the existing materials into the following five types according to the principle of basic material composition and structure (Bomberg *et. al.*, 2003b).

- Type C Asphalt -impregnated cellulose fibre based WRB
- Type P Polymeric fibrous WRB
- Type PP Perforated polymeric film
- Type LA Liquid-applied (trowel) WRB
- Type M Micro-porous film WRB

In the present study, three types of products are referred to, i.e. type C, type P, and type PP. As the name states, asphalt-impregnated cellulose fibre based (type C) WRB are made from cellulose fibers and asphalt. Generally, the cellulose fibers are hydrophilic materials by nature. However, when the pore structure of cellulose fibers is impregnated with

asphalt, the materials become hydrophobic. Therefore, water resistance of the type C products depends on both the pore size and the ratio of asphalt to cellulose. This fact explains an existing suspicion on the durability of type C membranes. Namely, it is assumed that type C products may decay due to losing of their asphalt when chronically exposed to high temperature or high moisture content conditions.

Polymeric fibrous (type P) WRB are made from hydrophobic polymer such as polyethylene or polypropylene. The properties of these WRB mainly depend on their pore structure and the dimension of the fibers. It is suggested that type P WRB are susceptible to photodegradation caused by ultraviolet radiation, which is the nature of polymeric materials.

Perforated polymeric film (type PP) WRB are also made from polymer materials but during the manufacture process they have been mechanically punctured to make the materials more vapour permeable. Typically, the size of the mechanically punctured holes is an order of magnitude higher than that of the pores in polymeric materials. Therefore, the size of the holes is crucial for the air and water resistance of the type PP membranes.

2.2 A review of researches on WRB

Since the original research on air leakage through frame walls conducted by University of Minnesota, and when building paper was formally introduced in the 1930's and through the 1980's when spun-bonded polyolefin membranes were developed, WRB have been recognized as a critical element to control moisture and air passing through wood frame walls. However, research work on the methods for evaluation of the WRB performance is inadequate.

Over the past ten years, a significant number of moisture-related building problems have appeared with many of the recently constructed wood framed buildings in the coastal areas of the southwest Canada and the northwest U.S., i.e. the Vancouver and the Seattle areas. The problems commonly include water penetration, damage to cladding systems, and rotting and decay of wood components, which are primarily caused by moisture accumulation within the walls. Among the damaged buildings in Vancouver, all types of cladding systems experienced performance problems, wherein it was found that the number of problems reported on stucco walls was greater. Some field investigations (MHL, 1996; CMHC, 1999; NHW, 1995; and Kadulski, 1997) on failed stucco walls and exterior insulation and finish systems (EIFS) have shown some common failures on WRB field performance, as following:

- WRB section missing,
- improper installation,
- WRB damages (ripped, punctured or torn),
- type C membranes degradation, and
- reduction of water resistance due to surfactants or chemical interaction presence.

After reviewing some design, construction, and material factors affecting the durability of stucco-clad structures and observing failed stucco walls, Marcus *et. al.* (1997) found that stucco is subject to a bond with WRB when applied directly on them. This prevents water from draining between the two materials. The trapped water may eventually penetrate through the WRB at their defect points.

Surveys conducted by MHL (1996), CMHC (1999), and NHW (1995, 1996) implied that

type C WRB could deteriorate in repeated wetting and drying. Lstiburek (2001) also suggested that directly applied hardcoat stucco could cause a lack of drainage between the stucco and the WRB. Lstiburek explains that earlier buildings outperform those that are recently constructed as they employ two layers of traditional type C WRB, which are able to debond from the back of hardcoat stucco as they dry.

For developing more representative data to understand durability issues regarding the use of WRB within building enclosures, a survey of in-place conditions and installation practices was carried in Pennsylvania (Burnett *et. al.*, 1998; Bosack *et. al.*, 1999; and Burnett, 2001). It was noted that the location of WRB membranes, the method of attachment, and the type of cladding system all greatly influenced the contribution of WRB to the performance of the wall assemblies. In addition, the laboratory tests on a few brands of WRB clearly demonstrated that each of the proprietary WRB had very different in-place characteristics especially with regard to controlling air leakage. It was also suggested that the effects of outdoor exposure, which may happen during construction slowdown over winter, on WRB durability should be investigated. Located alongside of WRB, to some extent, wood-based sheathing and exterior cladding protect the barriers against adverse climatic conditions, such as wind, sunlight, rain, and snow. However, during construction these factors may act on the WRB and change their physical or chemical properties. The performance of the WRB may be significantly affected by these changes. The industry has noticed these assumed situations and has proposed some weathering resistance tests for evaluating WRB products in standards.

CGSB 51.32-M77 (1977), "Technical Guide for Sheathing Membrane, Breather Type", is a Canadian standard for type C WRB products. It requires materials being tested to

undergo 25 accelerated aging cycles as following:

- 3 hours placed in an air-circulating oven at a temperature of 65°C,
- 3 hours submerged in distilled water at a temperature of 23°C, and
- 18 hours placed in a cold box at a temperature of -10°C.

Following the aging cycles, tensile strength and water vapour permeance tests are employed as the tools to evaluate the aging effects.

Because there was no existing Canadian standard for type P WRB, CCMC (1996) published a technical guide, "Sheathing, Membrane, Breather-Type, for Polyethylene-based or Polypropylene-based, Woven or Non-woven WRB". It proposes two aging processes to evaluate type P material resistance to weathering or aging. First, WRB specimen is required to go through successively 28-cycle aging as following

- 8 hours exposed to UV radiation UVA-340 lamps in a Q-UV apparatus operated in accordance with ASTM G 53 at 60°C and
- 4 hours of condensation at 40°C.

After the UV exposure test, the specimen is required to be heated in accordance with ASTM D 3045 for 168 hours at 90°C. Tensile strength, water vapour permeance, and water ponding test are utilized for the quality inspection.

As the standards show, potential effects of some aging or weathering on WRB have been noticed currently, however, to some extent the concerns are not adequate and can merely serve for quality assurance purposes. Further investigation on the influences of the aging or weathering on the durability of overall building envelopes is needed. Moreover, the

designated test methods in the standards cannot adequately examine the comprehensive performance of materials. For example, as a critical property of WRB, resistance to airflow is not examined in the standards. Therefore, more research work should be done and the aging or weathering evaluation parts in the material standards need to be improved. Detailed discussion on methods for testing WRB properties will be discussed in later parts of this chapter.

Early reports about reduction in water resistance of WRB due to surfactant presence can be traced to Lstiburek (1996) and Cushman (1997). An experimental work by Cushman (1997) demonstrated that water flow rate through some WRB membranes increased to varying extents when the membranes were exposed to an extractive solution, which was made by soaking cedar shavings in water. Similarly, Fisette (1999) tested three type P products with soap and wood extract solutions and observed slight reduction in WRB resistance to water flow. To relate this phenomenon to material field performance Fisette (2000) conducted another laboratory demonstration. In this test, same size of water saturated wood board, WRB, blotter paper and plywood were held together firmly from bottom to top with an elastic band. The blotter paper served as a visual indicator for water leaking through the WRB. The observation showed that among six WRB products, three type PP membranes immediately leaked water when bound between the blotter paper and the saturated wood board, and two type P WRB and a type C WRB had no signs of liquid water leakage through in two days. In addition, Fisette noted that all types of WRB leaked various amount of water within 2 hours in the same test when the sandwich composites were pierced with nails. EREC[1] (2002) suggested that lignin exists as a

[1] Energy Efficiency and Renewable Energy Clearinghouse

natural occurring and water-soluble substance in many species of wood and it can act as a surfactant.

Another laboratory investigation conducted by Weston *et. al.* (2001) also showed that WRB water resistance was reduced when the water involved extracts from cedar siding. In this investigation, a few WRB specimens were measured with a hydrostatic pressure test (AATCC 127, 1985) before and after they were exposed to an aqueous solution of cedar extracts obtained by soaking chipped cedar siding in distilled water for 24 hours. Two kinds of exposure processes were respectively employed. One was to immerse the WRB specimens in the extract solution for 24 hours. The other was to deposit the extracts on the WRB by evaporating a certain amount of the solution. The test results showed that only the deposition treatment resulted in reduction of the water resistance of the membranes reduced. In the report (Weston *et. al.*, 2001), mold resistance of several WRB products was also evaluated by a modified ASTM D3273-94 method, which calls for exposing the samples in an incubation chamber to mold spores. Mold resistance is defined as the ability of a sample to resist fungal growth that can cause discoloration and ultimate decomposition of sample medium. The comparison of the mold growth of the samples indicated that type C membranes are more susceptible to mould growth than type P products. The phenomenon was explained by the fact that the cellulose in type C can absorb water and is a good food source for mold.

In general, the conclusions from the previous researches on WRB emphasize that the industry and building designers should take the field conditions of WRB into consideration in order to make the materials to fulfill their designed functions. However, as discussed later in this chapter, current test methods employed to investigate WRB

performance are not all effective. Therefore, to evaluate the material performance and the significance of various environmental effects, which may be induced during construction phase and service life on WRB, appropriate test tools are needed.

2.3 A review of test methods used in evaluation of WRB products

A WRB product is not allowed to enter building market unless it passes evaluation tests designated by specified building codes or standards. In general, the tests are focused on examination of the material physical properties that relate to its performance. To test WRB membranes a few test methods have been adopted from various standards used by the textile, paper, and polymeric material industries. The physical properties being tested include moisture and air transmission characteristics. Generally, these tests should serve for at least one of two purposes, meaning that the test is capable either to characterize the material for comparative rating, or to provide input characteristics to heat, air and moisture (HAM) models, which in turn are able to simulate the performance of the building envelopes when all the constituent material characteristics, climatic and other boundary conditions are available.

2.3.1 Methods for testing liquid or vapour transmission through WRB

Table 2.1 lists several test methods currently utilized by the industry. Their sources, applicable standards/codes, and applicable material types are also shown in the table.

Table 2.1 Current methods for testing moisture transmission through WRB

Test title	Test standard reference	Applicable building standard or code	Applicable material type
Dry indicator test	ASTM D 779-94 Standard test method for water resistance of paper, paperboard, and other sheet materials by the dry indicator test (ASTM, 1998)	ICBO AC38 Acceptance criteria for weather-resistive barriers (ICBO, 2000)	Type P (not Grade D*) and type C
Water ponding test	CCMC 07102, Technical guide for Sheathing, membrane, breather-type section 6.4.5 (CCMC, 1996)	CCMC 07102 (1996)	Type P
		ICBO AC38 (2000)	
Hydrostatic pressure test	AATCC-127 Water resistance: Hydrostatic pressure test (AATCC, 1985)	ICBO AC38 (2000)	Type P
Dry cup test	ASTM E 96 Standard test methods for water vapour transmission of materials	CAN/CGSB 51.32-M77 (1977) National standard of Canada, Sheathing, membrane, breather type	Type C
		CCMC 07102 (1996)	Type P
		ICBO AC38 (2000)	Type P and type C

*Note: Grade D material is defined that: the dry tensile (tested with ASTM D 828) is minimum 20 pounds per inch width on both directions, the water resistance (tested with ASTM D 779) is minimum 10 min, and the water vapour transmission (tested with ASTM E 96 dry cup method) is minimum of 35 grams per square meter per 24 hours. (US Federal Specification, 1968)

2.3.1.1 Dry indicator test

Dry indicator test was developed by the paper industry and published in ASTM D 779, "Standard Test Method for Water Resistance of Paper, Paperboard, and Other Sheet Materials by the Dry Indicator Test." This method is currently adopted by ICBO AC38 "Acceptance Criteria for Weather-Resistive Barriers" to evaluate type C and type P WRB except for the type P membranes equivalent to Grade D. (ICBO, 2000) In fact, the dry indicator test can be considered as a modified method of the traditional "boat test", which is referred as a "Method 181" in the US Federal Specification UU-P-31b (1949). The boat test requires fabricating a 2.5-inch-square WRB specimen into a small boat. A dry indicator, which can change its colour in case of absorbing moisture, is sprinkled in the boat. To conduct the test, the boat is floated on water and the time, which it takes for the dry indicator to change colour, serves as a measure of the material resistance to water penetration.

With similar principle to the boat test, the dry indicator test employs a float arrangement, which allows the lower surface of specimen barely contacting with water and a watch glass being clamped over the specimen. The duration, which water takes to permeate through the specimen and change the colour of the dry indicator on the specimen under near-zero hydrostatic pressure, is used as the measure of material water resistance (ASTM D 779, 1998).

Although some improvements have been induced on the design of the boat test and the dry indicator test, their inherent shortcomings still have not been overcome, such as: (Bomberg *et. al.*, 2003)

- Colour change of the dry indicator has to be judged by naked eyes of test operators
- Unevenly sprinkled dry indicator with an unspecified amount may not be adequately sensitive to the moisture transmission
- Manual processes, such as creasing or folding specimen, for specimens may alter their resistance to water transfer.
- The condition on the upper surface of specimen being tested is not defined and the vapour existed in the ambient air may change the colour of the dry indicator
- The test cannot differentiate the liquid transmission from vapour transmission and the fraction between liquid and vapour is unknown.

2.3.1.2 Water ponding test

To evaluate type P WRB, CCMC adopted a water ponding test from roofing industry and standardized it in its "Technical Guide 07102 for Sheathing, Membrane, Breather-Type" section 6.4.5. The ponding test was also specified to test type P WRB in the ICBO AC38. To determine the material resistance to moisture transmission, this method uses a 250 Pa hydrostatic pressure on the upper surface of the specimen and the lower surface is exposed to the ambient condition as temperature $20 \pm 2°C$ and relative humidity $65 \pm 3\%$ RH. In order to pass this test, no more than two water drops are allowed to pass through the 160-cm2 specimen within 2 hours (CCMC, 1996). The appearance of the drops has to be judged by naked eyes of test operators, which is a disadvantage of the test. In addition, when the penetrated water does not flow vertically through the specimen but runs horizontally along the fibres of the material, it is difficult to make the judgment. Although the standard specifies the ambient temperature and humidity conditions, the varying

ventilation rate may evaporate the penetrated water in different rates so that the precision of the test may be affected.

2.3.1.3 Hydrostatic pressure test

In the ICBO AC38 (2000), a hydrostatic pressure test referred as AATCC 127-1985 is adopted to test type P WRB as an alternative water resistance test method. This method measures material resistance to water penetration under a high hydrostatic pressure by recording the onset period of liquid flow through the specimen being tested. To conduct the AATCC 127 test, two distinct apparatuses can be chosen. They introduce a hydrostatic head, ranging from 5.5 m to 2.8 m, either from the upside or the underside of the specimen with diameter of 114 mm. As specified by the ICBO A38, 55cm of hydrostatic head has to be kept on the specimen and for acceptance one requires no more than 3 water drops to pass through the specimen within the five hours test (ICBO AC38, 2000).

Added to all the disadvantages of the water ponding test, the hydrostatic pressure test falls short to establish a practical correlation between the material performance in this test and that in field because it is impossible for WRB to encounter such high hydrostatic pressure (0.55 m water column) in the service life. Therefore, this method can only serve for purposes of quality assurance. (Bomberg *et. al.*, 2003a)

2.3.1.4 Dry cup test

In 1953, ASTM specified a dry cup method and a wet cup method to determine water vapour transmission through various materials, for thickness less than 32 mm as ASTM E96-53T, named "Standard Test Methods for Water Vapour Transmission of Materials".

Figure 2.1 and Figure 2.2 are the schematic drawings of the dry cup test and the wet cup test.

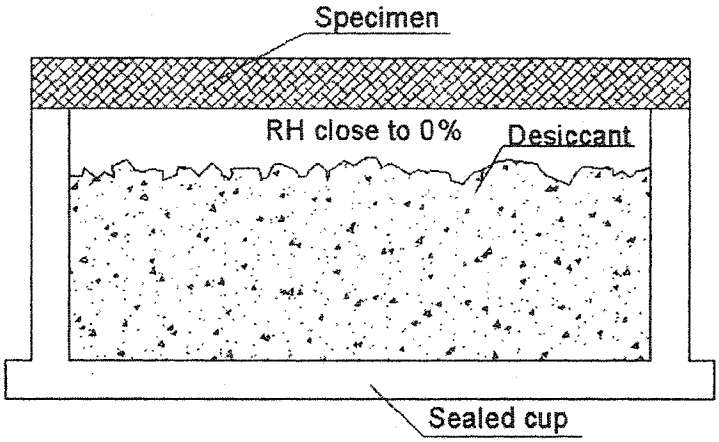

Figure 2.1 Schematic drawing of the dry cup test

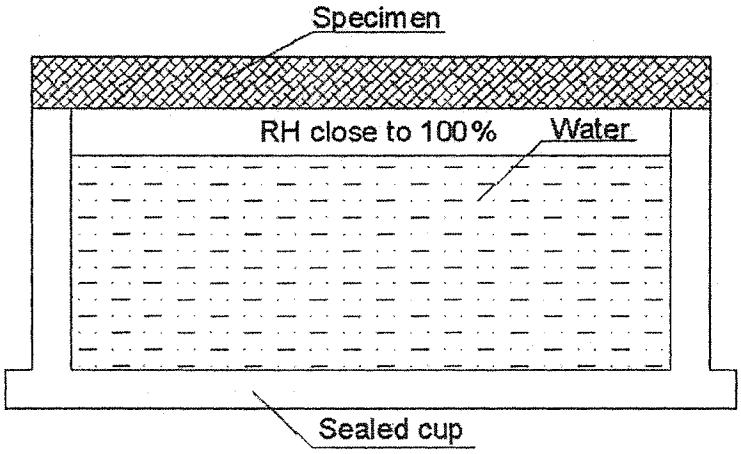

Figure 2.2 Schematic drawing of the wet cup test

As shown in the figures, the dry cup and the wet cup methods respectively use desiccant and water in their cups to keep relative humidity (RH) close to 0% and 100%. In ASTM E96-00, the outside RH of the cups is controlled at 50% by using a climatic chamber. In fact, water vapour permeability of materials is dependent on local relative humidity levels (McLean *et al.*, 1990 and Lackey *et al.*, 1997). The dry cup method in the ASTM E96-00

measures water vapour permeability of the specimen corresponding to the mean relative humidity of 25% (ASTM, 2000).

In the recent decades, the dry cup method has been used worldwide for determination of water vapour transmission properties of various building materials. It is also adopted by CCMC (1996), CAN/CGSB (1977), and ICBO (2000) standards to evaluate the performance of the type C and the type P WRB. Moreover, because it can measure single-phase moisture flow (water vapour), the measurement commonly is used as a necessary material property by heat, air and moisture model. (Grunewald, *et. al.* 2002 and Bomberg *et. al.*, 2003b)

However, some applications of this method have raised a difficulty of comparing results measured from different laboratories on the same material although all of them use the same measuring technique. It is found that the sources of uncertainty of this method include: barometric pressure, surface diffusion resistances at the specimen surfaces, air layer thickness inside the cup, boundary effects by specimen connection to the cup, relative humidity oscillation, errors in measuring instruments, determination of the onset of the steady state flow, and calculation technique for water vapour transmission properties from measured values. (Babbitt, 1939; Bomberg, 1989; Hansen *et. al.*, 1990; and Burch *et. al.*, 1992) To diminish the effect from ambient varying relative humidity on the measurement with dry cup or wet cup methods, ASTM (Schwartz *et. al.*, 1989) introduced a method called modified cup method, which combines a dry cup above the specimen and a wet cup under the specimen to keep two constant relative humidity conditions. This method does not require relative humidity control in the ambient environment of the test set-up because it is a closed system. Furthermore, since this

method allows monitoring the weight gain of the upper cup and the weight loss of the under cup by separately measuring the them and the specimen, the moisture accumulation in the specimen can be obtained and onset of the steady state flow can be known. The modified cup method is further examined in a parallel thesis work. (Mungo, 2003)

2.3.1.5 Conclusions of the methods for testing moisture transmission through WRB

The above review on the current methods for testing moisture transmission through WRB show that the dry cup method specified in ASTM E96-00 is capable to measure single-phase moisture transmission (water vapour flow). It is appropriate to not only characterize WRB performance but also provide WRB property as input of HAM model. The other methods, such as dry indicator test, water ponding test, and hydrostatic pressure test, commonly assume water flow to be dominant factor in moisture transmission through WRB and disregard the possible effects of water vapour flow. Actually, since they measure a mixed moisture flow, which includes liquid and vapour transport in an arbitrary ratio, one cannot use them to separately judge the performance of water and vapour transmissions through WRB. In addition, some inherent design shortcomings of the methods, such as uncertainties of operation or lack of well-defined boundary conditions, prevent them from giving adequate information of material performance to meet the objectives of the present study.

2.3.2 Methods for testing airflow through WRB

Air leakage is a very important parameter in the analysis of the building performance. In 1995, National Building Code of Canada (NBCC) proposed installation of air barrier system and its requirements: airtightness, continuity, structural integrity, and durability.

The NBCC also provides a material requirement for air barrier systems; specifically, where a material is to provide the principal resistance to air leakage, the material shall have an air leakage characteristic no greater than 0.02 L/s.m2 at a pressure difference of 75 Pa.

For testing of building assemblies, there are two widely referenced standards, which are ASTM E283 (1999), entitled "Standard Test Method for Rate of Air Leakage Through Exterior Windows, Curtain Walls, and Doors" and ASTM E783 (1999), entitled "Standard Method for Field Measurement of Air Leakage Through Installed Exterior Windows and Doors." As the titles state, both of the standards are limited to windows and doors. Two suitable methods for testing airflow resistance of WRB are reviewed as following.

2.3.2.1 Test of airflow resistance of exterior membranes and sheathing

Institute of Research in Construction (IRC) developed an experimental set-up and published it in the Building Research Note 227 titled "a Test Method to Determine Air Flow Resistance of Exterior Membranes and Sheathing" (Bomberg and Kumaran, 1985). Figure 2.3 shows a schematic drawing of the method. Chamber A and B are made of Plexiglas cylinders with an inside diameter of 12.57 cm. Specimen is placed between the chambers to separate them and held air tight with help of a rubber "O" ring with diameter of 13.66 cm and a pressure jack to keep airtight. Figure 2.4 shows detail configuration of the two chambers. To conduct the test, compressed dry air from a regulating valve is admitted to the chamber A; then the air flows through the specimen into the chamber B, which is open to atmosphere. Consequently an appropriate steady state is maintained in the assembly.

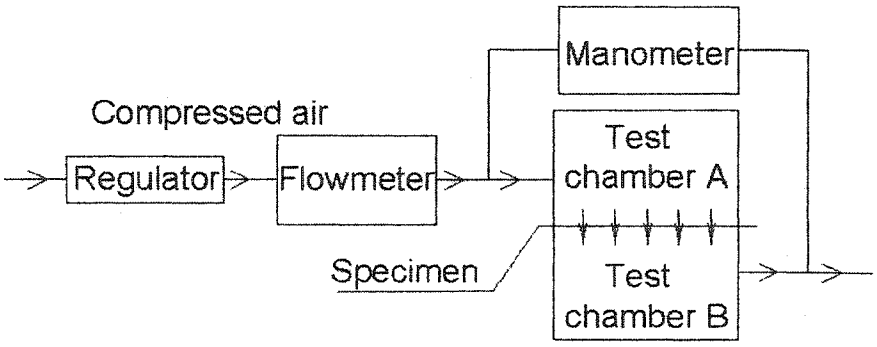

Figure 2.3 Schematic of the test assembly (IRC method)

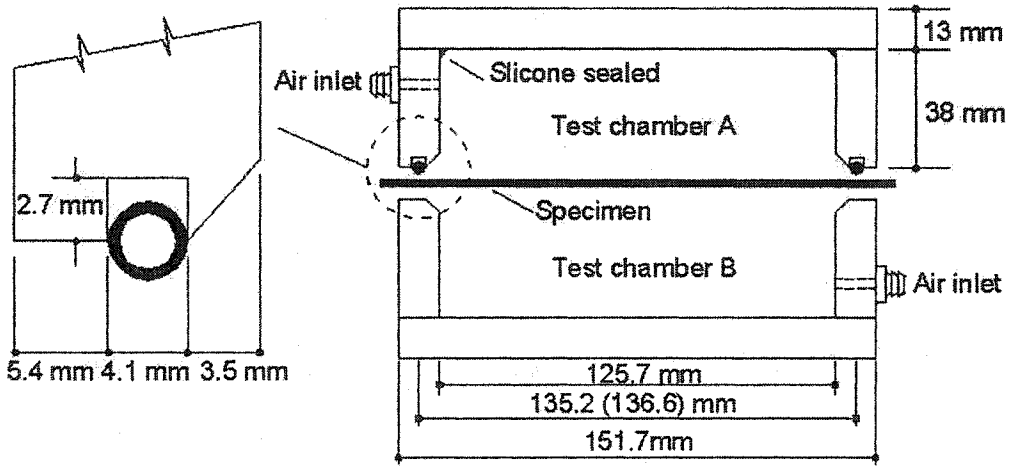

Figure 2.4 Detail configuration of the test chambers of the IRC air resistance test

In the test, the relevant experimental quantities to be measured by a manometer a flowmeter and are pressure differences applied across the specimen and their corresponding volumetric air flow rate. From the data produced, a graph of air flow rate versus pressure difference can be generated and the airflow resistance can be calculated by using equation 2.1.

$$R = \Delta p \, A / Q \tag{2.1}$$

Where,

R = airflow resistance of the material, (Pa m^2 s/L),

Q = volumetric air flow rate through the material, (L/s),

Δp = pressure difference cross the material, (Pa),

A = normal cross-sectional area of the material (It is defined by the "O" ring), (m^2).

One may notice that when the air flows into the material it could leak out from the material cross section at its unsealed edge. Therefore, if the method had defined how to avoid unexpected air leakage at the connections between the specimen and the chambers it would have given more reliable material property. In addition, to make the test results reproducible among different laboratories, the operating temperature of the dry air should be specified.

Since the IRC method was developed for testing the air resistance of WRB materials, for practical purposes it approximately assumes that the mode of air flow through WRB is laminar flow. Therefore, it employs a linear dependent relation between air flow rate and pressure difference to calculate air resistance of WRB. Actually, since building materials are heterogeneous by nature, the mode of air flow may change from laminar to turbulent at several locations within the material. Furthermore, entrance and exit effects may also be different from the mode of air flow existing within the material. Therefore, in order to cover all possibilities, the dependent relation should be exponential. The following method includes the instances.

2.3.2.2 Test for air permeance of building materials

In 1988, AIR-INS Inc. proposed and validated a test method to determine air permeance or flexible or rigid sheet building materials. Recently, this method was published as

ASTM E 2178 entitled as "Standard Test Method for Air Permeance of Building Materials". The experimental set-up assigned for flexible materials such as WRB is shown in Figure 2.5. To conduct the test, the material measuring 1.1 m by 1.1 m should be wrapped in a sheet of polyethylene and anchored to the open side of the test chamber by means of a compression frame and clamping devices. Due to lack of rigidity, the flexible specimen must be tested over a rigid support having an air permeance much greater than the specimen. A wire mesh, fabricated with welded wire having a minimum of 25 mm by 25-mm-square grid, can be used for this purpose.

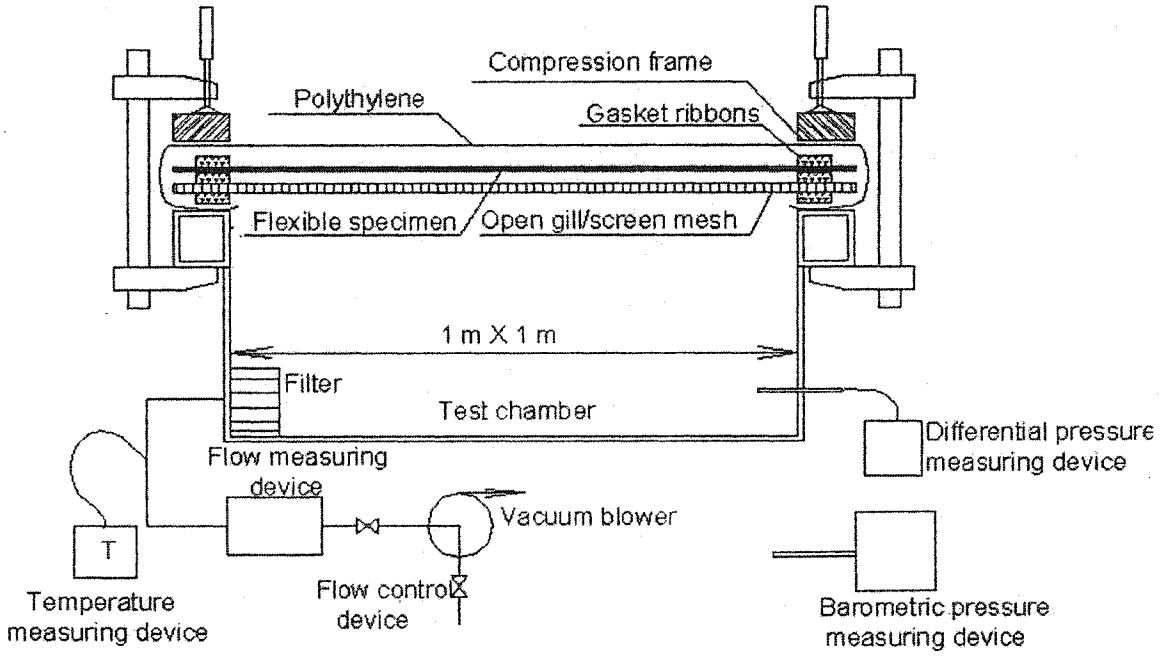

Figure 2.5 Schematic drawing of the ASTM E 2178 test

A vacuum machine is utilized to create lower air pressure in the chamber than the ambient air pressure. The air leakage rate through the chamber is measured with the chamber exposed to various pressure differentials (25, 50, 75, 100, 150 and 300 Pa) to determine the leakage, if any, of the test apparatus. The top section of the polyethylene

should be then cut from the sample along the inner line of the compression frame, and the air leakage rates are again measured with the chamber exposed to various pressure differentials (25, 50, 75, 100, 150 and 300 Pa). The air leakage rate through the sample is determined as Equation 2.2 by subtracting the air leakage rate of the chamber.

$$Q = Q_{ti} - Q_{ei} \tag{2.2}$$

Where,

Q = volumetric air flow rate through the material, (L/s),

Q_{ti} = total air leakage rate through the specimen and the test apparatus, (L/s),

Q_{ei} = extraneous air leakage rate through the test apparatus, (L/s)

The flow rate equation (shown in Equation 2.3) should be established by fitting the test data (Q and Δp) and errors estimated.

$$Q = C\ A\ (\Delta p)^n \tag{2.3}$$

Where,

C = airflow coefficient, ($L/s \cdot m^2 \cdot Pa^n$)

A = normal cross-sectional area of the material, (m^2),

n = air pressure exponent,

Δp = pressure difference cross the material, (Pa).

The air permeance of the specimen at a given pressure difference should be calculated by following equation 2.4.

$$P = q / (A)(\Delta p) \quad (2.4)$$

Where,

P = air permeance of the material, (L/s·m^2·Pa),

q = volumetric air flow rate calculated from Equation 2.3, (L/s).

To validate the ASTM E 2178 method, AIR-INS Inc. (1988) tested 126 specimens from 36 building materials by using the IRC and the ASTM methods at static pressure differences varying from 25 to 100 Pa. The validation process shows that test results from IRC and ASTM are very close to each other. In addition, the study confirms that at pressure differences from 25 to 100 Pa, the air flow regime through building materials is mainly laminar.

2.3.2.3 Conclusion of the review of the methods testing airflow through WRB

Two reviewed methods have their respective merits. Since ASTM E 2178 method tests a large size specimen (1 m by 1 m), the significance of material inhomogeneity on the result can be dwindled. The method using two airtight chambers provides more stable air pressure conditions across the specimen whereas the ASTM E 2178 method is subjected to effects from fluctuating barometric pressure because the top surface of the specimen is exposed. Therefore, the latter requires well-controlled laboratory environment to obtain reliable results. In general, both of the methods are suitable to characterize WRB performance on air resistance.

CHAPTER 3 MEASURING MATERIAL PROPERTIES

In the last 20 years, a number of moisture-related building envelope problems have triggered some suspicions about the performance of WRB. To validate or refute them one needs to understand the WRB performance in their envelope systems. The first step in this direction is to characterize the critical properties of the materials. This chapter examines WRB characteristics in respect to the way in which they contribute to the performance of a wall system. As the main functions of WRB are to resist water enter to water sensitive parts of walls, allow moisture within the walls to escape to exterior by vapour diffusion, and reduce air leakage through the walls, the material physical properties being examined in this chapter include their resistance to moisture transmission, either in liquid phase or in vapour phase, as well as their resistance to airflow.

The merits and shortcomings of the existing test methods, which are utilized in current standards or codes, have been reviewed in Chapter 2. It has been found that some of them do not provide adequate information for studying material property variations, which could happen in service life. Therefore, the present study develops an experimental set-up for testing air permeance of WRB and adopted a modified inverted cup (MIC) method and a moisture flux (MF) method, which are developed in a complementary project of the

EMC research consortium by Pazera (2003), for characterizing moisture transmission through WRB. As discussed later, the MIC and the MF tests conducted on type C and type P membranes measure moisture flow, which is dominated by water vapour, thereby, a water absorption test is developed to characterize water transmission through WRB. These four test methods will be described in the following sections in detail.

3.1 Description of WRB samples

The present study totally involved eleven brands of WRB products, which were all randomly obtained in standard roll size as manufactured from their respective product lines. According to the proposed classification in Chapter 2, these products include five type C (Asphalt -impregnated cellulose fibre based) membranes, coded as C1, C2, C3, C4, and C5; three type P (Polymeric fibres) products, coded as P6, P7, and P8; and three type PP (Perforated polymeric film) products, coded as PP9 PP10 and PP11.

Before any test or treatment was conducted, all material samples were stored in a laboratory condition at temperature of $23 \pm 2°C$ and relative humidity of $50 \pm 5\%$ for at least 40 hours. All specimens being tested were randomly cut from their respective sheets. If not specified, all test results, which are shown in this thesis, are averages of three specimen results for the sake of diminishing the result inaccuracy caused by material variation.

3.2 Characterization by means of air permeance test

It has long been recognized that the control of airflow is a crucial and intrinsic part of heat and moisture control in modern building enclosures (Wilson, 1963; Garden, 1965). WRB serves as an important component to resist airflow through building envelops. To evaluate overall performance of a WRB product, its resistance to airflow should be mentioned. To this end, an experimental set-up for testing WRB air permeance is developed in the present study. It is based on following theory.

3.2.1 Theory of air flow through WRB

According to the literature review in Chapter 2, unidirectional steady air flow through WRB at pressure difference ranging from 25 to 100 Pa is mainly laminar flow, which can be represented in Figure 3.1.

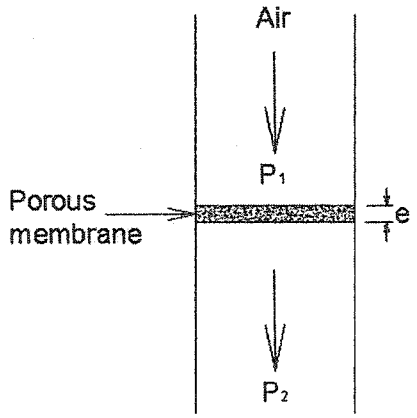

Figure 3.1 Unidirectional laminar flow of air through a porous material

According to Darcy's law, the relation between the rate of airflow and the pressure

difference can be expressed by following equation:

$$\frac{Q}{A} = -\frac{\kappa_i}{\eta} \bullet \frac{\Delta P}{e} \tag{3.1}$$

Where,

Q = volumetric air flow rate through the material, (m^3/s),

A = normal cross-sectional area of the material, (m^2),

κ_i = intrinsic permeability of the material, (m^2),

η = dynamic viscosity of air, (Pa·s),

ΔP = pressure difference across the material, (Pa), and

e =material thickness, (m).

Equation 3.1 is applicable to homogeneous materials. However, WRB are non-homogeneous membranes. For practical application a material property, air permeance p, is defined as Equation 3.2.

$$p = \frac{\kappa_i}{\eta e} \tag{3.2}$$

Where,

p = air permeance of the material, ($m^3/s \cdot Pa \cdot m^2$).

According to Equation 3.1 and 3.2 the material air permeance can be written as

$$p = \frac{Q}{A\,\Delta P} \tag{3.3}$$

There have been several attempts to derive a general relationship between material porosity and its intrinsic permeability. It is reasonable to assume that the permeability should increase with porosity. Air permeability as a function of the average pore radius can be very roughly estimated as Equation 3.4 (Massmann, 1989; Fetter, 2000)

$$k_i = \alpha\, D^2 \tag{3.4}$$

Where,

α = dimensionless constant,

D = mean pore diameter, (m).

According to Equation 3.2, material air permeance is proportional to its intrinsic permeability. In other words, the air permeance can roughly represent material porosity. Therefore, in the present study the measured air permeance serves not only for characterizing material resistance to airflow but also indicating material porosity.

3.2.2 Description of the air permeance test

The experimental set-up of the air permeance test entails sealing a WRB specimen between two airtight chambers, keeping a steady pressure differential across the specimen and measuring the air flow rate through the specimen. The pressure difference and the

corresponding air flow rate are used to calculate the specimen air permeance according to Equation 3.3.

3.2.2.1 Test apparatus

i . Airtight chamber A and B (shown in Figure 3.2)

Two similar chambers that are made of 3 mm thickness polyvinyl chloride (PVC) board, are prepared. The chamber inside measures 20 cm by 22 cm by 25 cm. Each chamber has two outlets on its top and bottom surface (20 cm by 22 cm). A circle opening with diameter of 14.2 cm is made on a side surface (20 cm by 25 cm). Around the opening there is a 15.5 cm diameter groove with depth of 1 mm and a rubber ring is embedded in it. Six 0.5-cm-diameter holes are symmetrically drilled on the brims of two side surface (20 cm by 25 cm) but do not penetrate the inside wall of the chamber. Three 50-cm-length screwed rods are inserted in the holes for clamping the two chambers together. In addition, because WRB are flexible, a metal mesh (25mm by 25mm square grid) is fastened in chamber B and its surface is in same surface as the opening of the chamber B. Chapter A does not have this metal mesh.

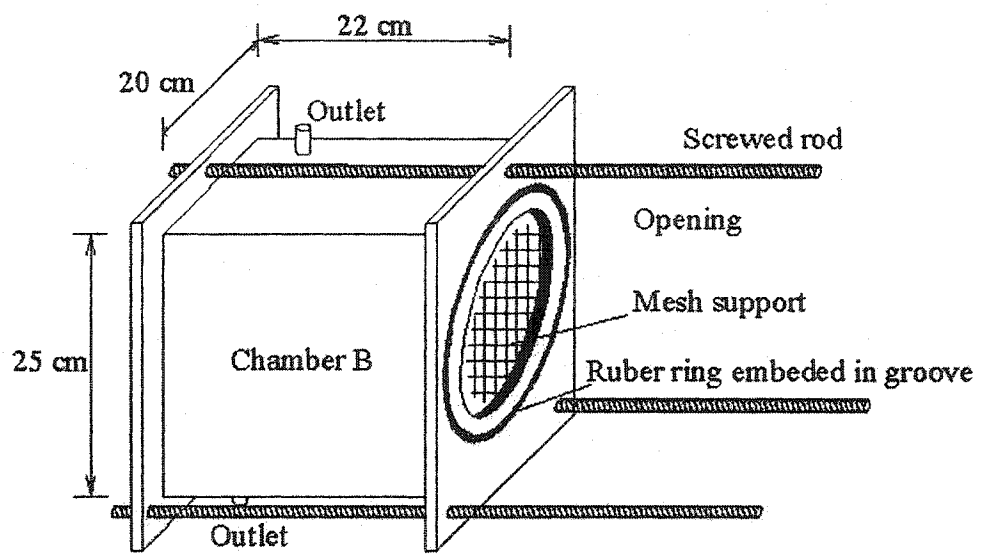

Figure 3.2 Schematic diagram of the airtight chamber

ii . Two PVC rings

To seal and fasten WRB specimen, two rings, which are cut from 3 mm thickness PVC board, are prepared. The inside diameter is 13 cm and outside diameter is 17 cm.

iii. Piping

The piping connecting air source, flow measuring device, pressure measuring device, and the chambers, is airtight and contain following four components:

- a flow control valve (regulator) to regulate the flow rate through specimen,
- an air filter to prevent dusts or particulate matters from affecting the flow measuring device reading,
- a temperature measuring device, which is capable of measuring air temperature

within ±0.5°C, and

- an airflow buffer (a airtight metal box measuring 30 cm by 30 cm by 50 cm with two outlets) to stabilize the air flow rate and temperature.

iv. Flow Measuring Device

Steady air flow rate is measured by one of following flow meters, which are located between the regulator and the chambers.

- Jour Digital Flowmeter, with a measuring range of 0.1 to 500 ml/min and accuracy of ±2% of the reading. It was calibrated with Drycal DC-2M calibrator.
- Cole-Parmer Flowmeter (Model 32907-00) manufactured by Cole-Parmer instrumental company. Its measuring range is 0 to 1 ml/min and its accuracy is ±1% of full scale. It was calibrated by its manufacturer.

v. Pressure measuring device

The pressure measurement was obtained by using a Magnehelic Differential Pressure Gage (Model 2000-250Pa), manufactured by the Dwyer Instruments Inc., with a range of 0 to 250 Pa and accuracy of 2%. The instrument was calibrated with a Dwyer Microtector Manometer (Model 1470 M745).

vi. Vacuum pump

Vacuum pump was used to suck air through tested specimens. The present study used Force 2 pump (air flow rate range: 500 to 3000 cc/min), which is manufactured by Rolf C. Hagen Inc.

vii. Compressed air bottle

In this study, another way to provide airflow is to use a compressed air cylinder, which is supplied by Praxair Inc.

3.2.2.2 Specimen preparation

To conduct the test, WRB specimen with diameter of 18.9 cm should be first sealed between the PVC rings by brushing mixture of wax and rosin on the outside and inside perimeters of the rings (see Figure3.3). The outmost edge of the specimen has to be covered by the wax mixture as well. Thus, practical exposed area of the specimen is 116.8 cm2, which is defined by the interior perimeter of the sealing wax.

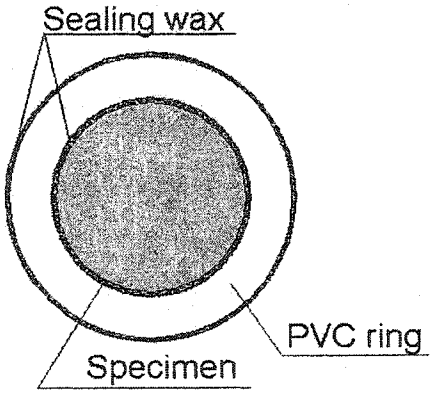

Figure 3.3 Sealing detail of specimen

3.2.2.3 Test procedure

The test procedure includes following four steps:

i . Installing the sealed test specimen between the test chambers.

The sealed specimen with the rings should be clipped between chamber A and B with their openings facing each other. Then, the chambers are clamped together by tightening the three screwed rods. Figure 3.4 shows the methods for assembling the specimen and the chambers.

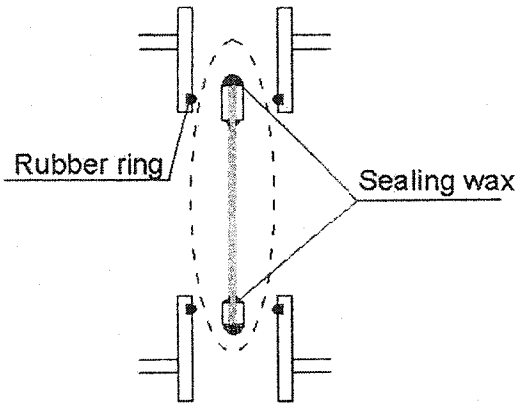

Figure 3.4 Methods for assembling the specimen and the chambers

ii . Verifying the assembly

Before conducting the test, the airtightness of the assembly has to be verified. To this end, three outlets of the chambers are blocked and the remaining one is used for compressing air into the assembly to keep the inside pressure approximately 1000 Pa higher than that of atmosphere. Then, the manometer is connected to this outlet to monitor the pressure

difference. If there is not pressure decay in 10 minutes, the assembly can be used to conduct further test.

iii. Connecting the test apparatuses

In case of the dry air cylinder is used as the source of airflow, the apparatus should be connected as shown in Figure 3.5. If the vacuum pump is employed, the connection should follow Figure 3.6.

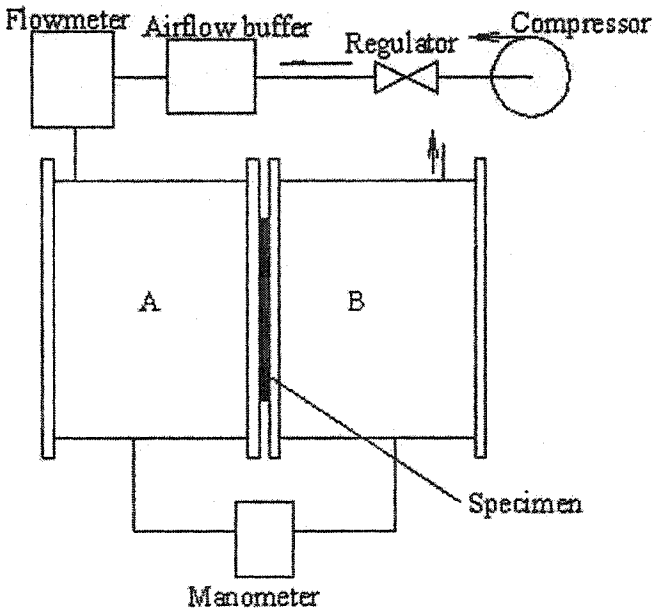

Figure 3.5 Connection method 1 of the air permeance test apparatuses

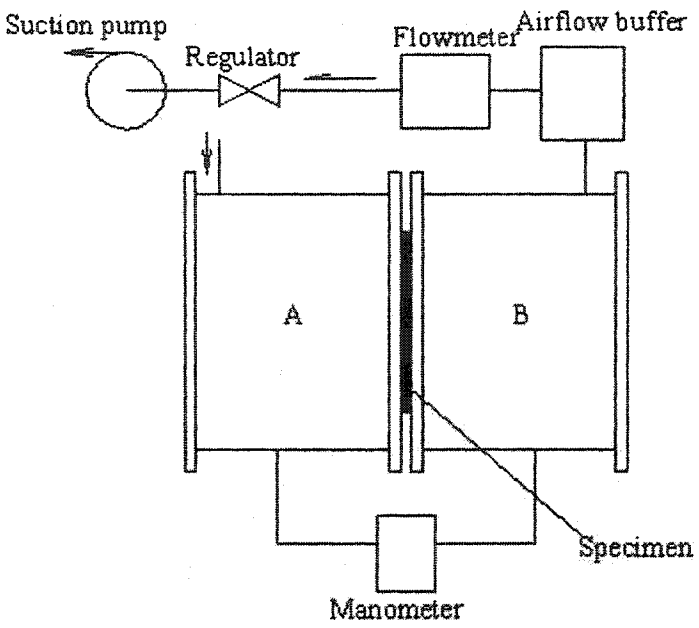

Figure 3.6 Connection method 2 of the air permeance test apparatuses

iv. Taking measurements

After opening the valve of the compressed air cylinder or turning on the vacuum pump, air is admitted in the chamber A, then, it flows through the specimen into chamber B. Consequently, a steady state is maintained in the assembly. At several static pressure differences near 12, 24, 36, 48, and 60 Pa, the flow rates and the pressure difference are measured by using the flowmeter and the manometer. Different steady states can be achieved by adjusting the regulator to change the air flow rate.

v. Calculation of air permeance

The air permeance of a specimen, p, is calculated by using Equation 3.3. By least-square method, several measured data pairs of air flow rates versus the pressure

differences are linearly analyzed to determine p, which represents the best fit.

3.2.3 Validation of the air permeance test

Three C4 specimens were tested and their measurements are shown in Table 3.1.

Table 3.1 Measurements of the air permeance test conducted on C4

C4 -1		C4 -2		C4 -3	
Pressure difference Pa	Air flow rate L/s·m^2	Pressure difference Pa	Air flow rate L/s·m^2	Pressure difference Pa	Air flow rate L/s·m^2
0	0	0	0	0	0
8	0.019	8	0.018	7	0.021
17	0.046	21	0.048	22	0.060
29	0.080	30	0.070	31	0.086
45	0.117	45	0.104	47	0.125
59	0.149	58	0.156	61	0.166

The linear dependences of two measurements are shown in Figure 3.7. The slopes of the regressed lines represent the specimen air permeance.

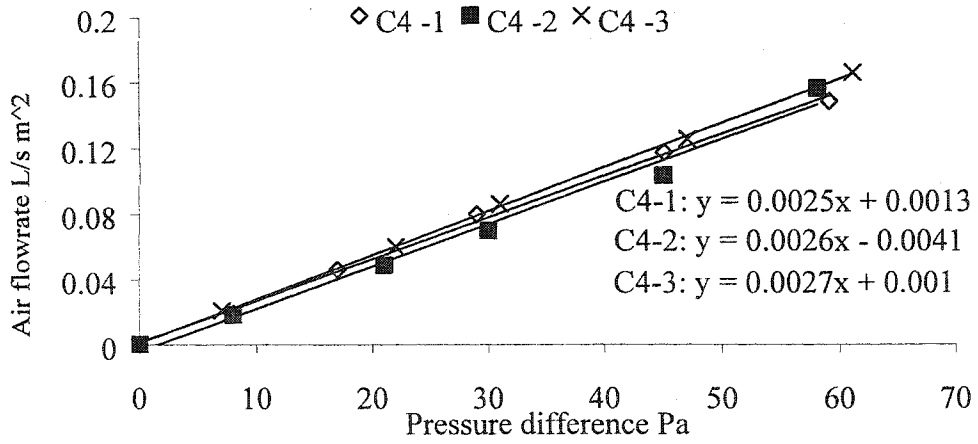

Figure 3.7 Linear dependence of pressure difference and air flow rate for three C4 specimens

Results of the linear least-squares analyses for the three series of measurements are given in Table 3.2.

Table 3.2 Linear least-squares analyses of the air permeance measurements

Specimen code	Intercept $L/s \cdot m^2$	Standard deviation $L/s \cdot m^2$	Linear correlation coefficient	Air flow rate $L/s \cdot m^2 \cdot Pa$
C4-1	0.0013	0.003	0.9988	0.0025
C4-2	-0.0041	0.007	0.9934	0.0026
C4-3	0.0010	0.002	0.9997	0.0027

The linear correlation coefficients and standard deviations of the three specimens indicate the test results are stable and repeatable. Theoretically, the intercepts of the regressed lines should be equal to zero. Yet, in practice, the values of the intercept are considered as the experimental imprecision.

3.2.4 Examining precision of the air permeance test

While developing a test method, to obtain accurate test results one should analyze effects of various experimental factors on test results. For this purpose, the present study adopts a ruggedness test method, ASTM E 1169 "Standard Guide For Conducting Ruggedness Tests". This method recommends a Placett-Burman (P-B) design, which can be used to evaluate relative significance of N-1 experimental factors on test results (N is the number of tests to be conducted and the recommended P-B design requires that N must be an integer multiple of four). In the P-B design, it is assumed that the effect of each factor on

test results is not dependent on those of other factors. In another word, there is no coupled influence. When the levels of the factors simultaneously change, the observed effects on test results can be described as simple addition of the fixed effects for each factor. Therefore, by repeatedly testing same material with systematically changing the levels of the factors, corresponding test results will allow one to evaluate the relative significance of the each factor.

To examine the effects of several test parameters on the air permeance results, the present study selects C4 membrane as a representative. Seven experimental factors (N=8 in the present study) being evaluated are listed as following. According to ASTM E 1169, the calculation of effects of each factor is based on the test result variations caused by systematically and simultaneously changing the setting of the factors between their two controllable extreme levels, called here a high and low setting. Therefore, the settings of the each factor are defined and listed as well.

Description of selected factors and their settings

Factor A: Testing area of specimen

The effective testing area of the specimen was varied in the evaluation. A circle area defined by the inner edge of the sealing wax was set as a low setting. By masking half of the circle with the wax (see Figure 3.8), half circle area was set as a high setting.

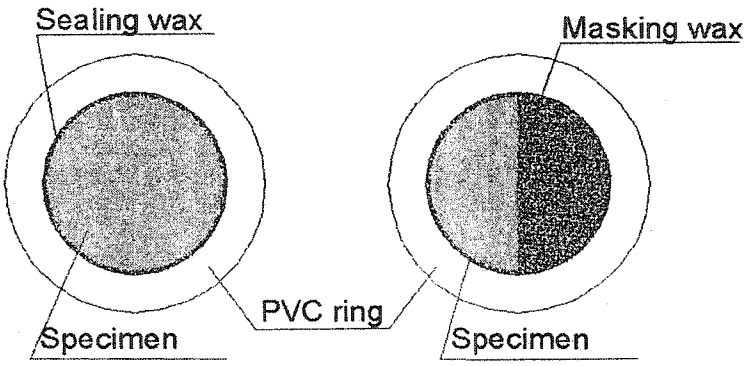

Figure 3.8 Low setting (full circle) and high setting (half circle) of the Factor A for the ruggedness test

Factor B: Use of airflow buffer

In order to find if test results would be affected by tubing connection, test set-up with the airflow buffer was set as a high setting and that without the airflow buffer was set as a low setting.

Factor C: Measurement range

To find if test results are dependent on range of pressure difference applied across specimen, at a high setting, pressure difference was selected within range of 0 to 60 Pa. Yet, at a low setting, pressure difference was selected within range of 0 to 120 Pa.

Factor D: Use of metal mesh support

Owing to lack of rigidity, WRB air permeance results may be influenced. At a high setting, specimens were supported by the metal mesh fixed in the chamber B. At a low setting, no support was provided.

Factor E: Frequency of reading

In order to achieve steady states, a certain time interval must elapse before one takes a reading. 20 minutes and 10 minutes were selected as high and low settings of the time interval, respectively.

Factor F: Approach of airflow supply

At a high setting, the compressed air bottle was used to press air through specimens. At a low setting, the suction pump was employed to suck air through specimens.

Factor G: Order of taking measurements

The order of taking measurements was varied. At a high setting, readings were taken from low pressure difference to high pressure difference within a specific range and at a low setting, in reverse.

Table 3.3 summarizes the seven factors and their corresponding settings. The high and low settings of each factor will be symbolized by "+" and "-".

Table 3.3 Factors and their settings for the ruggedness test

	Factor	Settings	
		High (+)	Low (-)
A	Testing area of specimen	Half circle	Full circle
B	Use of airflow buffer	No	Yes
C	Measurement range	0-60 Pa	0-120 Pa
D	Use of metal mesh support	Yes	No
E	Frequency of reading	20 min	10 min
F	Approach of airflow supply	Pressing	Sucking
G	Order of taking measurements	Increasing	Decreasing

Design calculation and result

The selected P-B design defines eight test setups, which combine the high or low setting of the seven factors together by a specific arrangement shown in Table 3.4. In this table, each row represents one setup. To obtain accurate results, the present study tested two specimens for each setup and their results are listed Table 3.4 as series 1 and 2. According to the P-B design, the estimation for the significance of each factor is done by comparing the value of effect of each factor, which can be calculated by using Equation 3.5.

$$Effect\ of\ a\ factor = \frac{\sum factor\ (+)}{N/2} - \frac{\sum factor\ (-)}{N/2} \tag{3.5}$$

Where,

factor (+) = Test result obtained at the high setting for a given factor,

factor (–) = Test result obtained at the low setting for a given factor, and

N = Number of the setup (here N is equal to 8).

Further, a statistic analytic method, t-test, is recommended to judge whether a factor is statistically significant. The method entails calculating a t value of each factor and comparing it with a reference value. If the absolute value of t value of a factor is larger than the reference value, effects of the factor are suggested to be relatives significant. Equation 3.6 indicates calculation method of the t value.

$$t_{N-1} = \frac{average \quad effect \quad of \quad a \quad factor}{2 \cdot \sqrt{[\sum d^2/(N-1)](N/8)}/\sqrt{2N}} \tag{3.6}$$

Where

t_{N-1} = t value of a given factor,

average effect of a factor = average of the effects of a factor from its two series of results, and

d = difference between effects of a factor from its two series of results.

Table 3.4 Results of the ruggedness test of the air permeance test

Setup	Factors							Air permeance $10^3 \cdot L/s \cdot m^2 \cdot Pa$	
	A	B	C	D	E	F	G	Series 1	Series 2
1	+	+	+	-	+	-	-	2.71	2.60
2	-	+	+	+	-	+	-	2.69	2.44
3	-	-	+	+	+	-	+	2.73	2.69
4	+	-	-	+	+	+	-	1.90	1.95
5	-	+	-	-	+	+	+	2.57	2.62
6	+	-	+	-	-	+	+	2.07	2.30
7	+	+	-	+	-	-	+	1.88	2.29
8	-	-	-	-	-	-	-	1.93	2.96
Av.Eff.*	-3.6E-04	1.6E-04	2.7E-04	-1.5E-04	1.5E-04	-1.6E-04	-3.1E-06		
t value	-2.58	1.11	1.89	-1.06	1.06	-1.11	-0.02		

Note: Av. Eff. is *average effect of a factor*

According to statistical tables, for normal error distribution, 15 degrees of freedom, and a two-tailed significance level of 0.05, the critical t value is 2.13 (Weinberg and Schumaker, 1969).

Conclusions of the ruggedness test

The result of the ruggedness study shows that among the seven factors only Factor A, i.e. specimen testing area, had relative significant effect on test results. This conclusion implies that when one conducts the air permeance test, exposed area of specimens should be carefully controlled.

Since the remaining factors did not show significant effects on the test results, it is suggested that the present test method is capable to measure stable airflow through WRB

in pressure difference between 0 and 120 Pa and the measured air permeance results are reliable and accurate.

3.2.5 Material property measured with the air permeance test

Following the examination for the precision of the air permeance test method, the eleven WRB products were tested and their results are shown in Table 3.5.

Table 3.5 Air permeance test results on the eleven WRB products

Material code	Air permeance of fresh WRB L/s·m^2·Pa				Standard deviation
	Specimen 1	Specimen 2	Specimen 3	Average	
C1	1.69E-03	1.63E-03	1.67E-03	1.66E-03	2.64E-05
C2	8.08E-04	9.77E-04	8.76E-04	8.87E-04	8.50E-05
C3	5.34E-04	5.97E-04	5.61E-04	5.64E-04	3.16E-05
C4	2.55E-03	2.60E-03	2.70E-03	2.62E-03	7.28E-05
C5	2.18E-03	2.27E-03	2.21E-03	2.22E-03	4.52E-05
P6	1.29E-04	1.20E-04	1.12E-04	1.20E-04	8.50E-06
P7	1.13E-04	1.01E-04	1.09E-04	1.07E-04	6.26E-06
P8	2.55E-05	2.77E-05	2.57E-05	2.63E-05	1.20E-06
PP9	2.90E-02	2.70E-02	2.41E-02	2.67E-02	2.49E-03
PP10	1.20E-02	1.55E-02	1.35E-02	1.37E-02	1.76E-03
PP11	2.81E-02	2.61E-02	2.67E-02	2.70E-02	1.01E-03

From Table 3.5, it could be inferred that standard deviations of the results are one or two orders of magnitude lower than the mean results of three specimens. This fact again indicates that the air permeance test developed in the present study is a reliable method. Therefore, this method will be employed as a tool to relate material performance and pore

structure variation, which may be caused by laboratory aging or weathering.

3.3 Characterization by means of moisture flux test

In stucco-clad wall, WRB are located between stucco layer and wood-based sheathing, typically oriented strand board (OSB) or plywood. When rainwater penetrates through the stucco layer, it may directly have contact with the WRB. The moisture flux test is to simulate this situation. As shown in Figure 3.9, to conduct the test a 30-mm-high plastic ring is cut from a PVC pipe with inside diameter of 100 mm and outside diameter of 105 mm. A 105-mm-diameter WRB specimen is sealed to the underside of the ring by using wax and rosin mixture inside the ring. Thus, the exposed upper area of the specimen is defined by the inner edge of the wax and it measures 72.8 cm^2. Then, an OSB disk having same area as the specimen is dried in an air-circulated oven at 65°C until steady weight is obtained. After the disk cools down to temperature of 23 ± 2°C in a desiccator (moisture isolated chamber), its smoother surface is placed in contact with the specimen underside. The disk and the PVC ring are sealed together by dipping or brushing the wax mixture on their seam as well as the exposed area of the disk. Similar to the water ponding test, a 25 mm water head is kept on the specimen. It gives the specimen a comparable pressure with air pressure differentials caused by wind load under normal service conditions. The weight of the whole set-up after removing all water is measured periodically. The increased weight is considered as the amount of moisture transmitted.

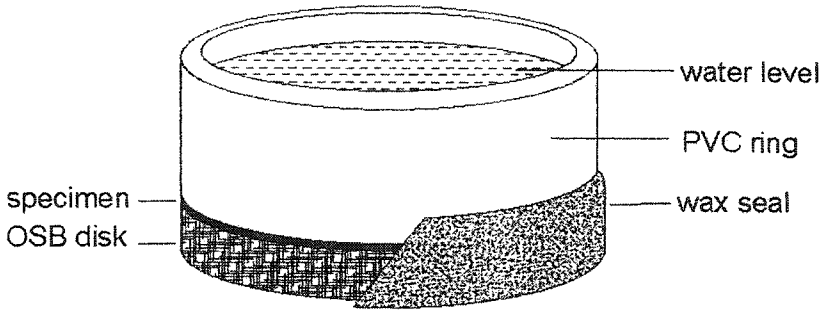

Figure 3.9 Schematic drawing of the moisture flux test

Figure 3.10 shows results of the moisture flux test conducted on fresh C4, C5, P6 and P8 membranes. A 48-hour interval was chosen between two weight measurements and the moisture transmission rate is calculated by dividing the weight increase in the time interval and the specimen testing area.

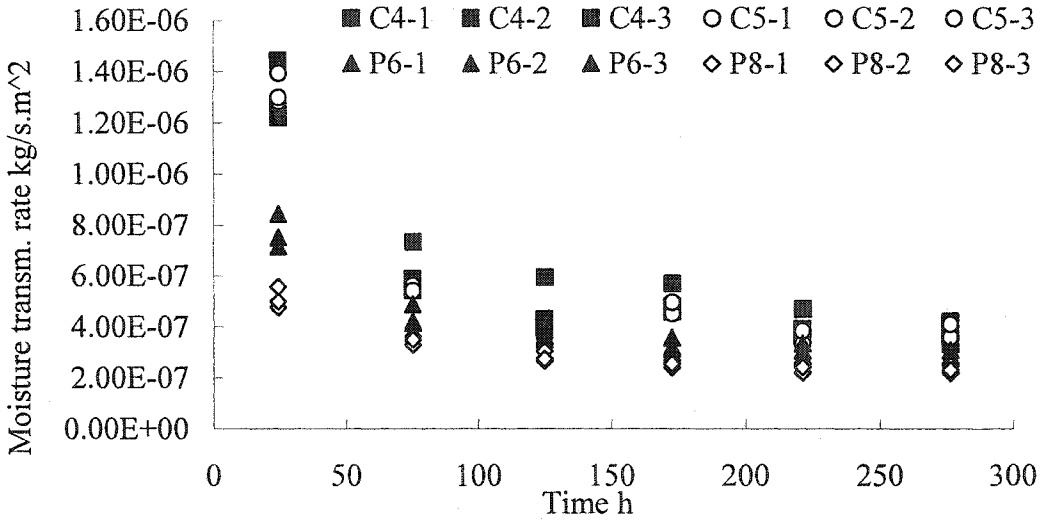

Figure 3.10 Results of the moisture flux test conducted on fresh WRB

In Figure 3.10 results for same material but different specimens are shown by same symbol and they indicate good stability and repeatability of the test method. Yet, the

figure also indicates that all the transmission rates of the different specimens evidently decreased after an initial period and became relatively constant with elapse in time. Perhaps the superposition process of a few effects can explain this variation. In addition to the variation in the transmission properties of the WRB product caused by the change in its moisture content, there may be a change in the moisture content of the OSB substrate. This may change the driving force of the moisture transfer. In the present study, the first 96 hours moisture flow is assumed to be in a transient stage. The measurements following this period are employed to calculate the average moisture transmission rate. Table 3.6 lists the MF test results for C4, C5, P6, and P8 products.

Table 3.6 Results of the moisture flux test conducted on fresh WRB

Material code	Moisture transmission rate $kg/s \cdot m^2$	Standard deviation
C4	4.79E-07	6.68E-08
C5	4.36E-07	5.21E-08
P6	3.55E-07	3.60E-08
P8	2.76E-07	2.39E-08

The moisture flux test conducted in a parallel thesis with various substrate materials, such as OSB, plywood, blotter, and vacuum cast gypsum, showed that results with different substrates were various. This implies that while the method allows obtaining an average moisture transmission rate within a specific interval, evidently, this rate is influenced by the substrate condition. It was also found that the measured moisture transmission through type C and type P membranes are dominated by water vapour flow (Pazera,

2003). The application validity of the test method to evaluate the material characteristics for moisture transmission will be again discussed in Chapter 5.

3.4 Characterization by means of modified inverted cup test

Having the experience of the moisture flux test and for the sake of obtaining constant moisture transmission, the moisture flux test was improved to use more stable boundary conditions on both surfaces of specimen by using 25 mm water head on the specimen and frequently regenerated desiccant under it. The method is named modified inverted cup (MIC) test.

The set-up of MIC method is shown in Figure 3.11. To conduct the test, a circular specimen with 105-mm diameter is firstly sealed between a 30-mm-high top ring (cut from a PVC pipe with 100-mm inside diameter and 105 outside diameter) and a 10-mm-high middle ring by brushing mixture of wax and rosin on the seams between the rings and the specimen. Thereby, the exposed specimen area becomes 72.8 cm^2, which is defined by the inner edge of the sealing wax. Further, dry desiccant (anhydrous calcium chloride) is filled in a 30-mm-deep bottom cup, which is made of same material as the rings. Then, the top composite is sealed on the bottom cup by using an adhesive tape to eliminate moisture leakage. A 25 mm water head is kept on the specimen to drive moisture through. With the purpose of keeping constant moisture condition under the specimen the desiccant is periodically replaced by regenerated desiccant. The weight

increase of the set-up excluding the water is the amount of moisture transmission through the specimen. The moisture transmission rate is calculated by dividing the weight increase by the specimen area and the time interval between the weight measurements.

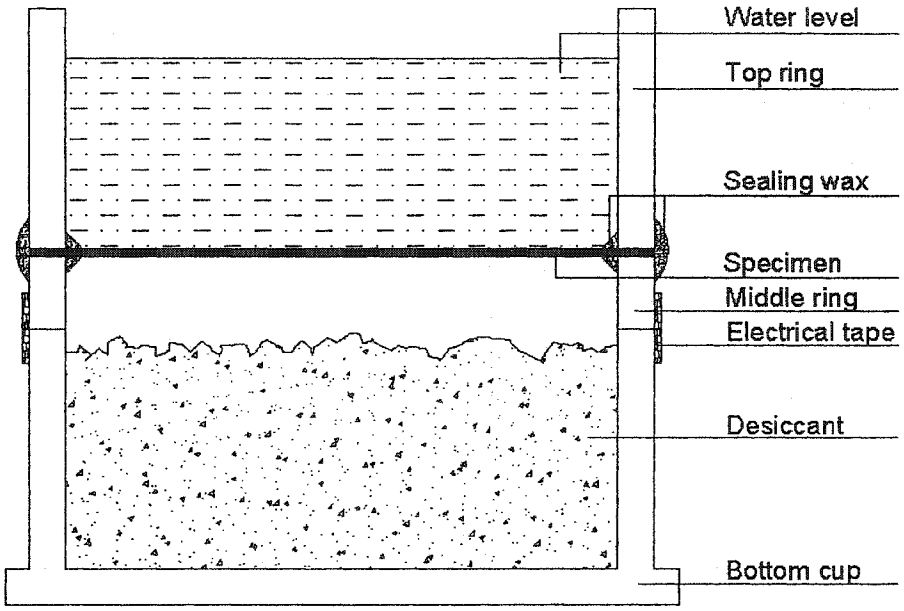

Figure 3.11 Schematic drawing of the modified inverted cup test

To examine the reliability of the test, three specimens of each WRB product were tested and their results are shown in Figure 3.12 with same symbol.

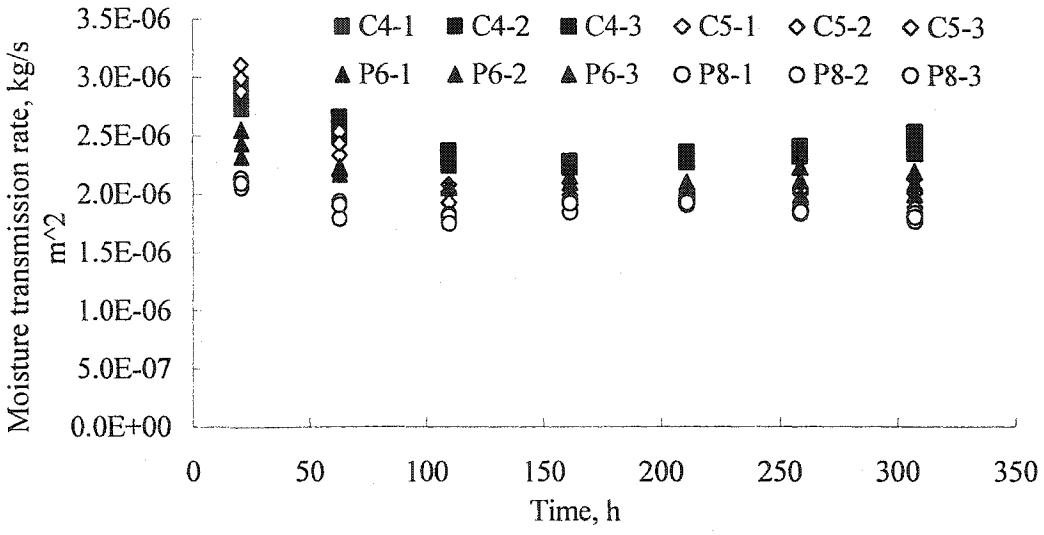

Figure 3.12 Results of the MIC test conducted on fresh WRB

From Figure 3.12, it could be inferred that while all specimens had higher moisture transmission rate at their first measurement (average transmission rate during the first 48 hours), the rates all became relatively constant from the second measurement. The variation may result from the transient variation of the material moisture content. Therefore, the first measurement of every specimen is not used to calculate average rate of moisture transmission in this thesis. Table 3.7 lists MIC test results of C4, C5, P6, and P8 products. These results will be used as moisture transmission characteristic of the fresh products to compare with results of various treated materials in order to evaluate effects of the treatments on the moisture flow performance of the materials.

Table 3.7 Results of the MIC test conducted on fresh WRB

	Moisture transmission rate $kg/s \cdot m^2$	Standard deviation
C4	2.94E-06	1.16E-07
C5	3.22E-06	1.99E-07
P6	4.53E-06	4.99E-08
P8	3.38E-06	5.56E-08

While operating the MIC test on type C and type P materials, observation on the specimens showed that there was not visible liquid water on the lower surfaces of the specimens (desiccant side). Another study conducted in the parallel thesis (Pazera, 2003) showed that when various water levels (25, 50, 75, 150, 200, 250 mm) were utilized to perform the MIC test on type C and type P materials, the rates of moisture transmission with high water level were slightly higher than those with low water level and no proportional increase could be identified. These two phenomena may be explained by fact that the measured moisture transmission through the type C and type P membranes was dominated by water vapour.

3.5 Characterization by means of water absorption test

Since there was not test techniques available to measure liquid phase moisture transfer through WRB membranes, an alternative experimental method, water absorption test, was adopted.

3.5.1 Test theory

When a homogenous material, which allows liquid moisture diffusion through its boundary surface, is contacted with liquid water, it would change its weight with time. It is suggested that the increase in weight of the test specimen is a linear function of the square root of the time before the specimen comes close to the saturation limit. (Kumaran, 1999) The slope of this linear variation is called the water absorption coefficient (A_w). Water absorption process can be mathematically written as:

$$m_w = A_w \sqrt{T} \tag{3.7}$$

where,

m_w = mass of absorbed water, (kg/m^2),

A_w = water absorption coefficient, (kg/m^2 s$^{0.5}$),

T = duration of contact, (s).

It has been suggested that water absorption coefficient together with capillary saturation moisture content can be used to calculate an average liquid diffusivity (Krus and Künzel, 1993; de Wit and van Schindel, 1993) by using Equation 3.8.

$$D_w = \frac{\pi}{4}\left(\frac{A_w}{W_c}\right)^2 \tag{3.8}$$

where,

D_w =material specific liquid diffusion coefficient, (m^2/s) and

W_c =the saturated volumetric moisture content of the material, (kg/m^3).

The usefulness of this simplified method has already been confirmed through a series of laboratory measurements using the gamma-ray attenuation technique (Kumaran, 1999).

According to Equation 3.8, the water absorption coefficient can represent the rate of liquid water transmission through the material. Therefore, a modified water absorption test was designed to test WRB membranes. The method entails wrapping up a hygroscopic substrate (drywall) with a WRB specimen and allowing one-dimensional water uptake to the composite. Although the interface between the WRB and the substrate would unavoidably affect the liquid diffusion through the WRB specimen to the substrate, the method was expected to show the WRB resistance to water transmission.

3.5.2 Experimental set-up of water absorption test on WRB

Figure 3.13 shows a schematic diagram of the water absorption test. WRB membrane being tested is cut to square size of 120 mm by 120 mm. A standard drywall board (brand Sheetrock) with thickness of 0.5 inch is cut to square size measuring 90 mm by 90 mm. The specimen and the drywall sample are dried in air-circulated oven ($60\pm5°C$) until their weight become constant. To guarantee one-dimensional water transport through the drywall sample, its four side surfaces are sealed by brushing mixture of wax and rosin on. The bottom and the side surfaces of the drywall samples are wrapped by the WRB

specimen with the help of two rubber bands. The extra margins of the membranes are folded up and the fold seams are sealed with the wax mixture. All the preparation should be done in a short time. Following that, the samples are conditioned in a desiccator for 24 hours. To conduct the test the composite of the drywall and the specimen is submerged in a water tank with a water depth of 1 ± 0.5 mm. The weight of the composite is periodically measured.

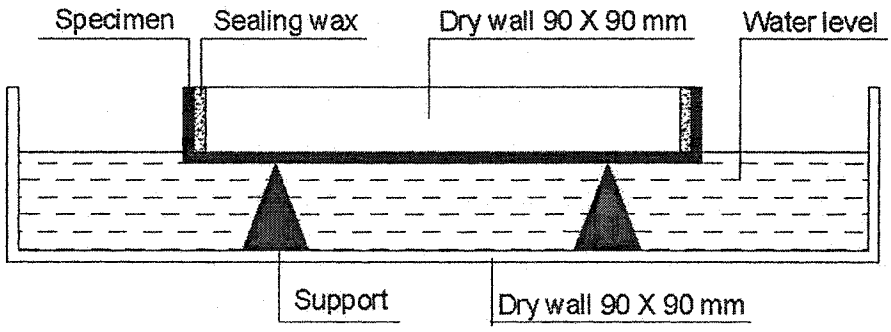

Figure 3.13 Schematic diagram of the water absorption test for WRB

3.5.3 Validation of the water absorption test

Figure 3.14 shows the measurements from the water absorption test conducted on three C4 specimens, three P6 specimens and three drywall samples. The composite weight increase per square meter and the corresponding square root of time are plotted on the figure.

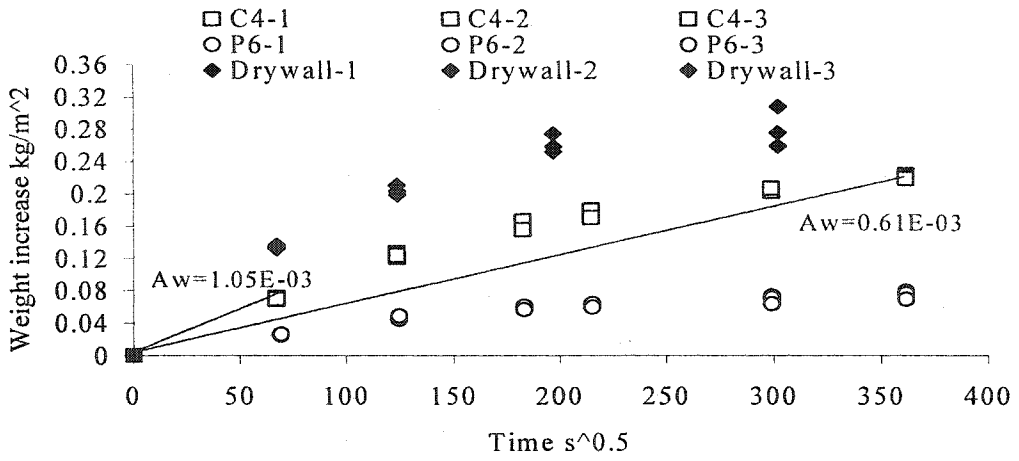

Figure 3.14 Measurements of the water absorption test conducted on fresh WRB and drywall alone

The figure indicates that the results for replicas of same product are stable and repeatable. Yet, it could be inferred that the shape of the curves obtained from type C and type P is not linear and the average absorption coefficient of the C4 WRB with their substrates changes from A_w=1.05E-03 kg/m^2·s$^{0.5}$ at the first point to A_w=0.61E-03 kg/m^2·s$^{0.5}$ at the sixth measurement. From theoretical analysis one may infer that the water absorption coefficient of a composite may vary. At the initial stage of water absorption, the coefficient is governed by the properties of the material surface. When water penetrates deeper into the composite the properties of the substrate will play more important role and after a sufficiently long period the water absorption coefficient of this composite will depend mainly on that of the substrate. In addition, the interface between the membrane and the substrate also affect the moisture transmission. Therefore, to understand the retardation of water flow provided by the WRB, a comparison of different materials at the initial stage of the absorption process is more meaningful. As a result, the first hour

measurement is employed to calculate the absorption coefficient in this thesis.

3.5.4 Characterization results with the water absorption test

Table 3.8 lists the test results obtained from the water absorption test on C4, C5, P6, and P8 membranes with drywall substrates.

Table 3.8 Results of the water absorption conducted on fresh WRB with drywall substrates

	Aw, Absorption coefficient $kg/m^2 \cdot s^{0.5}$	Standard deviation
C4	1.05E-03	1.57E-05
C5	1.39E-03	8.19E-05
P6	3.81E-04	7.20E-06
P8	2.58E-04	2.62E-05

Note the drywall substrate has Aw =2.01E-03 $kg/m^2 \cdot s^{0.5}$

3.6 Discussion and result analysis

To evaluate overall performance of WRB membranes, the present study is firstly targeted to find effective test methods. It was found that four test methods, i.e. air permeance test, moisture flux test, modified inverted cup test, and water absorption test, can characterize different aspects of WRB performance.

Air permeance test equipment was developed to evaluate WRB resistance to airflow. The ruggedness study indicated that among the seven experimental factors, which were examined in the present study, only Factor A "effective testing area" had statistically significant effects on test results. Therefore, when one uses the air permeance method,

careful control of specimen testing area is important to obtain accurate results. Meanwhile, the ruggedness study and result analysis (see Figure 3.7, Table 3.2, and Table 3.5) indicated that test results from the method are reliable.

Having a contact with water on top surface with a 25 mm water head and a wood substrate on bottom surface, moisture flux test is designed to simulate a WRB field situation. It had been proved that the measured moisture flow through type C and type P materials is dominated by water vapour. The test results in Figure 3.10 indicate that the measured moisture transmission rates were repeatable for same products. However, one may find that all the material had a faster transmission rate at initial times, and the value gradually fell down about 30% to 50% of the first measurements after two weeks. Changes of material boundary moisture conditions during the test period may be the main reason.

To avoid the effect of the changing boundary conditions on the moisture transmission through the WRB membranes, MIC method, which can measure constant vapor dominated moisture flow, was adopted in the present study. Frequently changed desiccant and 25 mm water head provide a constant moisture gradient across specimen. This gradient could drive moisture to constantly flow through specimens. Measured results indicated results from MIC test are stable and repeatable (see Figure 3.12).

Relation between water absorption coefficient and liquid diffusivity allows one to use the

water absorption method to compare rate of water flow through materials. A particular water absorption test, which entails warping a drywall in WRB membrane and contacting the composite with 1 mm deep water, was developed for testing WRB materials. Theoretical analysis and experimental results (see Figure 3.14) indicated that the first hour water absorption coefficient of WRB and drywall composite is repeatable and can be used to characterize water transmission through WRB.

To conduct further evaluation two asphalt impregnated cellulose fibre products, (C4 and C5) as well as two polymeric fibrous membranes (P6 and P8) were selected. The properties measured on fresh products were employed to analyze probable material property variations caused by laboratory weathering or aging, which are entailed in following chapters.

CHAPTER 4 EFFECTS OF MECHANICAL FORCES AND OUTDOOR WEATHERING ON WRB

Prior to installing claddings, WRB are exposed to outdoor environment and are subjected to numerous environmental stress factors, caused by sun radiation, freezing temperature, rain, snow, or wind. These might impact WRB or their additives used. The exposure can last several days or even a few months in case of winter construction. This chapter is focused on examining the influence of outdoor weathering and mechanical forces, which may be caused by wind or other stretching actions, on the performance of WRB.

4.1 Effects of mechanical forces on WRB

Canadian Construction Materials Center (CCMC, 1996) has specified a requirement for tensile strength on WRB in its Technical Guide 07102, which indicates that the WRB tensile strength measured on by employing ASTM D 882 method has to be more than 3.5 N/mm. This requirement is also utilized as a criterion of quality control to evaluate material resistance to weathering and aging. Although all WRB products in the market have passed this requirement, the level, to which mechanical forces impact material performance, is still not fully understood. Therefore, a laboratory method for applying mechanical forces on WRB specimens was used and the procedure is described as following.

4.1.1 Application of mechanical forces on WRB

As shown in Figure 4.1, a WRB membrane is cut into a rectangular sample measuring 20 cm by 100 cm. One of the 20 cm margins is folded and clamped between an edge of a table and a 20-cm-length wood strip by using four clamping devices. Further, two metal bars are clamped to the other 20 cm margin of the specimen. In this way, the membrane is vertically hung under the table. All the clamping devices are equally located along the material margins to keep even strain on the sample along horizontal direction. The total pull created by the suspenders (including the clamping devices and the metal bars) is 200 N. For each sample the stretching process was maintained for 120 hours.

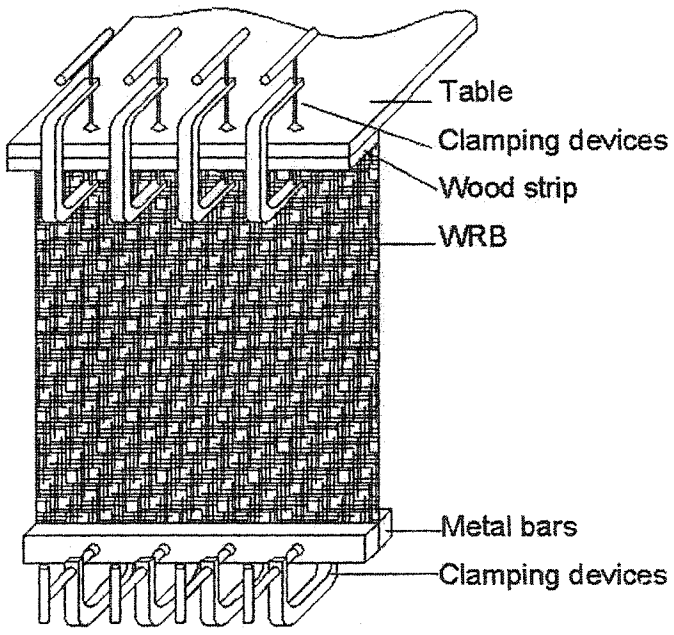

Figure 4.1 Application of mechanical forces on WRB

4.1.2 Evaluation of the effects of the mechanical forces

Following the application of mechanical forces, the samples were cut into suitable sizes and examined with MIC, water absorption, and air permeance tests. Table 4.1 lists the results, which were obtained from MIC test conducted on type C and P products subjected to the stretching process.

Table 4.1 Results of the MIC test conducted on the fresh and the stretched WRB

	Fresh WRB		Stretched WRB	
	Moisture transmission rate $kg/s \cdot m^2$	Standard deviation	Moisture transmission rate $kg/s \cdot m^2$	Standard deviation
C4	2.94E-06	1.16E-07	2.80E-06	1.04E-07
C5	3.22E-06	1.99E-07	2.67E-06	1.88E-07
P6	4.53E-06	4.99E-08	4.51E-06	9.14E-08
P8	3.38E-06	5.56E-08	3.22E-06	6.67E-08

Tables 4.1 shows that change of the moisture transmission rate measured by MIC test is slight. Similar to it, the results from water absorption test performed on the stretched WRB did not show evident difference from fresh WRB (see Table 4.2).

Table 4.2 Results of the water absorption test on the fresh and the stretched WRB

	Fresh WRB		Stretched WRB	
	Absorption coefficient $kg/m^2 \cdot s^{0.5}$	Standard deviation	Absorption coefficient $kg/m^2 \cdot s^{0.5}$	Standard deviation
C4	1.05E-03	1.57E-05	1.01E-03	3.59E-05
C5	1.39E-03	8.19E-05	1.32E-03	5.02E-05
P6	3.81E-04	7.20E-06	3.65E-04	2.64E-05
P8	2.58E-04	2.62E-05	2.80E-04	8.04E-05

To examine whether the mechanical forces changed the porosity of the membranes, air permeance test was also utilized and the results are listed in Table 4.3.

Table 4.3 Results of the air permeance test conducted on the fresh and the stretched WRB

	Fresh WRB		Stretched WRB	
	Air permeance $L/s \cdot m^2 \cdot Pa$	Standard deviation	Air permeance $L/s \cdot m^2 \cdot Pa$	Standard deviation
C4	2.62E-03	7.28E-05	1.54E-03	1.51E-05
C5	2.22E-03	4.52E-05	1.69E-03	3.32E-05
P6	1.20E-04	8.50E-06	1.14E-04	2.51E-06
P8	2.63E-05	1.20E-06	2.01E-05	1.62E-06

It is found that the air permeance of the stretched membranes was slightly lower than that of the fresh WRB, however the variation was not significant. In addition to the results from the MIC and the water absorption tests, one may suggest that applying the mechanical forces on the membranes did not evidently influence the membranes' performance.

4.2 Effects of outdoor weathering on WRB

Outdoor weathering, discussed in this thesis, is defined as physical and chemical property changes of materials due to exposing the materials to various climatic conditions and lasting some time. Before applying cladding, WRB may be subject to ultraviolet radiation, temperature, moisture (rain, snow, and humidity), wind, ozone, carbon dioxide, atmospheric pollutants, and effects of freeze and thaw. To determine the influences of weathering on WRB performance, WRB industry has adopted different weathering methods from interrelated paper and plastics industries. Generally, these methods involve either cyclic ultraviolet exposure for polymer-based products or humidity and temperature oscillations for paper-based products (CAN/CGSB 51.32, 1977). This distinction is determined by the differences of two types of products in physical and chemical properties. The performance of polymer materials depends largely on their molecular structure, where the molecules are arranged in long, chain-like configurations. These chains are broken up into shorter chains when subjected to an ultraviolet radiation. This process is known as photodegradation. For paper-based materials, however, paper fibers are prone to moisture-related swelling and shrinkage. In addition, decomposition of organism could degrade paper-based products when they are in high moisture contents. To investigate the effects of short-term weathering, the present study employed an actual outdoor exposure to both type C and type P products.

4.2.1 Application of outdoor weathering on WRB

As shown in Figure 4.2, WRB sample with size of 60 cm by 90 cm was fastened to a wood grid by clamping material four edges between plywood strips. Four grids with different membranes were nailed on a large wood frame, which can stand in a vertical position with its bracket support. This frame was put on the roof of the Department of Building, Civil, and Environmental Engineering at Concordia University and oriented in southwest direction. In this way, both the surfaces of WRB were subjected to effects of various climatic factors, e.g. wind, rain, snow, sunlight and ultraviolet radiation. The weathering was started on November 27th 2001 and lasted 120 days. After the exposure the samples were removed and stored in laboratory condition at a temperature of 23 ± 2°C, and a relative humidity of 50 ± 5 RH.

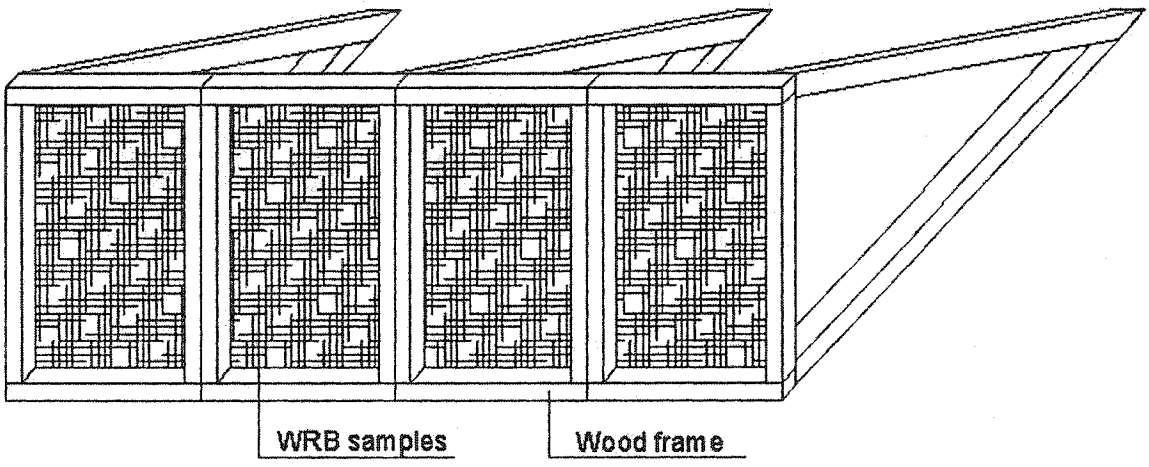

Figure 4.2 Application of the outdoor weathering

Scanning Electron Microscope (SEM) technique was utilized to observe the effect of the

outdoor weathering on material microscopic structure. Figures 4.3 (C4) and 4.4 (P6) show the images of fresh and weathered membranes.

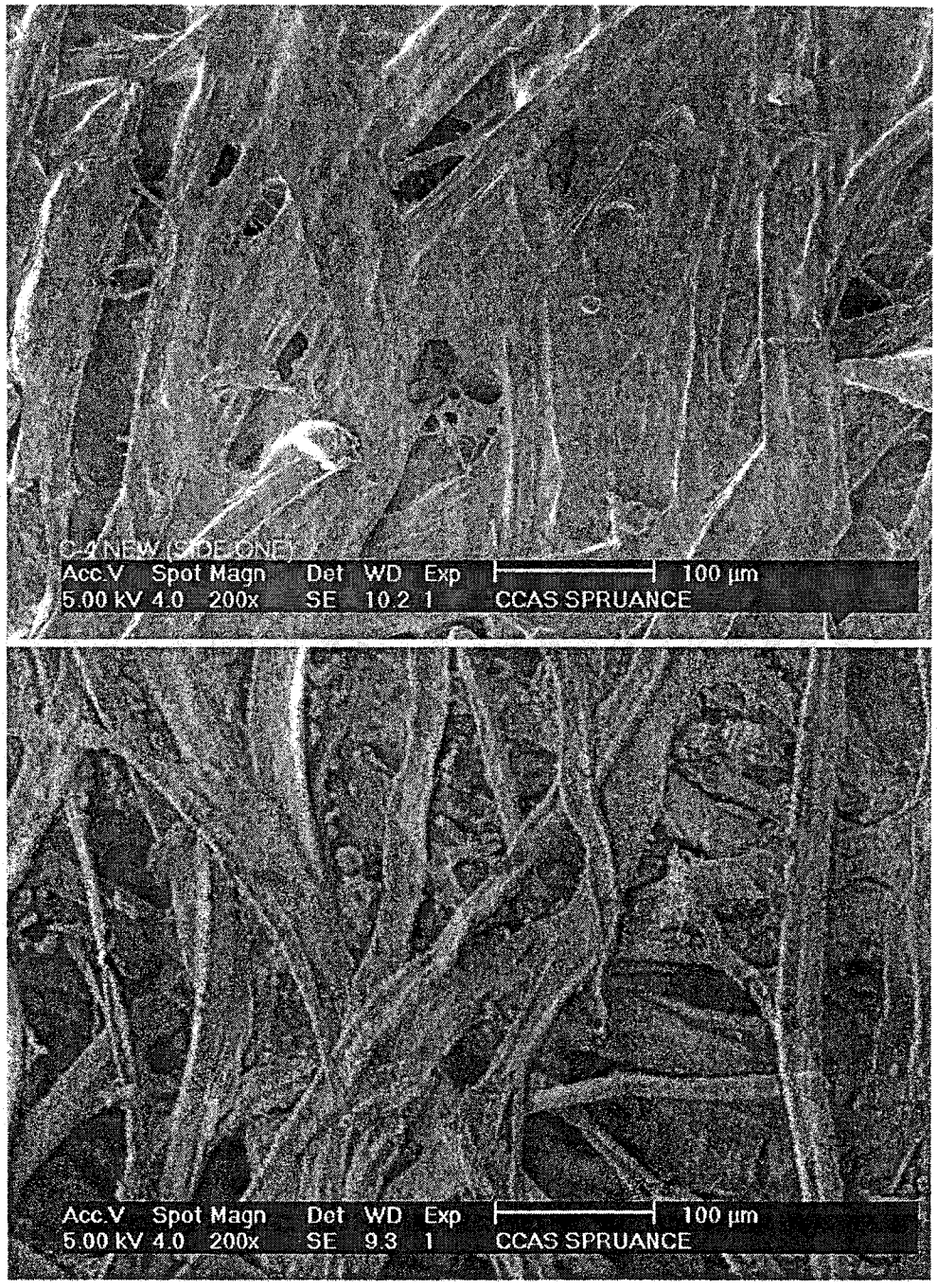

Figure 4.3 200-time magnified images of the fresh (top) and the outdoor weathered (bottom) C4 membranes viewed with a SEM

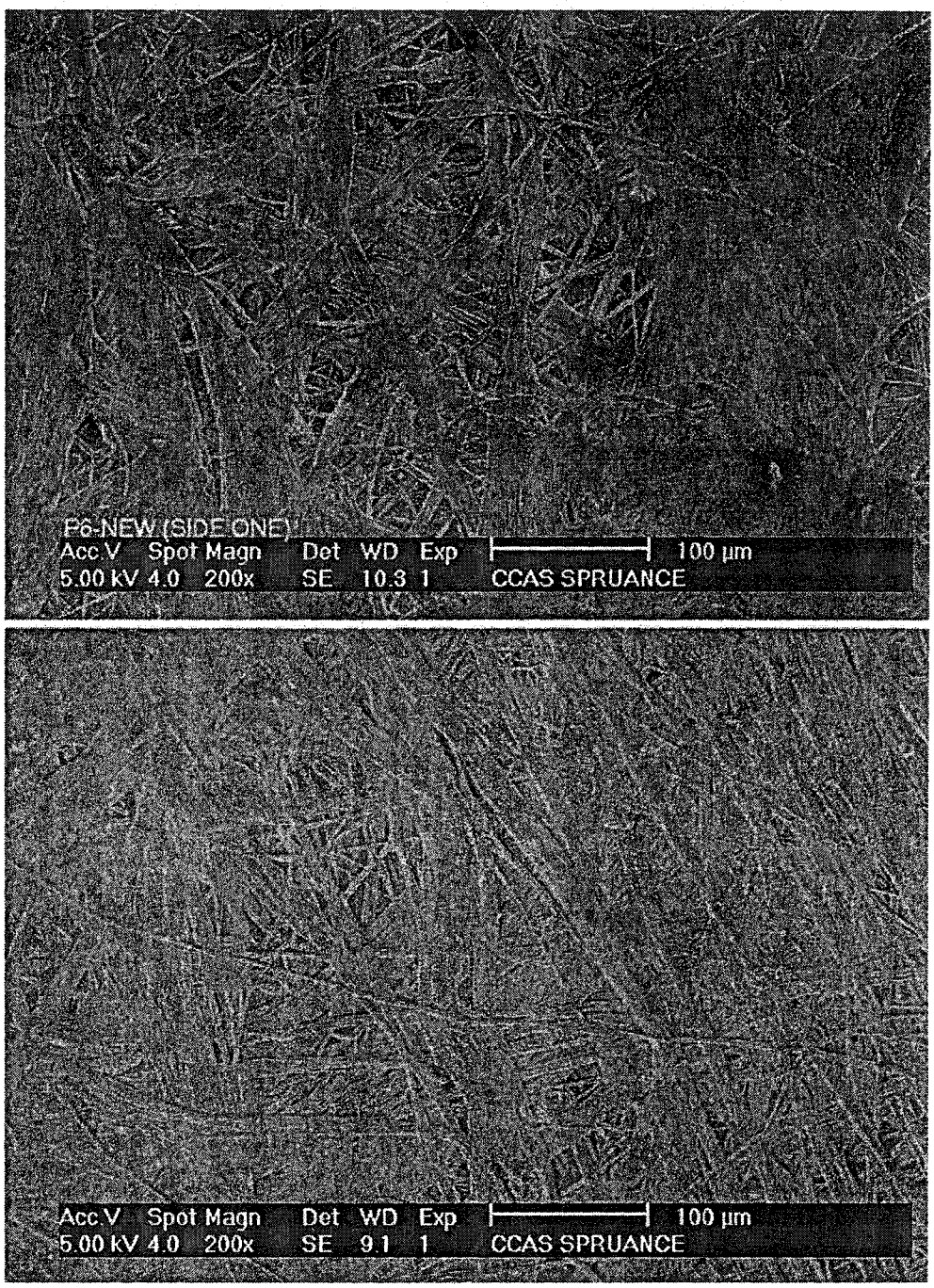

Figure 4.4 200-time magnified images of the fresh (top) and the outdoor weathered (bottom) P6 membranes viewed with a SEM

4.2.2 Evaluation of the effects of the outdoor weathering

To evaluate the influences of the weathering on the performance of WRB, three test

methods, namely MIC test, water absorption test, and air permeance test were applied to the weathered membranes. Table 4.4 lists the results from the MIC test conducted on the four fresh and the weathered WRB products.

Table 4.4 Results of the MIC test conducted on the fresh and the outdoor weathered WRB

	Fresh WRB		Outdoor weathered WRB	
	Moisture transmission rate kg/s·m^2	Standard deviation	Moisture transmission rate kg/s·m2	Standard deviation
C4	2.94E-06	1.16E-07	2.02E-06	1.51E-07
C5	3.22E-06	1.99E-07	2.66E-06	3.34E-07
P6	4.53E-06	4.99E-08	5.26E-06	2.04E-07
P8	3.38E-06	5.56E-08	4.65E-06	4.62E-07

Following the weathering, the measured moisture transmission rates of type C products had 17% to 31% reduction, yet, those of type P products experienced an increase between 16% to 38%.

The water absorption test was also conducted to determine the effects of the weathering. Table 4.5 lists the measured water absorption coefficient of the WRB prior to and following the weathering.

Table 4.5 Results of the water absorption test conducted on the fresh and the outdoor weathered WRB

	Fresh WRB		Outdoor weathered WRB	
	Absorption coefficient $kg/m^2 \cdot s^{0.5}$	Standard deviation	Absorption coefficient $kg/m^2 \cdot s^{0.5}$	Standard deviation
C4	1.05E-03	1.57E-05	7.06E-04	5.07E-05
C5	1.39E-03	8.19E-05	1.16E-03	8.44E-05
P6	3.81E-04	7.20E-06	4.31E-04	2.02E-05
P8	2.58E-04	2.62E-05	3.42E-04	1.92E-05

The absorption coefficient results are similar to those obtained with the MIC method. The weathered type C membranes showed a decrease of value from 33% to 17% and the weathered P6 and P8 experienced an increase from 13% to 33% in the liquid flow rate.

Air permeance test results (see Table 4.6) showed that the weathering introduced 29% decrease for C4 material, and, 6%, 21%, and 30% increase for C5, P6 and P8 products, respectively.

Table 4.6 Results of the air permeance test conducted on the fresh and the outdoor weathered WRB

	Fresh WRB		Outdoor weathered WRB	
	Air permeance $L/s \cdot m^2 \cdot Pa$	Standard deviation	Air permeance $L/s \cdot m^2 \cdot Pa$	Standard deviation
C4	2.62E-03	7.28E-05	1.87E-03	7.15E-04
C5	2.22E-03	4.52E-05	2.35E-03	2.12E-04
P6	1.20E-04	8.50E-06	1.45E-04	2.07E-05
P8	2.63E-05	1.20E-06	3.42E-05	5.88E-06

4.3 Analysis of results and discussion

As shown in Tables 4.1, 4.2 and 4.3, the results did not show that the laboratory

stretching produced a significant impact on the membranes.

With the exception of air permeance result of weathered C5 membrane (see Table 4.6), which had 6% increase in air flow rate, all measured values (see Table 4.4, 4.5, and 4.6) of the vapour, water, and air transfer rates, decreased for the type C materials. However, those values increased for type P material. It could be inferred that the outdoor weathering had contrary effect on the performance of type C and type P products, while they are not significant. These different effects may be due to the difference of the material compositions.

CHAPTER 5 EFFECTS OF WOOD EXTRACTS ON WRB PERFORMANCE

In stucco-clad walls WRB are in contact with wood-based sheathings on one side and stucco on the other side. High moisture content in the assembly may cause some soluble chemicals, such as wood extracts or surfactants, to be dissolved and leached out from OSB or plywood sheathings. These chemicals, in turn, may affect the performance of WRB. One needs to examine what effects these chemicals can impose on WRB properties.

Generally, soluble chemicals could affect WRB performance in two ways. When the soluble substances are dissolved into rainwater, they can change water properties and cause the water to have differences in hydromechanical characteristics from ordinary water. On the other hand, soluble chemicals may be deposited on WRB surfaces when repeated wetting and drying take place on WRB materials. Both of the possibilities will be investigated in this chapter.

5.1 Preparation of water solutions for testing

5.1.1 Preparation of surfactant solutions

As surfactant solution was only used for comparative purposes, an ordinary liquid soap

(brand Tide) was selected for the present testing program. The concentration of the solution is presented in an arbitrary scale using the percentage of the soap in the water solution.

5.1.2 Preparation of wood extracts

To investigate the effects of wood extracts on physical properties of water, which has dissolved wood extracts from wood-based sheathings, initially, the present study employed the wood extracts prepared at Louisiana Pacific Laboratory (LPL). The procedure utilized in preparation of the wood extracts is described in detail in Appendix A. The principle procedure includes pulverizing OSB and then leaching (digesting) out soluble chemicals at a controlled temperature. The procedure was carried out at two temperatures: room temperature (by using an ambient-temperature liquid bath, called ambient bath) and an elevated temperature (by using a controlled-temperature liquid bath, called warm bath). Since two groups of OSB powders, which were cut from different regions of same OSB board, were separately digested in the two bathes, total four batches of wood extract solutions (named as extracts from ambient bath 1, extracts from ambient bathes 2, extracts from warm bath 1, and extracts from warm bath 2) were obtained.

As discussed later in the text, differences between the two preparation methods and between the locations, at which the OSB powders were taken, were not significant on the solutions properties (surface tension and kinematic viscosity), therefore another batch of

extract solution was made at Concordia University (CU). The preparation procedure is described in Appendix B in detail.

5.2 Physical characterization of the solutions

Since the two assumed effects of leached wood extracts on WRB are related to their hydrodynamic features and composition, properties of the extract solution such as surface tension, kinematic viscosity and total solid fraction, were examined.

5.2.1 Measurement of surface tension

The present study employed a Du Nouy Ring technique to measure surface tension of various solutions. The use of the instrument, i.e. Fisher Tensiomat model no. 21, is specified by ASTM D 971 and ASTM D 1331. The measurement technique and its validation are in detail described in Appendix C.

5.2.1.1 Surface tension of the soap solution

Figure 5.1 shows results of surface tension measurements performed on the soap solution with concentration ranging from 0.02% to 10%.

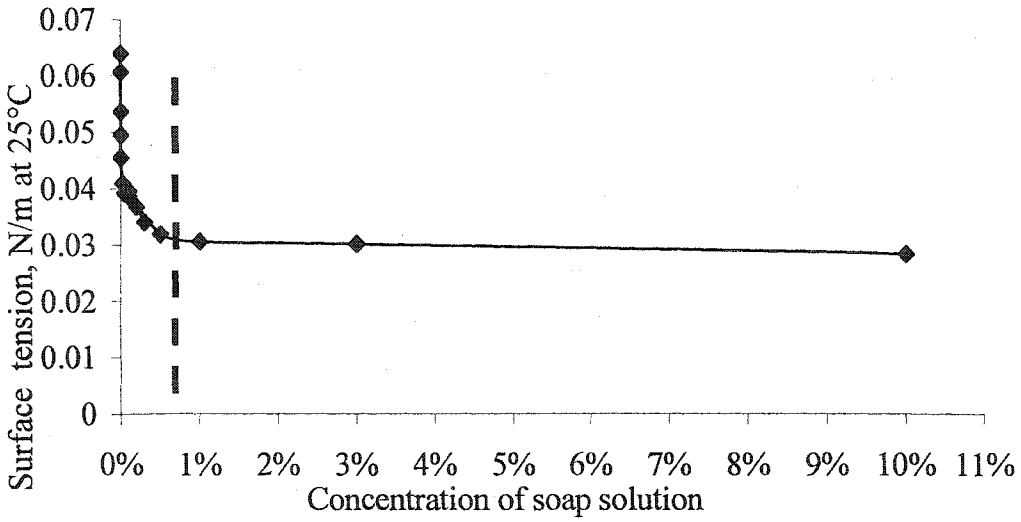

Figure 5.1 Surface tension measurements performed on the soap solution

The measurement results shown in Figure 5.1 highlight that more than 50% of reduction in the solution surface tension occurred at low concentrations, approximately 0.5%. Increasing the concentration above 1% did not affect the results much. Therefore, a threshold point can be established at about 1% of concentration. Before this point the solution surface tension decreased steeply with increasing concentration and a reduction of about 50% was achieved.

5.2.1.2 Surface tension of the wood extract solution

Surface tension measurements performed on a few diluted extract solutions made at LPL from the ambient bath 1 extracts are shown in Figure 5.2.

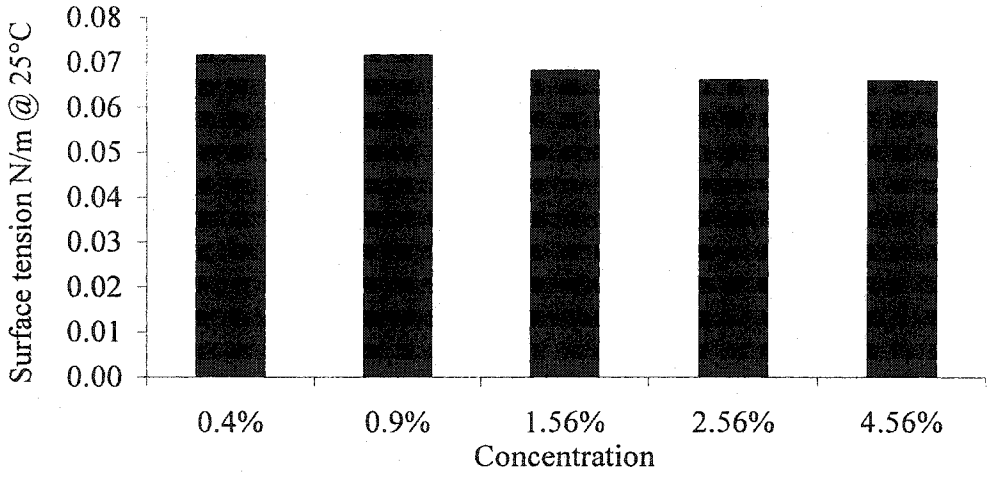

Figure 5.2 Surface tension measurements performed on the extract solution from ambient bath 1 (low range of concentration)

Figure 5.2 indicates that within a range of zero to 5 percent concentration of the extracts did not show significant effects on surface tension value of water. As a result, the study was continued for higher concentration (see Figure 5.3).

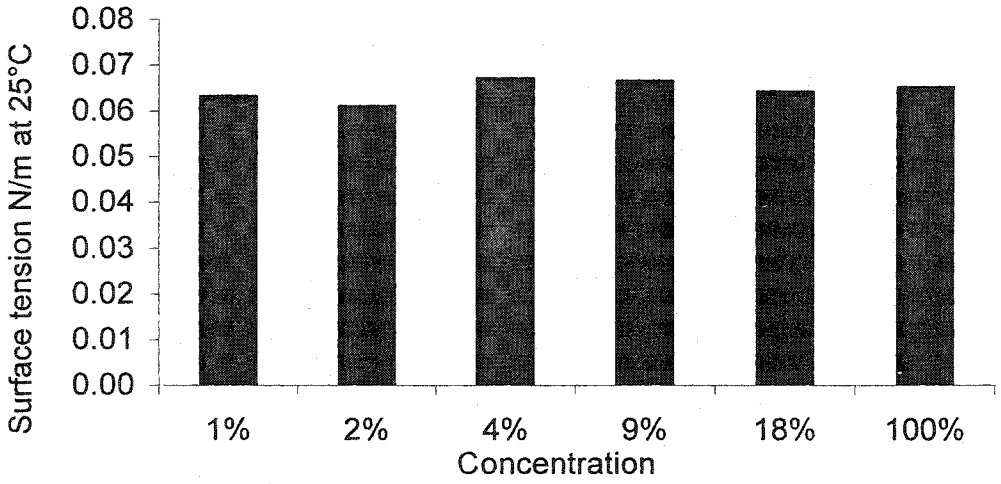

Figure 5.3 Surface tension measurements performed on the extract solution from ambient bath 1 (whole range of concentration)

Differing from the soap solution, surface tension of the extract solution did not show a changing trend when its concentration increased. All the values were slightly lower than that of water. For example, the surface tension of undiluted extract solution from ambient bath 1 was 0.065 N/m and that of water was 0.072 N/m. Measurement results on the extract solutions from ambient bath 2, warm bath 1 and warm bath 2 are shown in Figure 5.4 and Figure 5.5.

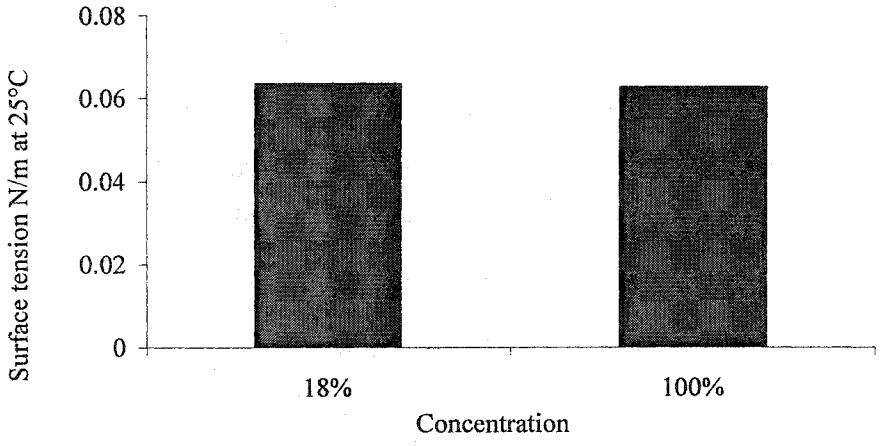

Figure 5.4 Surface tension measurements performed on the extract solution from ambient bath 2

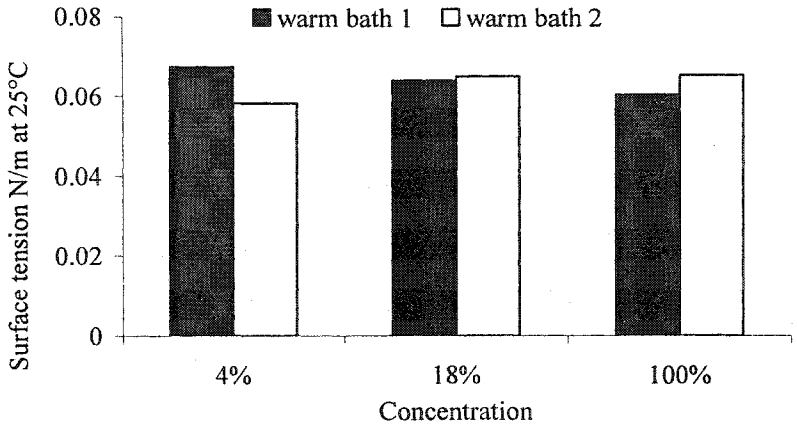

Figure 5.5 Surface tension measurements performed on the extract solution from warm bath 1 and warm bath 2

The results also show that all the extract solutions, which differ in concentration preparation method, or source, had similar surface tension to each other. Therefore, three interim conclusions can be drawn from the measurements:

- Wood extracts slightly reduced surface tension of water when they were dissolved in the water.
- The source of the wood extracts was not found to introduce differences in surface tension of the wood extract solution.
- The difference in preparation processes to make wood extracts, i.e. ambient bath and warm bath, did not result in obvious change in surface tension of the extract solution.

Hence, in following investigation, the undiluted wood extract solution made at CU was employed. Figure 5.6 shows a few surface tension measurements performed on this solution.

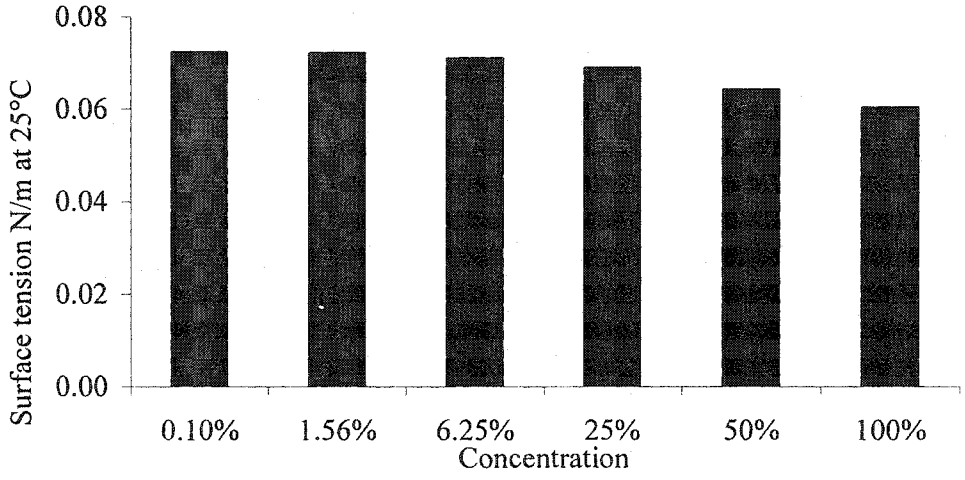

Figure 5.6 Surface tension measurements performed on the extract solution made at CU

Figure 5.6 shows that the trend of surface tension change with increasing concentration of the extract solution made at CU are more uniform than that of the extract solutions prepared at LPL. The average surface tension of the undiluted extract solution made at CU is 0.0601 N/m.

5.2.2 Measurements of kinematic viscosity

Rate of liquid transport in porous materials can be different when surfactants are present in. This is due to the fact that surfactants can result in change of liquid viscosity. The technique to measure kinematic viscosity of liquid is described in Appendix D. Table 5.1 lists kinematic viscosity measurement results of various solutions.

T able 5.1 Kinematic viscosity measurements conducted on different solutions

No.	Solutions	Kinematic viscosity mm^2/s at 40°C
1	Distilled water	0.6834
2	Tap water	0.6721
3	50% extract solution from warm bath made at LPL	0.6888
4	50% extract solution from ambient bath made at LPL	0.6936
5	100% extract solution from warm bath made at LPL	0.6988
6	100% extract solution from ambient bath made at LPL	0.6977
7	100% extract solution made at CU	0.7720

The different batches of extracts prepared at LPL did not significantly change the kinematic viscosity of water. The test result of the extract solution prepared at CU is slightly higher than those from LPL. It is assumed that the result difference between LPL

extracts and CU extracts is related to the storage duration of the extracts as the time, at which the measurements were taken, was a few months later than the preparation of the LPL extract. To avoid this influence, the undiluted extract solution made at CU was used right after it was prepared in the present study.

5.2.3 Measurement of total solids fraction

The capability of WRB to resist water flow may be altered not only by changes in fluid properties but also by the presence of extracts on WRB surface. Extract deposition on WRB surface may cause the hydrophobic feature of WRB to change. Therefore, it is useful to know how much deposit can be left after extract solution is evaporated. For this purpose, a total solid fraction test was conducted.

Total fraction of solids is the term applied to the material residue left in a vessel after evaporation of a solution in an oven at an elevated temperature. Method of measuring total fraction of solids is described in Appendix E. The test entails evaporating a certain amount of well-mixed extract solution in a weighed dish and drying to constant weight in an oven at 105 °C. The increase in the weight over that of the empty dish represents the total solids. Test result shows that the total solid fraction of the extract solution is about 0.5g/l.

5.3 Effects of the wood extract solution on moisture transmission through WRB

To evaluate the effects of wood extracts on moisture transmission through WRB, moisture flux test and modified inverted cup test were employed.

5.3.1 Evaluation of the effects of the wood extracts by means of moisture flux test

To examine the effects of wood extracts, distilled water and the extract solution were respectively used to conduct moisture flux test on fresh C4, C5, P6 and P8 WRB products. The test results are shown in Table 5.2.

Table 5.2 Results of the MF test with distilled water and the extract solution

	Distilled water		Wood extract solution	
	Moisture transmission rate $kg/s \cdot m^2$	Standard deviation	Moisture transmission rate $kg/s \cdot m^2$	Standard deviation
C4	4.79E-07	6.684E-08	5.391E-07	1.043E-07
C5	4.36E-07	5.205E-08	4.808E-07	5.282E-08
P6	3.55E-07	3.599E-08	3.986E-07	4.556E-08
P8	2.76E-07	2.394E-08	3.295E-07	7.887E-08

From Table 5.2, one may find that the transmission rates of wood extract solution through the specimens are slightly higher than those of water. The wood extract solution did not cause significant acceleration on the moisture transport. These results may be explained by fact that moisture transmission measured with MF method is water vapour dominant. The hydrophobic feature of the WRB prevented water breaking through the materials;

even with the changes in water surface tension and kinematic viscosity there is no acceleration of moisture transmission.

5.3.2 Evaluation of the effects of the wood extracts by means of modified inverted cup test

As discussed in Chapter 3, MIC test measures water vapour dominant moisture flow and it provides more stable moisture driving force than moisture flux method. In addition, MIC method provides higher moisture gradient across WRB specimens than MF test because desiccant can create lower relative humidity than OSB disk. Therefore, MIC test was used to evaluate effects of wood extracts as well. Result of tests conducted on fresh WRB specimens with distilled water and wood extract solution are listed in Table 5.3

Table 5.3 Results of the MIC test with distilled water and the extract solution

	Distilled water		Wood extract solution	
	Moisture transmission rate $kg/s \cdot m^2$	Standard deviation	Moisture transmission rate $kg/s \cdot m^2$	Standard deviation
C4	2.94E-06	1.16E-07	3.871E-06	1.95E-07
C5	3.22E-06	1.99E-07	3.288E-06	1.703E-07
P6	4.53E-06	4.99E-08	5.698E-06	7.387E-08
P8	3.38E-06	5.56E-08	4.245E-06	7.25E-08

Similar to the MF test results, all the WRB showed a slight increase in moisture transmission rate when the wood extract solution was used instead of distilled water. The changes for C4, C5, P6 and P8 are 32%, 2%, 26%, and 26%, respectively.

5.4 Effects of wood extract deposition on WRB

Climatic variations can cause repetitive drying and wetting on WRB surface, which may result in deposition of dissolved wood extracts on the WRB surfaces. The deposited particles may either stay on material surface or infiltrate into micro pores of WRB. Laboratory investigation on this phenomenon was conducted by depositing wood extracts on WRB surface and examining the material performance.

5.4.1 Deposition of the wood extracts on WRB

WRB membrane measuring 0.5 m by 0.5 m is spread on a flat table and 100 ml of the extract solution is uniformly spread on the material surface. The solution is allowed to evaporate at 23 $\pm$ 1°C temperature and 50 $\pm$ 2% relative humidity. Such a wetting and drying procedure is called here one cycle deposition. 5 cycles of deposition were applied on four WRB products, C4, C5, P6, and P8.

5.4.2 Evaluation of the effects of the extract deposition by means of modified inverted cup test

To find the effects of extract deposition, the treated WRB were tested using modified inverted cup method. The results are listed in Table 5.4.

Table 5.4 Results of the MIC test conducted on the fresh WRB and the WRB with extract deposition

	Fresh WRB		WRB with wood extracts deposited	
	Moisture transmission rate kg/s·m^2	Standard deviation	Moisture transmission rate kg/s·m^2	Standard deviation
C4	2.94E-06	1.16E-07	2.76E-06	1.17E-07
C5	3.22E-06	1.99E-07	2.74E-06	1.17E-07
P6	4.53E-06	4.99E-08	4.46E-06	2.53E-07
P8	3.38E-06	5.56E-08	3.32E-06	1.07E-07

Comparing with the test results of fresh materials, the results of MIC tests, which were conducted on the treated WRB, showed 6%, 15%, 2%, and 2% reduction in the moisture transmission rate.

5.4.3 Evaluation of the effects of the extract deposition by means of water absorption test

To find effects of the deposition on liquid transmission through WRB, another batch of treated WRB were tested using water absorption method. The results are compared with fresh WRB and shown in Table 5.5.

Table 5.5 Results of the water absorption test conducted on the fresh WRB and the WRB with extract deposition

	Fresh WRB		WRB with extract deposited	
	Absorption coefficient $kg/m^2\ s^{-2}$	Standard deviation	Absorption coefficient $kg/m^2\ s^{-2}$	Standard deviation
C4	1.05E-03	1.57E-05	1.03E-03	1.21E-04
C5	1.39E-03	8.19E-05	1.57E-03	1.71E-05
P6	3.81E-04	7.20E-06	6.78E-04	4.04E-05
P8	2.58E-04	2.62E-05	6.55E-04	9.18E-05

All the materials, except C4, showed an increase in absorption coefficient due to the wood extract deposition. The increase was small for type C products (zero and 12%) and somewhat larger for type P products (78% and 154% respectively).

5.4.4 Evaluation of the effects of the extract deposition by means of air permeance test

WRB air permeance was examined in this study for understanding if the deposition of wood extracts can change the material porosity by chemical interactions and thereby affect airflow through WRB.

Table 5.6 Results of the air permeance test conducted on the fresh WRB and the WRB with extract deposition

	Fresh WRB		WRB with extract deposited	
	Air permeance $L/s \cdot m^2 \cdot Pa$	Standard deviation	Air permeance $L/s \cdot m^2 \cdot Pa$	Standard deviation
C4	2.62E-03	7.28E-05	1.14E-03	3.15E-04
C5	2.22E-03	4.52E-05	1.71E-03	5.73E-05
P6	1.20E-04	8.50E-06	1.21E-04	9.90E-06
P8	2.63E-05	1.20E-06	3.12E-05	6.58E-06

While the treated C4 and C5 showed a 57% (C4) and 23% (C5) of decrease in the air permeance; nevertheless, 1% and 19% increase of air permeance were observed for P6 and P8 respectively, after depositing the wood extracts on WRB surface.

5.5 Analysis of results and discussion

Measurements performed on various wood extract solutions (made at different laboratories) showed that the wood extracts did not significantly change such properties of water, as the surface tension and the kinematic viscosity. (See Figure 5.2, 5.3, 5.4, 5.5 and 5.6 for surface tension and Table 5.1 for kinematic viscosity) The measurement of total solid fraction shows that there is about 0.5 gram of solid substance in one litre extract solution, which was used to evaluate wood extract influence on WRB performance.

It is assumed that wood extracts can impact WRB performance by two ways. When they are dissolved in water, it may accelerate moisture transfer through WRB. On the other

hand, when they are deposited on WRB surface, they may affect the hydrophobic feature of the WRB surface. MIC and MF test results showed that the measured values of water vapour permeance were not significantly affected by the wood extracts in both the ways.

Yet the results, which were obtained with water absorption test conducted on the WRB with extract deposition, showed a somewhat large difference between type C and type P membranes. (See Figure 5.7)

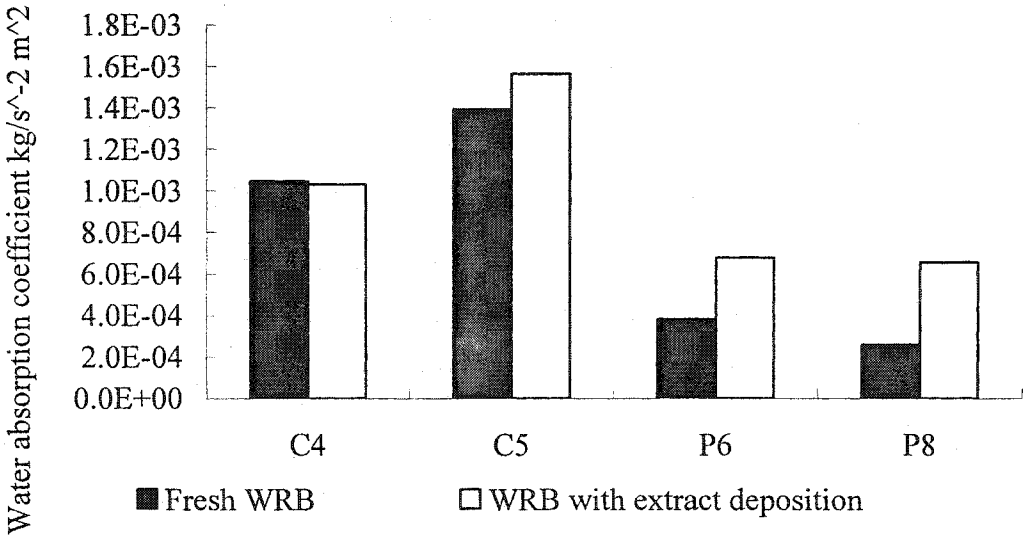

Figure 5.7 Comparison of the water absorption coefficients of the fresh WRB and the WRB with wood extract deposition

According to Figure 5.7, changes in water absorption coefficient (from the first hour measurement) was zero for C4 and 12% for C5, while increase in the flow rate was 78% for P6 and 154% for P8. Furthermore, from Figure 5.8 one may find that while the treated C4 material performed almost same as the fresh material, there was a significant increase of water absorption coefficient for P6 specimens when the test lasted about 4 hours.

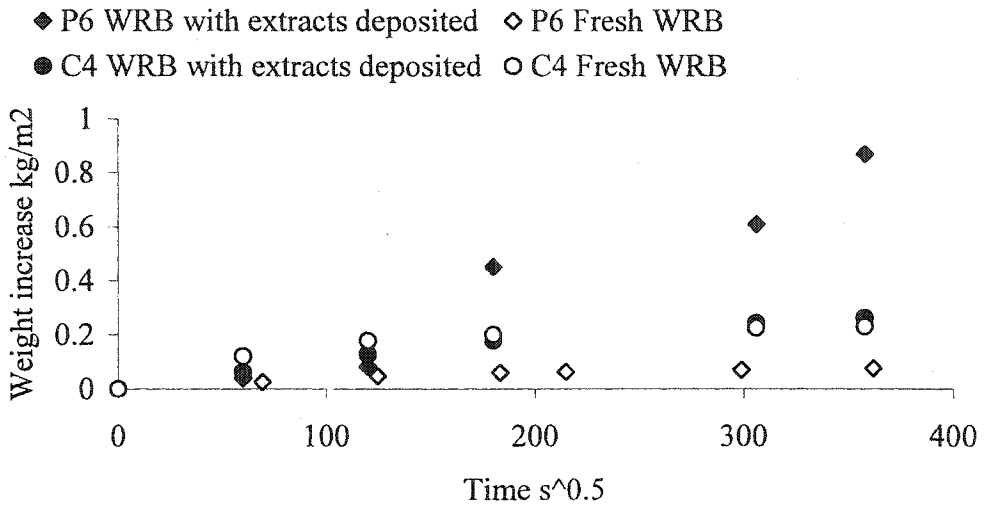

Figure 5.8 Measurements of the water absorption test conducted on C4 and P6

No definitive conclusion could be reached from these results. Yet, there is another difference in the effect of the wood extracts deposits between types C and P: air permeance results showed a small reduction of the porosity available for air flow through type C material and increase for type P. Thus the increase of the liquid and air flow rate through type P products is probably related to the electric or osmotic interaction of the deposits. This issue will be examined further in the next chapter using a different test method.

CHAPTER 6 EFFECTS OF CHEMICALS LEACHED FROM STUCCO ON WRB PERFORMANCE

Rainwater can reach the interface between stucco and WRB. As a continuation of investigating effects of wood extracts from wood-based sheathing on WRB, the study in this chapter is directed to find whether the rainwater could leach chemicals out from stucco and change WRB performance. The first step of this laboratory investigation was to verify a possibility of leaching chemicals from stucco.

6.1 Water leaching out soluble substances from stucco

Two batches of Portland cement plaster (stucco A and stucco B) comprised of cement, lime and sand with a volume ratio at 1: 0.5: 4.5 were prepared. Stucco A was mixed with 1% soap solution and stucco B was mixed with tap water. Every batch of stucco plaster was separately cast into 5 disks with a height of 5mm and a diameter of 100mm, by using PVC molds (rings) (see Figure 6.1). After curing, the stucco disks were bonded to the interior surface of the rings and their seams were sealed by mixture of beeswax and rosin. As a "cup bottom", every disk with its ring was sealed to underside of a same diameter ring with height of 200mm by using the beeswax mixture (see Figure 6.2). All the high "cups" were filled with distilled water, so that the water was slowly leaked out through the stucco bottom by gravity and collected in a container up to about 100 ml.

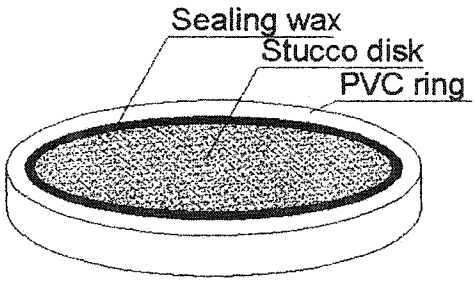

Figure 6.1 Stucco disk for leaching water

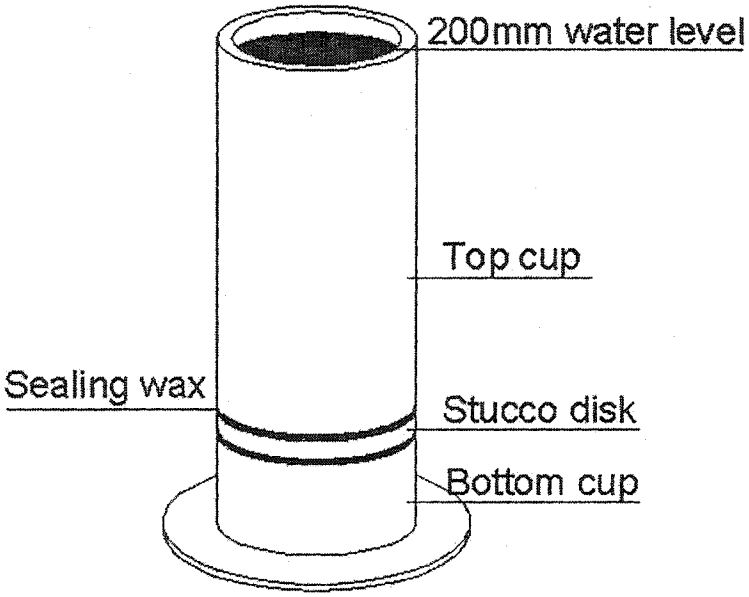

Figure 6.2 Test set-up for leaching chemicals from stucco disk

After being separately filtered through filter paper (Whatman model 40), 10 collected water samples were obtained. It was verified that detergent can evidently reduce surface tension of water when dissolved in the water. (See Figure 4.1) This fact allows using surface tension measurement to justify the existence of the soap in water. The measurement performed on the ten water samples are shown in Table 6.1.

Table 6.1 Surface tension measurements performed on the leaked water samples

Sample code	Water surface tension, N/m at 40 °C	
	From stucco A	From stucco B
1	0.0281	0.0632
2	0.0332	0.0667
3	0.0293	0.0606
4	0.0305	0.0595
5	0.0256	0.0676
Average	0.0293	0.0635
St. Dev.	0.0028	0.0036

The average surface tension of the five water samples leaked from the stucco A (with soap additive) is 46% of the stucco B. The stucco B had a 14% reduction in surface tension comparing with distilled water (0.0733 N/m). Evidently, some surfactants had been dissolved in the water during the water penetration.

6.2 Laboratory interactive weathering of WRB

With the verification of the leaching action the investigation was further directed to examine the influence caused by the chemicals leached on WRB performance. As shown in Chapter 5 the presence of soluble substances, such as wood extracts, did not induce significant impact on the rate of moisture transmission as measured in MIC and water absorption methods. The investigation in this chapter tries to find whether the chemicals leached from stucco can change the WRB performance. A kind of stucco additive,

bentonite, was used as a representative of the chemicals. It is an absorbent aluminium silicate clay formed from volcanic ash and sometimes it is used as an admixture in concrete.

A laboratory weathering procedure employed for pretreating fresh WRB is described as following: WRB sample with a dimension of 0.5 m by 0.5 m was spread out flat on a table, then 100ml of mixture of bentonite and wood extracts, which were prepared at Concordia University and same as those described in Chapter 4, with a ratio at 25g/L was spread on the material surface. The solution was allowed to evaporate at air temperature of 23 $\pm$ 2°C and relative humidity of 50 $\pm$ 5%. After the first wetting and drying cycle, the remaining 4 cycles were completed in the same way but using the solution without bentonite.

6.3 Modified inverted cup test on the weathered WRB

MIC test was utilized to evaluate the effects from bentonite and wood extract deposition on WRB moisture performance. The test results are shown in Table 6.2

Table 6.2 Results of the MIC test conducted on the fresh WRB and the WRB with extract and bentonite deposition

Material code	Fresh WRB		WRB after interactive weathering	
	Moisture transmission rate $kg/s \cdot m^2$	Standard deviation	Moisture transmission rate $kg/s \cdot m^2$	Standard deviation
C4	2.94E-06	1.16E-07	3.42E-06	1.44E-07
C5	3.22E-06	1.99E-07	3.39E-06	1.91E-07
P6	4.53E-06	4.99E-08	5.18E-06	1.49E-07
P8	3.38E-06	5.56E-08	4.01E-06	8.54E-08

After the weathering, both type C and type P materials showed slight increase in the moisture transmission rate when compared with the results of the fresh WRB.

6.4 Water absorption test on the weathered WRB

The weathering effects on liquid flow through the WRB was examined by the water absorption test as well. Table 6.3 lists the results of the test performed on the fresh and the weathered WRB.

Table 6.3 Results of the water absorption test conducted on the fresh WRB and the WRB with extract and bentonite deposition (5 cycles)

Material code	Fresh WRB		WRB after interactive weathering	
	Absorption coefficient $kg/m^2 \cdot s^{0.5}$	Standard deviation	Absorption coefficient $kg/m^2 \cdot s^{0.5}$	Standard deviation
C4	1.05E-03	1.57E-05	1.28E-03	4.81E-05
C5	1.39E-03	8.19E-05	1.83E-03	1.21E-04
P6	3.81E-04	7.20E-06	2.00E-03	2.85E-04
P8	2.58E-04	2.62E-05	1.35E-03	2.30E-04

While type C materials were not greatly influenced by the weathering procedure, more than five times increase in the water absorption coefficient can be identified for type P materials. Although the type C shows initially one magnitude higher water absorption coefficient, after the weathering four type C and type P products indicated the coefficient in the same order of magnitude.

For further examining the effect, another batch of products were tested with the water absorption test but with a more severe weathering process. The materials were successively subjected to two identical weathering exposures i.e., 10 cycles of wetting and drying, where bentonite was used in the first and the sixth cycles. Table 6.4 gives the results of the water absorption test performed on these 10-cycle weathered WRB.

Table 6.4 Results of the water absorption test conducted on the fresh WRB and the WRB with extract and bentonite deposition (10 cycles)

Material code	Fresh WRB		10-cycle weathered WRB	
	Absorption coefficient $kg/m^2 \cdot s^{0.5}$	Standard deviation	Absorption coefficient $kg/m^2 \cdot s^{0.5}$	Standard deviation
C4	1.05E-03	1.57E-05	1.76E-03	1.24E-04
C5	1.39E-03	8.19E-05	2.28E-03	1.63E-04
P6	3.81E-04	7.20E-06	2.50E-03	4.21E-04
P8	2.58E-04	2.62E-05	1.38E-03	1.64E-04

All 10-cycle weathered materials showed further increase in the water flow rate comparing with the 5-cycle weathered membranes, while the difference between the two weathering treatments was not significant. However, one may note that the absorption coefficients of C5 and P6 exceeded that of their substrates (drywall Aw =2.01E-03 $kg/m^2 \cdot s^{0.5}$). This indicates that water had accumulated at the interface between the membranes and their substrates, despite of the fact that this test does not use hydrostatic pressure. In this case, the measurement of water absorption coefficient is not adequate to characterize WRB performance since the membranes does not provide retardatory effect on the water absorption of the drywall substrates.

6.5 Liquid penetration resistance test on the weathered WRB

With the present study closing to its end, some progress on developing experimental techniques for measuring liquid transmission through WRB had been made by another

worker in the EMC group (Pazera, 2003). A Liquid Penetration Resistance (LPR) test involved the WRB subjected to 25 mm water layer on the top surface and 50 mm water layer on the lower surface i.e., 250 Pa hydrostatic pressure difference is used to push the water upwards through the WRB. The test measures the onset time of liquid penetration and the rate of filtration following liquid breakthrough. The detail description of the method is in Appendix I. As a tentative application, the method was utilized to verify the change of the water resistance of the laboratory interactive weathered WRB. Table 6.5 compares the results of the test with fresh WRB and 5-cycle weathered products.

Table 6.5 Results of the LPR test conducted on the fresh WRB and the WRB with extract and bentonite deposition

Material code	Fresh WRB (Pazera, 2003)		WRB after interactive weathering	
	Onset time, days	Moisture transmission rate $kg/s \cdot m^2$	Onset time, days	Moisture transmission rate $kg/s \cdot m^2$
C4	4	2.1E-05	1	7.6E-05
C5	6	2.2E-05	4	1.5E-04

Application of the LPR test on the materials exposed to combined depositions of bentonite and wood extracts showed significant reductions in period to the onset of liquid flow and increase in the flow rate on type C4 and C5 membranes. No quantification is, however, warranted because this test method has yet not been fully verified.

6.6 Air permeance test on the weathered WRB

The specimens subjected to 5-cycle interactive weathering were tested with the air

permeance method and the results are shown in Table 6.6.

Table 6.6 Results of the air permeance test conducted on the fresh WRB and the WRB with extract and bentonite deposition

Material code	Fresh WRB		WRB after interactive weathering	
	Air permeance $L/s \cdot m^2 \cdot Pa$	Standard deviation	Air permeance $L/s \cdot m^2 \cdot Pa$	Standard deviation
C4	2.62E-03	7.28E-05	1.44E-03	1.03E-04
C5	2.22E-03	4.52E-05	1.58E-03	5.41E-05
P6	1.20E-04	8.50E-06	1.23E-05	2.59E-06
P8	2.63E-05	1.20E-06	1.68E-06	3.06E-07

Contrary to the increases in moisture transmission rates measured with MIC and water absorption tests, the air permeance of all the materials was reduced after the WRB underwent the depositions.

6.7 Analysis of results and discussion

Vapour-dominant moisture flow measured by MIC method did not significantly change after the interactive weathering. When comparing the MIC results on the weathered WRB with wood extract deposition (examined in Chapter 5) and those WRB with wood extract and bentonite deposition (interactive weathering), one may find that the bentonite powders introduced slight a increase in the vapour transmission rate through the WRB (see Figure 6.4).

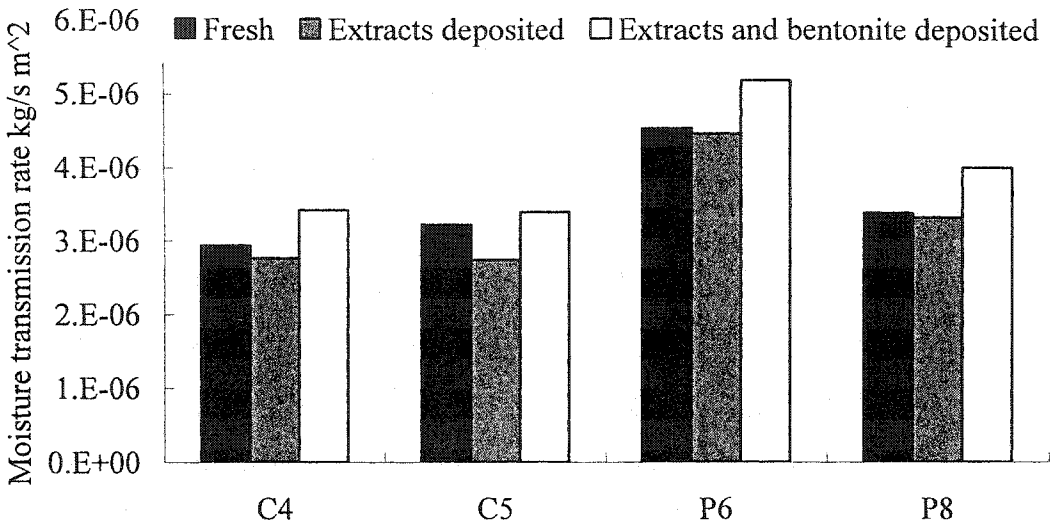

Figure 6.3 Comparison of the MIC test results of the fresh WRB, the WRB with extract deposition, and the WRB with extract and bentonite deposition

According to the water absorption test results (Figure 6.4), one can observe that test methods concur in highlight on increase in the rate of moisture flow. The water absorption test showed small increase for type C and much higher for type P materials. Incidentally, the absolute value of both measurements when undergone 5 or 10 cycles of interactive weathering come to about the same level of moisture flow rates as that of the substrate alone. Although in this case the water absorption test could not provide adequate information to quantify the level of the interactive weathering effect, the effect was evidently indicated by the method. The results of LPR also showed increase but the test method is not yet fully developed (see Table 6.5).

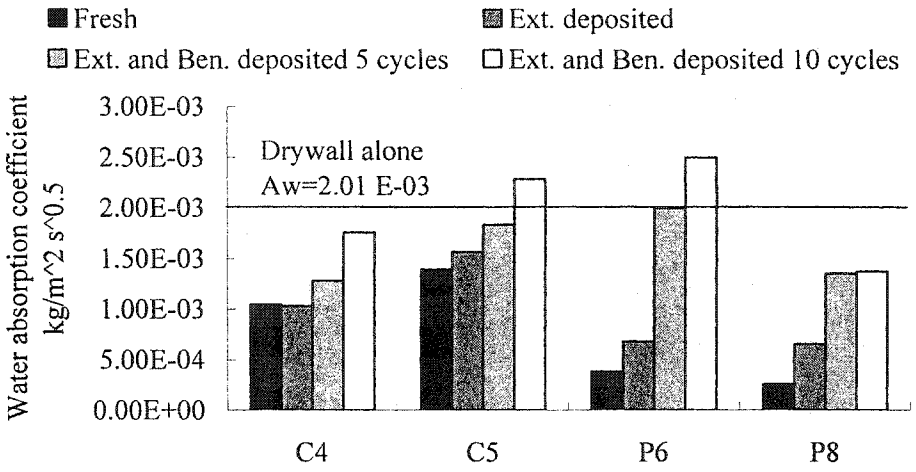

Figure 6.4 Comparison of the water absorption test results of the fresh WRB, the WRB with extract deposition, and the WRB with extract and bentonite deposition (5 cycles and 10 cycles)

To find the reason of the moisture flow increase, one may need to compare the pore structure of the fresh materials with that of the aged materials. Since air permeance can be used to describe material porosity, the air permeance results of the fresh and aged WRB are compared in Figure 6.5 (for type C) and Figure 6.6 (for type P).

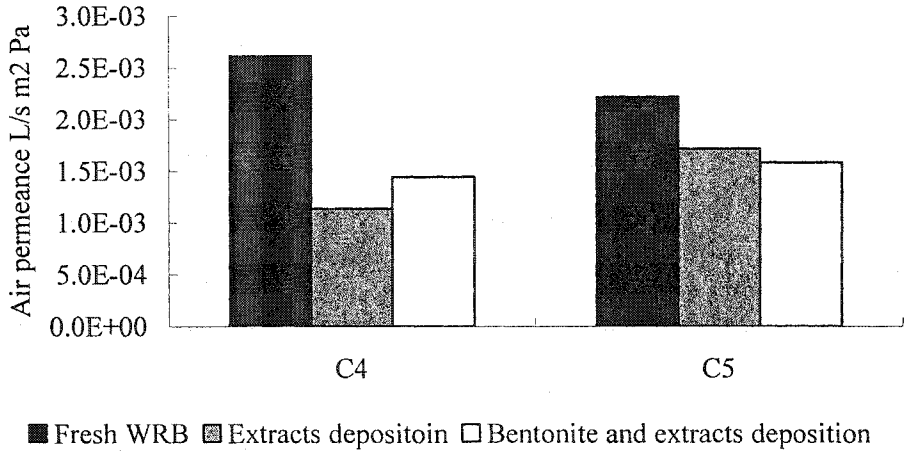

Figure 6.5 Comparison of the air permeance test results of the fresh WRB, the WRB with extract deposition, and the WRB with extract and bentonite deposition (type C WRB)

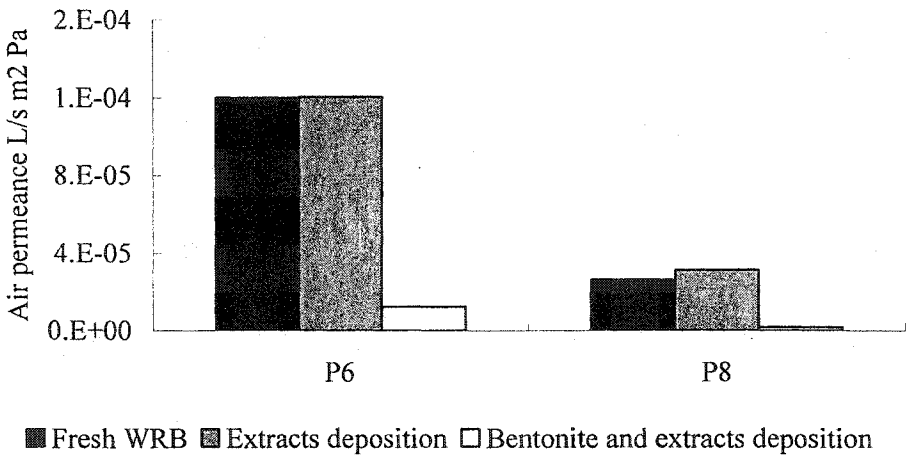

Figure 6.6 Comparison of the air permeance test results of the fresh WRB, the WRB with extract deposition, and the WRB with extract and bentonite deposition (type P WRB)

The reduction of air permeance results indicates the material porosity for airflow was reduced. This fact may imply that the change of moisture transmission rate would not be due to change of material structure but that of material surface condition. It is assumed that the interaction between the electrically charged particles (bentonite) and wood extract particles reduced the hydrophobic feature of WRB surface.

CHAPTER 7 CONCLUSIONS AND SUGGESTIONS FOR FUTURE WORK

7.1 Conclusions

WRB materials are designed to provide protection of moisture sensitive materials against the moisture-originated damage. However, the degree of the protection may be affected by the adjacent components of the WRB. Therefore this study was aimed at examining the effects of interaction between the WRB and adjacent materials on the WRB performance. The conclusions from this study are listed as following:

1. Reviewing the existing test methods, i.e. ASTM D 779 dry indicator test, CCMC 07102 water ponding test, AATCC-127 hydrostatic pressure test, it was found that they do not provide adequate characterization of the material performance. To alleviate the problem, several methods used for homogenous materials or those developed in a parallel research at Concordia University (Pazera, 2003) were employed in this study.

2. The equipment of air permeance test was developed and the precision of the method was verified with a ruggedness test. The repeatable results showed that the method can be used as a reliable tool to evaluate changes in porosity of WRB products.

3. Water absorption coefficient test was employed to evaluate WRB liquid transfer characteristic. Within a short duration of test conducted (1 hour in this study), the

measured absorption coefficient is repeatable. However, the method is not reliable, when the specimen resistance to water is similar to that of the substrate alone.

4. To evaluate field performance of the WRB one has to use two or three different test methods, since each of them addresses only one aspect of the performance. Air permeance defines the porosity alone and cannot predict effects of hydrophobic treatment on moisture transmission. The MIC measures vapour dominated moisture transmission and provides different qualification than a liquid dominated test such as water absorption coefficient or liquid penetration resistance test.

5. These three test methods were used to evaluate the effects of outdoor weathering and mechanical stretching of the membranes. It was found that changes in moisture and air transport introduced by these effects were small in type C and P products.

6. Two batches of Portland cement plaster (stucco) were prepared to examine the extent of chemical leaching in case rain penetrating through stucco layer. Water leached from the stucco prepared with 1% soap solution showed about 50% reduction in the surface tension. This highlighted the possibility of a chemical leaching.

7. Repeated testing on the laboratory weathered WRB with wood extracts showed that a significant impact on moisture transmission is achieved only when there is a chemical deposit on the surface of the WRB. Furthermore, only when a combination of chemical deposit from wood extracts with other particles was used one could observe a dramatic change on the material resistance to water flow. This change was demonstrated with water absorption coefficient test and liquid penetration resistance tests.

7.2 Future work

The following items are proposed for future research on performance of WRB.

- Further development on experimental methods for testing liquid transmission rate through WRB is needed. This should involve both the development of appropriate instrumentation as well as an evaluation of factors affecting the precision of the test method (Ruggedness study).

- Using tools developed in the research project for the External Moisture Control Consortium such as air permeance, double cup water vapour transmission, modified inverted cup and liquid penetration resistance methods, one should undertake a systematic study on durability of WRB in the field conditions.

- Further investigations on the reason, by which the laboratory interactive weathering changed WRB performance, should be undertaken. This may be an important factor in assessment of WRB durability.

RELATED PUBLICATIONS

Bomberg, M., Pazera, M., Zhang, J. and Haghighat, F., 2003, Weather resistive barriers: Assessment of their performance, *2nd International Conference on Building Physics*, Leuven, September, 2003

Bomberg, M., Pazera, M., Zhang. J. and Haghighat, F., 2003, Weather resistive barriers: Laboratory testing of moisture flow, *9th Canadian Building Science and Technology Conference*, Vancouver, February , 2003

Bomberg, M., Pazera, M., Zhang, J., Mungo, T. and Haghighat, F., 2003, Weather resistive barriers: New methodology for their evaluation, *24th Conference of the Air Infiltration & Ventilation Centre (AIVC BETEC 2003),* Washington DC, October, 2003

REFERENCES

AATCC-127 (American Association of Textile Chemists and Colourists), 1985, Water resistance: Hydrostatic pressure test.

ASTM Standard, ASTM D 1331, Test methods for surface and interfacial tension of solution of surface-active agent, *American Society for Testing and Materials*, Philadelphia.

ASTM Standard, ASTM D 3045, Heat aging of plastics without load, *American Society for Testing and Materials*, Philadelphia.

ASTM Standard, ASTM D 779-97, Standard test method for water resistance of paper, paperboard, and other sheet materials by the dry indicator test, *American Society for Testing and Materials*, Philadelphia.

ASTM Standard, ASTM D 828-97, Standard test method for tensile properties of paper and paperboard, *American Society for Testing and Materials*, Philadelphia.

ASTM Standard, ASTM D 882 Standard practice for conducting tests on paint and related coatings and materials using filtered open-flame carbon-arc exposure apparatus, *American Society for Testing and Materials*, Philadelphia.

ASTM Standard, ASTM D 971, Standard test method for interfacial tension, *American Society for Testing and Materials*, Philadelphia.

ASTM Standard, ASTM E 104, Standard practice for maintaining constant relative humidity by means of aqueous solutions, *American Society for Testing and Materials*, Philadelphia.

ASTM Standard, ASTM E 1169, Standard guide for conducting ruggedness tests, *American Society for Testing and Materials*, Philadelphia.

ASTM Standard, ASTM E 2178, Standard test method for air permeance of building materials, *American Society for Testing and Materials*, Philadelphia.

ASTM Standard, ASTM E 283, Standard test method for rate of air leakage through exterior windows, curtain walls, and doors, *American Society for Testing and Materials*, Philadelphia.

ASTM Standard, ASTM E 783, Standard method for field measurement of air leakage through installed exterior windows and doors, *American Society for Testing and Materials*, Philadelphia.

ASTM Standard, ASTM E96-53T, Standard Test Methods for Water Vapour, *American Society for Testing and Materials*, Philadelphia.

ASTM Standard, ASTM E96, Standard test method for water vapor transmission of materials, *American Society for Testing and Materials*, Philadelphia.

ASTM Standard, ASTM G 53. Standard practice for operating light- and water-exposure apparatus (fluorescent UV-condensation type) for exposure of nonmetallic materials, *American Society for Testing and Materials*, Philadelphia.

Babbitt, J. D., 1939, The diffusion of water vapour through various building materials, *Canadian journal of research*

Bomberg, M. T., 1989, Testing water vapour transmission: unresolved issues. Water vapour transmission through building materials and systems: mechanism and measurement, ASTM STP 1039, H.R. Trechsel and M. Bomberg, Eds., *American Society for Testing and Materials*, pp. 157-167

Bomberg, M. T. and Brown, W. C., 1993, Building envelope and environmental control: Part 1, *Construction Canada* **35**(1): pp.15-18.

Bomberg, M. T. and Kumaran, M., 1985, Determination of airflow resistance of exterior membranes and sheathing

Bomberg, M. T., Rousseau, M., Desmarais, G., Nicholls, M., and Lacasse, M., 2002, Description of 17 large scale wall specimens built for water entry investigation in IRC dynamic wall testing facility, Report from Task 2 of MEWS Project, October

Bomberg, M. T., Pazera, M. and Haghighat, F., 2002, On testing moisture flow through weather resistive barriers, 11th Building Physics Conference, Dresden, Sept 26-27, 2002

Bomberg, M. T., Pazera, M., Zhang. J. and Haghighat, F., 2003a, Weather resistive barriers: Laboratory testing of moisture flow, *9th Canadian Building Science and Technology Conf.*, Vancouver, February 24-25, 2003

Bomberg, M. T., Pazera, M., Zhang, J. and Haghighat, F., 2003b, Weather resistive barriers: assessment of their performance, submitted to *2nd Int. Conf. on Building Physics*, Leuven, Sept

Bosack, E. and Burnett, E., 1999, Durability of wall systems containing housewrap, *8th International conference on durability of building material and components*, Vancouver, Canada, May 30-June 3

Burch, D. M., Thomas, W. C., and Fanney, A. H., 1992, Water vapour permeability measurements of common building materials, *ASHRAE Transactions 98(2)*: pp. 486-494.

Burnett, E., 2001, The performance of exterior sheathing membranes in enclosure wall systems

Burnett, E. and Bosack, E., 1998, The use of housewrap in walls: installation, performance and implications

CAN/CGSB, 1977, CAN/CGSB 51.32-M77, National standard of Canada, Sheathing, membrane, breather type

CCMC, 1996, CCMC 07102, Technical guide: Sheathing, membrane, breather-type, for polyethylene-based and polypropylene-based, woven or non-woven WRB

CMHC, 1999, Comparative analysis of residential construction in Seattle, WA and Vancouver, B.C. Prepared for CMHC, January 27

Cushman, T., 1997, Can moisture beat housewrap, *June 1997 issue of journal of light construction*

de Wit, M. and van Schindel, J., 1993, The estimation of the moisture diffusivity, *IEA Annex XXIV*, Report T1-NL-93/04.

Dell, M., Busque, P. M., and Liaw, S., 1997, Distress of stucco-clad buildings in the Vancouver area

Douglas, J.S., Kuehn, T.H., and Ramsey, J.W., 1992, A new moisture permeability measurement method representative test data, *ASHRAE Transactions 98(2)*: 513-519.

EREC (Energy Efficiency and Renewable Energy Clearinghouse), 2002, Vapour diffusion retarders and air barriers

Fanney, A. H., Thomas, W. C., Burch, D. M., and Mathena, L. R., 1991, Measurements of

moisture diffusion in building materials, *ASHRAE Transactions 97(2)*: pp. 99- 112.

Fetter, C. W., 2000, Applied Hydrogeology (4th edition), pp. 81-84

Fisette, P., 1998, Journal of Light Construction, November.

Fisette, P., 2000, Leaky housewrap

Garden, G. K., 1965, Control of Air leakage is Important. *Canadian Building Digest 72,* National Research Council of Canada, Ottawa

Grunewald, J. and Bomberg, M. T., 2002, An engineering approximation of material characteristics needed for input to Heat, Air, and Moisture transport simulations, *11th Building Physics Conference*, Dresden, Sept 26-27

Hansen, K. K. and Lund, H. B., 1990, Cup method for determination of water vapour transmission properties of building materials. Sources of uncertainty in the method

Hutcheon, Neil, B., Handgord, and Gustav, O. P., 1995, Building science for a cold climate, NRCC, pp. 65.

ICBO (International Conference of Building Officials), 2000, ICBO AC38, Acceptance criteria for weather-resistive barriers

Kadulski, R., 1997, Keeping the water out: Building envelope performance, *Solplan*

Review, January

Krus, M. and Künzel, H. M., 1993, Determination of Dw from A-value, *IEA Annex XXIV*, Report T3-D-93/02.

Kumaran, M. K., 1999, Moisture diffusivity of building materials from water absorption measurements, *Journal of Thermal Envelope and Building Science*, Technomic Publishing Co., Vol. 22, April, pp. 349-355.

Lackey, J. C., Marchand, R. G. and Kumaran, M. K., 1997, A logical extension of the ASTM standard E96 to determine the dependence of water vapor transmission on relative humidity, *Insulation Materials: Testing and Applications*, Vol. 3, pp. 456-469.

Lstiburek, J., 1996, The effect of wood siding on Tyvek, *December 1996 issue of Energy Design Update*

Lstiburek, J., 2001, Brick, stucco, housewraps and building paper

Maref, W., Lacasse, M., Kumaran, M. K., and Swinton, M. C., 2002, Benchmarking of the advanced hygrothermal model – hygIRC with mid scale experiments, Proceedings of esim2002: pp. 171- 176. Sept. 11-13, Montreal, Canada.

Massmann, J. W., 1989, Applying groundwater flow models in vapour extraction system design. *Journal of Environmental Engineering ASCE* 115(1): pp.129-49.

McLean, R. C., Galbraith, G. H., and Sanders, C. H., 1990, Moisture transmission testing of building materials and presentation of vapour permeability values, *Building Research and Practice, The Journal of CIB 2: 82-91.*

MHL (Morrison Hershfield Limited), 1996, Survey of building envelope failures on the coastal climate of British Columbia, Prepared for CMHC, November 22

Mungo, T., 2003, Water vapour transmission through weather resistive barriers

NHW (New Home Warranty of British Columbia and Yukon), 1995, Building Insight (Monthly bulletin), August

NHW (New Home Warranty of British Columbia and Yukon), 1996, General problems with stucco clad buildings

Pazera, M., 2003, Evaluation of laboratory performance of weather resistive barriers

Schwartz N., Bomberg and Kumaran M., 1989, Water vapour transmission and moisture accumulation in polyurethane and polyisocyanurate foams.

US Federal Specification, 1968, UU-B-790a, Building paper, vegetable fiber: (kraft, waterproofed, water repellent and fire resistant.

US Federal Specification, 1949, UU-P-31b, Paper; general specifications and methods of testing.

Weinberg and Schumaker, 1969, Statistics an intuitive approach, 2nd edition Brooks/Cole Publishing Co., Belmont, CA

Weston, T. *et. al.* 2001 Development of a textured spun-bonded polyolefin weather resistive barrier for stucco and EIFS. *ASHRAE Transactions 107(1)*

Wilson, A. G., 1963, Air leakage in buildings, *Canadian Building Digest 23*, National Research Council of Canada, Ottawa, Dec.

Young, J. F., Mindess, Sidney, Gray, J. R., Bentur, Arnon, 1998, The science and technology of civil engineering materials, pp.66-67

APPENDIX A: PROCEDURE OF PREPARING THE WOOD EXTRACTS AT LOUISIANA PACIFIC LABORATORY[1]

An OSB was cut at selected points within the centre area of the board, through multiple cuts. The sawdust was obtained in this manner and it was collected until each sample reached 1000 g weight. 2 batches of sawdust sample were collected from different locations (called location 1 and location 2) of the board. Each batch of sample was divided in two shares. Therefore, overall 4 samples per board type were obtained. They were treated separately so that one can compare measurements on the samples. Two of them (one from location 1 and the other from location 2) were treated in a warm bath, and the other two were treated in a bath with an ambient temperature.

The OSB extracting commenced by preheating solvent (distilled water) in a beaker, which was in the warm bath at a temperature of 156°F. For the ambient bath the temperature was 71.5°F. To fully mix the sawdust in the water, the samples were stirred immediately when they were put in the bathes. Thereafter, the stir was done in every half hour. Due to solvent evaporation, the volume within the beakers was monitored and distilled water was added as needed to maintain the volume of 2000 (± 50) ml. Loss of the solvent was about 100 ml within 5.5 hours. All the baths were capped with aluminium foils to prevent organic contamination. After 5.5 hours, the baths were no longer stirred. Since the particles had been beneath the meniscus, it was certain that all particles had been completely saturated with the solvent over the 4 hours period of time.

[1] This procedure is quoted from operation note of Louisiana Pacific Laboratory

Once the 5.5 hours time period was ended, the solutions were filtered through Sark Skin ® filter paper by gravitation until all filtrates were collected. The residues were dried in an oven at 103°F until the weight reached constant. The weight of the soluble fraction was established as the difference in weight before and after the oven treatment.

APPENDIX B: PROCEDURE OF PREPARING THE WOOD EXTRACTS AT CONCORDIA UNIVERSITY

0.5 m2 OSB with a thickness of 128mm was completely cut through multiple cuts. Approximate 4000g of sawdust were obtained in this manner and were collected. 8 litres solvent (distilled water) in a clean metal container was preheated and kept at 70 ±1°C. The sawdust of 500g was put into the solvent and it was stirred immediately and every half hour thereafter. The container was capped with its cover to prevent organic contamination. The solution volume was monitored and maintained by adding distilled water (70 ±1°C). After 5 hours, the heating and stirring were stopped. Since the particles had been beneath the meniscus, it was certain that all particles had been completely saturated with the solvent. Solution was put in room temperature to cool for half hour. After the cooling, the solution was first filtered through an ordinary dense-mesh strainer and then through two layers of clean gauzes. Finally it was filtered through ashless filter paper (Whatman model 40) by gravitation. All residues were collected and dried in an oven at 50 °C until no change in weight was observed.

The above procedure was repeated five times; therefore 40 liters of wood extract solution was obtained. They were stored in a few clean sealed containers. Thus, the soluble fraction of the solution was 7.79g extracts per liter.

APPENDIX C: METHODS TO DETERMINE SURFACE TENSION[2]

Introduction: surface tension of water

When discussing surface tension it is important to know that each atom has an energy state, which is defined by temperature and pressure. It has an equal interaction energy in all directions within the bulk. However, when the atom is near the surface, it "feels" an asymmetric force field since its neighbours are not placed symmetrically on all sides, thus creating a greater potential energy for these atoms called the surface free energy or surface tension (Young *et. al.*, 1998).

Surface tension is an important factor in building materials. This is due to adsorbed water in materials that contain pores and capillaries. "Molecules at the surface of any body, whether liquid or solid, experience different forces of interaction from their fellow molecules at some distance from the surface" (Hutcheon *et. al.*, 1995). When discussing liquids this is known as surface tension, the reaction of surface tension is dependent on the material as well as the liquid being discussed. The wetting angle or contact angle is dependent on adhesive forces (Figure C-1). Different liquids react differently to a variety of surfaces. Surface molecules have fewer nearest neighbours than submersed molecules, thus fewer intermolecular interactions take place. There is then a free energy change that occurs with isothermal, reversible formation, which is more commonly known as surface tension.

[2] Based on work of Ines Sijercic, Tania Mungo and Jian Zhang at Concordia University

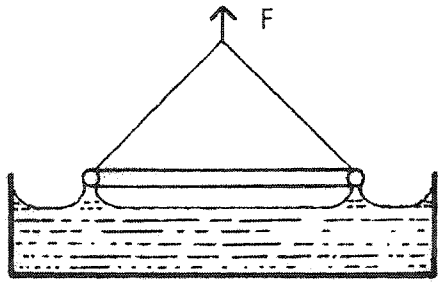

Figure C-1 Surface tension with use of platinum ring.

Method to determine surface tension (Fisher Tensiomat model no. 21)

Fisher Surface Tensiomat 21 a precise instrument, which can measure surface tension). It is based on the principles of operation created by Dr. Pierre Lecompte du Nouy, a noted biochemist. This method is specified by the ASTM D 971, "Standard Test Method for Interfacial Tension" and ASTM D 1331, "Test Methods for Surface and Interfacial Tension of Solution of Surface-Active Agent".

As shown in Figure 17, a platinum-iridium ring is attached to a counter-balanced lever-arm. This horizontal lever-arm is clamped to a taut stainless steel wire, which in turn holds the arm through torsion. The torsion is controlled and increased thus causing the suspended ring to be slowly lifted from the liquid being tested, it is at this time that a film around the ring occurs. The torsion is increased in small increments until it is released from the surface film, the force needed to release the ring is then measured.

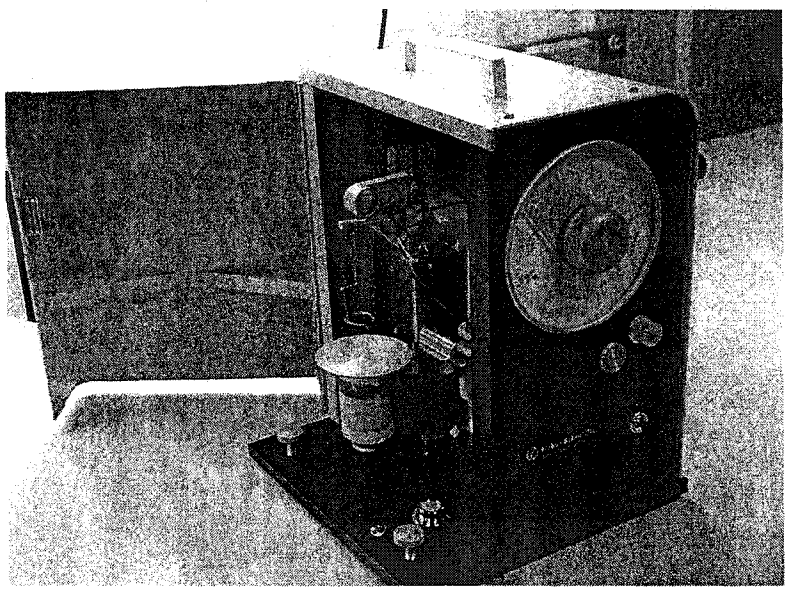

Figure C-2 Fisher Tensiomat model no. 21.

Description of the test protocol for testing with Fisher Tensiomat 21.

1. 35 ml of the liquid being tested was poured into a glass beaker.

2. The clean platinum ring was suspended from the lever-arm. The arrest mechanism was holding the arm at that time.

3. The sample was placed on the sample table and raised until the ring was immersed in the liquid.

4. The torsion arm was then released and the instrument adjusted to the zero reading.

5. The knob was adjusted until the index and the image were exactly in line with the reference mark on the mirror.

6. The sample table was lowered and the lever-arm raised by the knob at the same time while keeping the index in line with the marking on the mirror.

7. This was continued until the surface film was broken.

8. The reading on the dial was taken.

9. This was repeated five times.

10. The Tensiomat measures apparent surface tension, if necessary absolute surface tension can be calculated. This is accomplished by using Equation C-1.

$$S = p \cdot F \qquad \text{(C-1)}$$

Where

S = absolute value of surface tension, N/m

p = apparent value (Dial reading of the Fisher Tensiomat)

F = correction factor of the Fisher Tensiomat

APPENDIX D: METHODS TO DETERMINE KINEMATIC VISCOSITY

1. Introduction: kinematic viscosity

When a fluid is subjected to external forces, it resists flow due to internal friction. Viscosity is a measure of this internal friction. There are two basic methods for expressing viscosity: absolute (dynamic) viscosity and kinematic viscosity. Kinematic viscosity is a measure of the resistive flow of a fluid under the influence of gravity. Absolute viscosity, sometimes called dynamic or simple viscosity, is the product of kinematic viscosity and fluid density. The dimension of kinematic viscosity is L2/T, in which L is a length and T is a time, and commonly it unit is centistoke (cSt) (equal to mm2/s). Absolute viscosity is expressed in units of centipoise (cP). The SI unit of absolute viscosity is the milliPascal • second (mPa • s), where 1 cP = 1 mPa • s. The instruments measuring the viscosity can be classified into three major types:

2. Methods to determine kinematic viscosity

Capillary Viscometers

It measures the flow rate of a fixed volume of fluid through a small orifice at a controlled temperature. The rate of shear can be varied from near zero to 106 s-1 by changing capillary diameter and applied pressure. Types of capillary viscometers and their mode of operation are:

- Glass Capillary Viscometer (ASTM D 445) — Fluid passes through a fixed-diameter orifice under the influence of gravity. The rate of shear is less than 10 s-1. All kinematic viscosities of automotive fluids are measured by capillary viscometers.
- High-Pressure Capillary Viscometer (ASTM D 4624 and D 5481) — Applied gas pressure forces a fixed volume of fluid through a small-diameter glass capillary. The rate of shear can be varied up to 106 s-1. This technique is commonly used to simulate the viscosity of motor oils in operating crankshaft bearings. This viscosity is called high temperature high shear (HTHS) viscosity and is measured at 150°C and 106 s-1. HTHS viscosity is also measured by the Tapered Bearing Simulator, ASTM D 4683, and the Ravenfield Tapered Plug viscometer, ASTM D 4741 (see below).

Rotary Viscometers

It uses the torque on a rotating shaft (at constant rotational speed) or the rotational speed of the rotating shaft (at constant shear stress) to measure a fluid's resistance to flow. The Cold Cranking Simulator (CCS), Mini-Rotary Viscometer (MRV), Brookfield Viscometer, Tapered Bearing Simulator (TBS) and Ravenfield Tapered Plug viscometer are all rotary viscometers. Rate of shear can be changed by changing rotor dimensions, the gap between rotor and stator wall, and the speed of rotation.

- Cold Cranking Simulator (ASTM D 5293) — The CCS measures an apparent viscosity in the range of 500 to 200,000 cP. Shear rate ranges between 104 and 105 s-1. Normal operating temperature range is 0 to -40°C. The CCS has demonstrated excellent correlation with engine cranking data at low temperatures. The SAE J300 viscosity classification specifies the low-temperature viscometric performance of

motor oils by CCS limits and MRV requirements.

- Mini-Rotary Viscometer (ASTM D 4684) — The MRV test, which is related to the mechanism of pumpability, is a low shear rate measurement. Slow sample cooling rate is the method's key feature. A sample is pretreated to have a specified thermal history which includes warming, slow cooling, and soaking cycles. The MRV measures an apparent yield stress, which, if greater than a threshold value, indicates a potential air-binding pumping failure problem. Above a certain viscosity (currently defined as 60,000 cP by SAE J 300), the oil may be subject to pumpability failure by a mechanism called "flow limited" behaviour. An SAE 10W oil, for example, is required to have a maximum viscosity of 60,000 cP at -30°C with no yield stress. This method also measures an apparent viscosity under shear rates of 1 to 50 s-1.
- Brookfield Viscometer — Determines a wide range of viscosities (1 to 105 P) under a low rate of shear (up to 102 s-1).
- ASTM D 2983 is used primarily to determine the low-temperature viscosity of automotive gear oils, automatic transmission fluids, torque and tractor fluids, and industrial and automotive hydraulic fluids. Test temperature is held constant in the range -5 to -40°C.
- ASTM D 5133, the Scanning Brookfield technique, measures the Brookfield viscosity of a sample as it is cooled at a constant rate of 1°C/hour. Like the MRV, ASTM D 5133 is intended to relate to an oil's pumpability at low temperatures. The test reports the gelation point, defined as the temperature at which the sample reaches 30,000 cP. The gelation index is also reported, and is defined as the largest rate of change of viscosity increase from -5°C to the lowest test temperature. This method is

finding application in engine oils, and is required by ILSAC GF-2.

- apered Bearing Simulator (ASTM D 4683) and Ravenfield Tapered Plug Viscometer (ASTM D 4741)— These techniques also measure high-temperature high-shear-rate viscosity of motor oils (see High Pressure Capillary Viscometer). Very high shear rates are obtained by using an extremely small gap between the rotor and stator wall.

Miscellaneous instruments

They operate by a number of principles; for example, the falling time of a steel ball or needle in a fluid, the vibration resistance of a probe, and the pressure applied to a probe by a flowing fluid.

3. Viscosity Measurement Using Cannon-Fenske Viscometer

In the present study, we chose CANNON-Fenske Routine Viscometer because it is precise, easy to control and suitable for the transparent solutions, which we want to measure.

Apparatus

- Viscometer: calibrated Cannon-Fenske Routine viscometer (size 25)
- Viscometer holders: use viscometer holders to enable the viscometer, which has the upper meniscus directly above the lower meniscus, to be suspended vertically with 1° in all directions.
- Constant temperature liquid bath: Use the bath to provide constant temperature in range of 20° C to 100° C with temperature accuracy ±0.2°C
- Baker and temperature control: Use the baker with height 25cm capacity 3000ml.

Because the temperature accuracy of the bath is not enough the baker with 3000ml water is put in the liquid bath to provide a precise temperature control. The temperature of the medium does not vary by more than ±0.1°C of the selected temperature over the length of the viscometer.

- Thermometer with range from -40°C to 110°C with an accuracy after correction of 0.1°C.
- Timing device: Use the stopwatch that is capable of taking readings with a discrimination of 0.1 s.

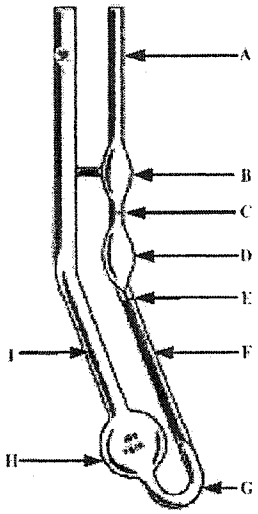

Figure D-1 Cannon-Fenske Routine viscometer

Test procedure

1) Clean the viscometer using suitable solvents, and by passing clean, dry and filtered air through the instrument to remove the final traces of solvents.
2) To charge the sample into the viscometer, invert the instrument and apply suction to tube I, immersing tube A in the liquid sample, and draw liquid to mark E. Wipe clean arm A, and turn the instrument to its normal vertical position.
3) Place the viscometer into the holder, and insert it into the constant temperature baker.

Align the viscometer vertically in the beaker by means of a small plumb bob in tube I.

4) Allow approximately 10 minutes for the sample to come to the beaker temperature at 40°C.

5) Apply suction to tube A and draw the liquid slightly above mark C.

6) To measure the efflux time, allow the liquid sample to flow freely down past mark C, measuring the time for the meniscus to pass from mark C to mark E

7) Calculate the kinematic viscosity in mm2/s (cSt) of the sample by multiplying the efflux time in seconds by the viscometer constant.

$$\nu = C_v \, t \qquad \text{(D-1)}$$

where:

ν = kinematic viscosity, mm2/s

C_v = calibration constant of the viscometer, mm2/s2, and

t = mean flow time, s.

APPENDIX E: DETAILED RESULTS OF THE MOISTURE FLUX TESTS

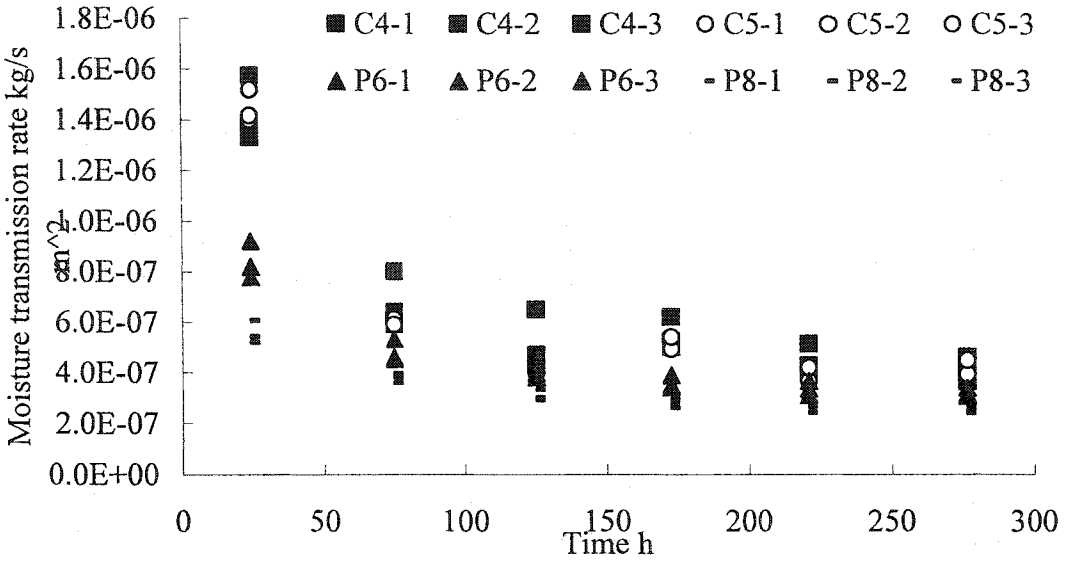

Figure E-1 Moisture flux test on fresh WRB with distilled water

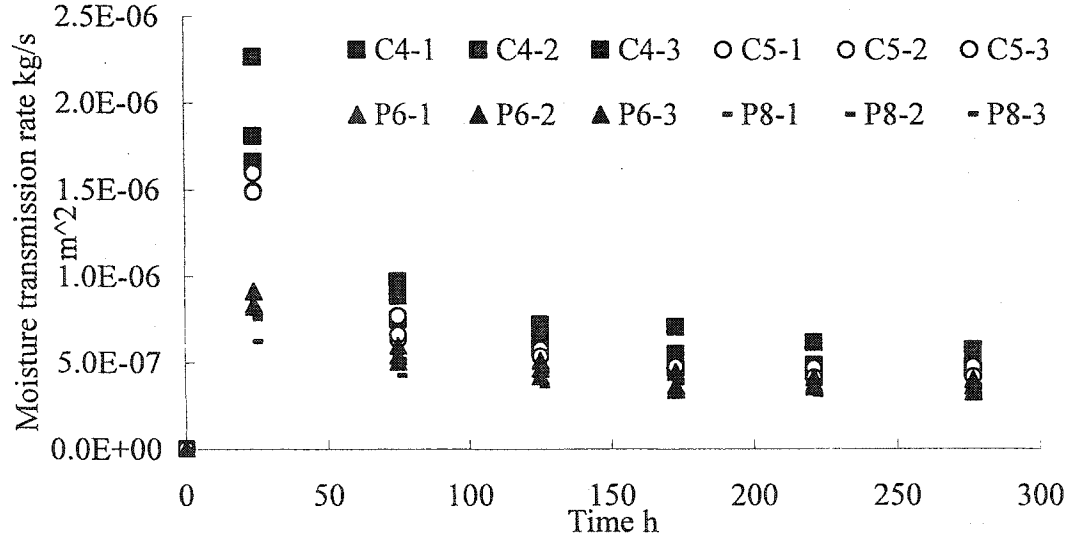

Figure E-2 Moisture flux test on fresh WRB with the extract solution

APPENDIX F: DETAILED RESULTS OF THE MODIFIED INVERTED CUP TESTS

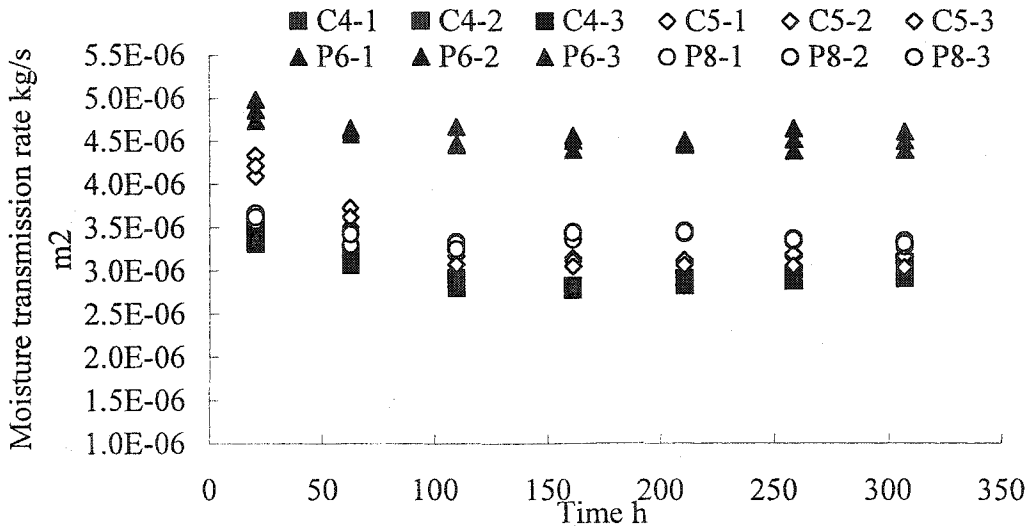

Figure F-1 Modified inverted cup test on fresh WRB

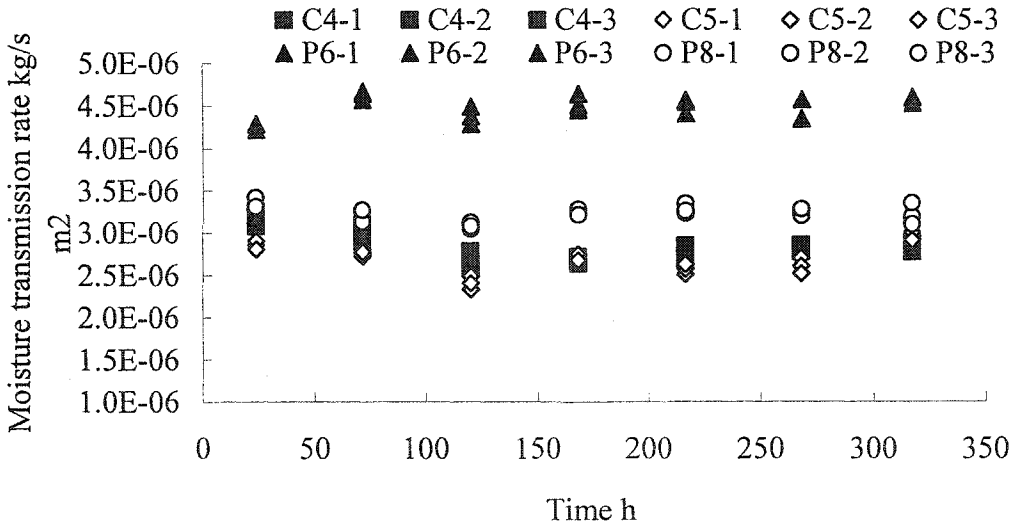

Figure F-2 Modified inverted cup test on the stretched WRB

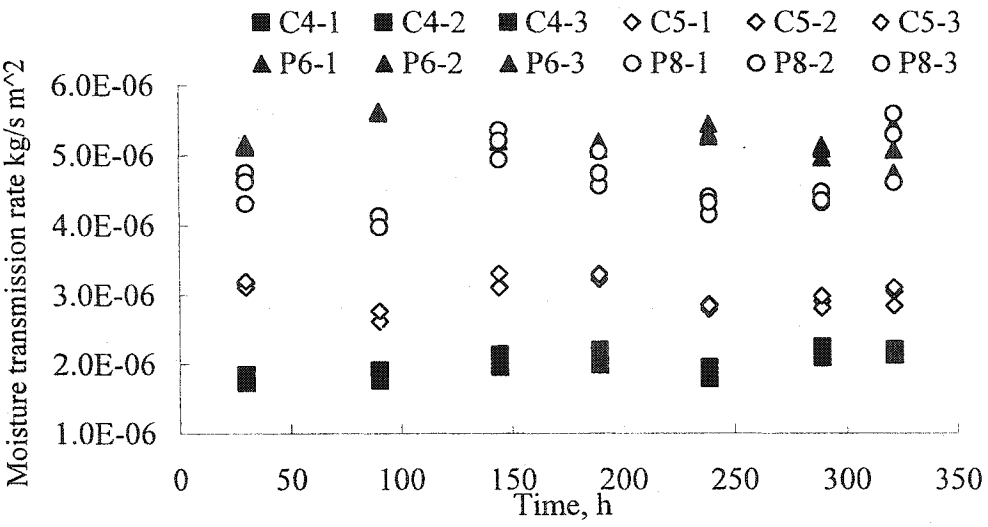

Figure F-3 Modified inverted cup test on the outdoor weathered WRB

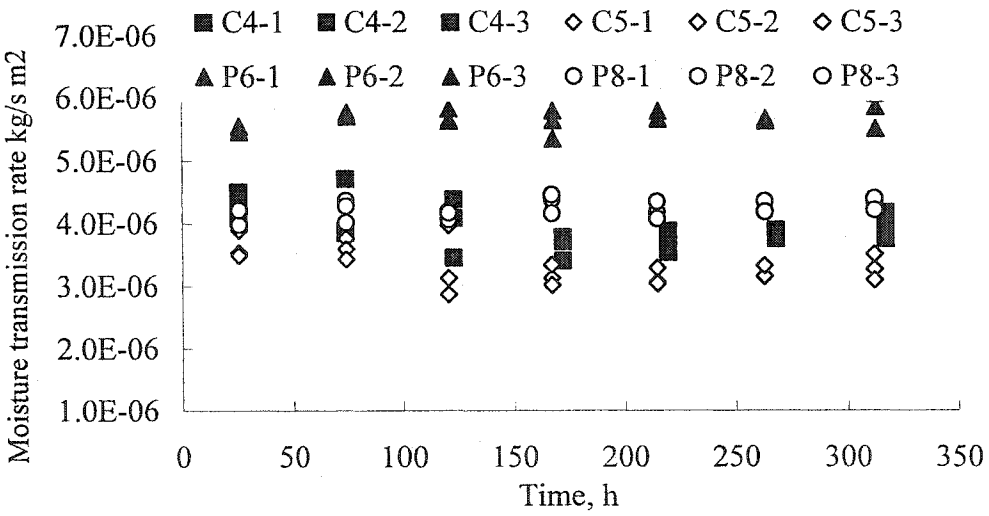

Figure F-4 Modified inverted cup test on fresh WRB with extract solution

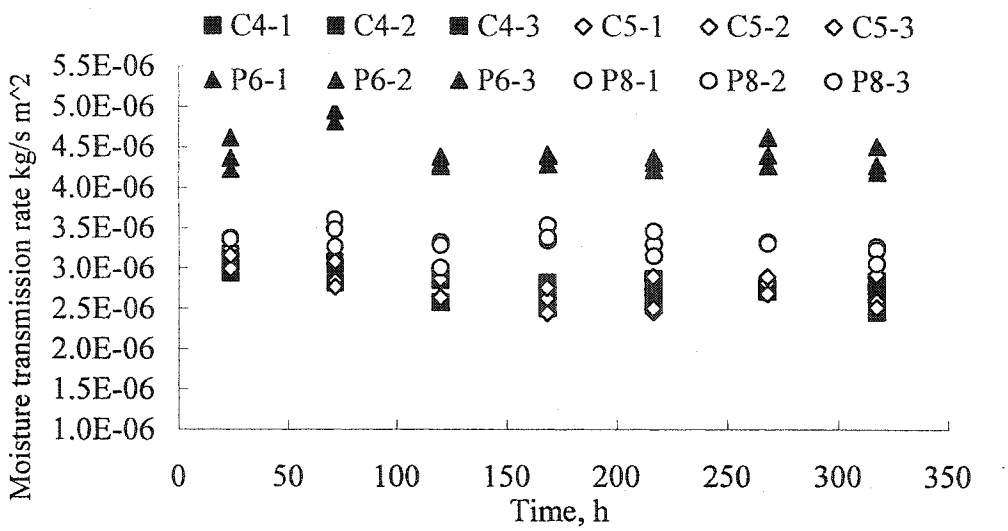

Figure F-5 Modified inverted cup test on the WRB with wood extract deposition

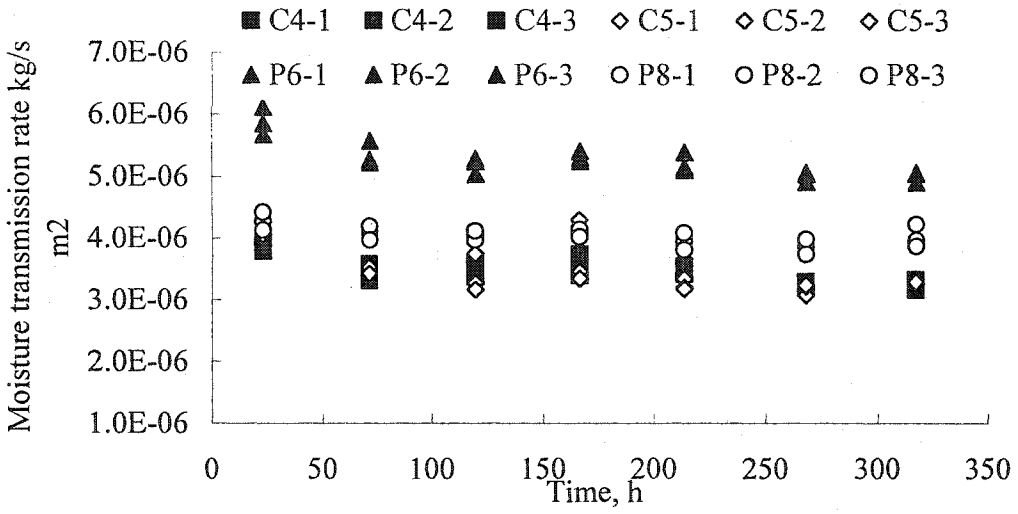

Figure F-6 Modified inverted cup test on the interactively weathered WRB (with wood extract and bentonite deposition)

APPENDIX G: DETAILED RESULTS OF THE WATER ABSORPTION TESTS

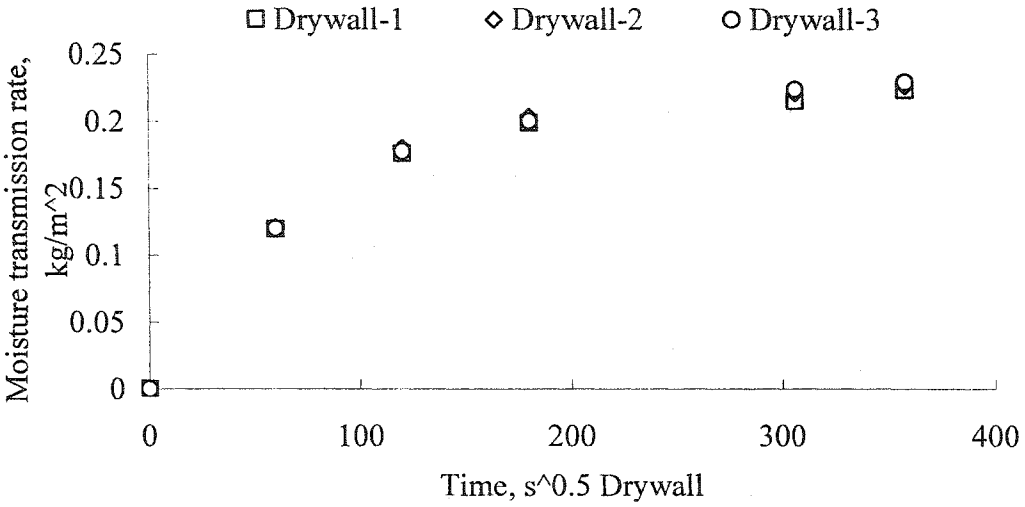

Figure G-1 Water absorption test on the drywall alone

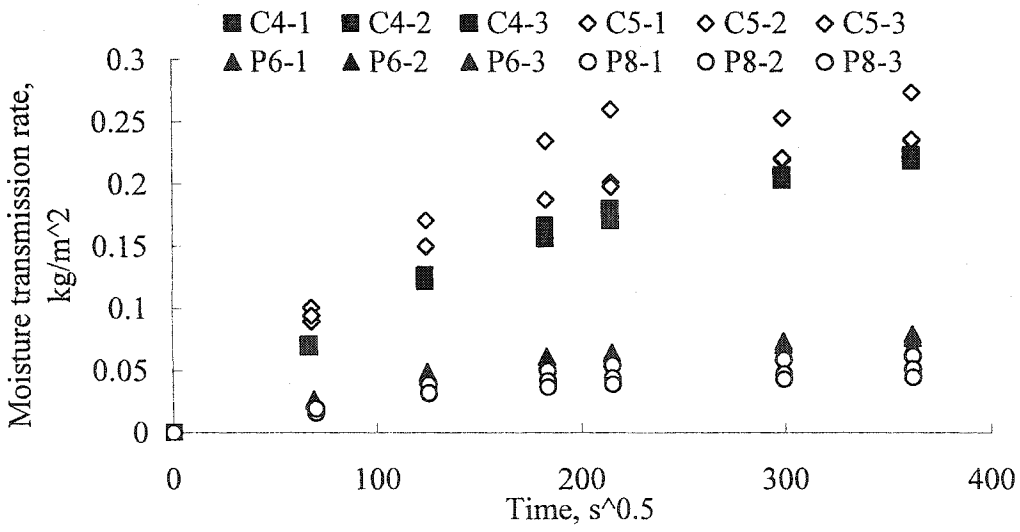

Figure G-2 Water absorption test on the fresh WRB

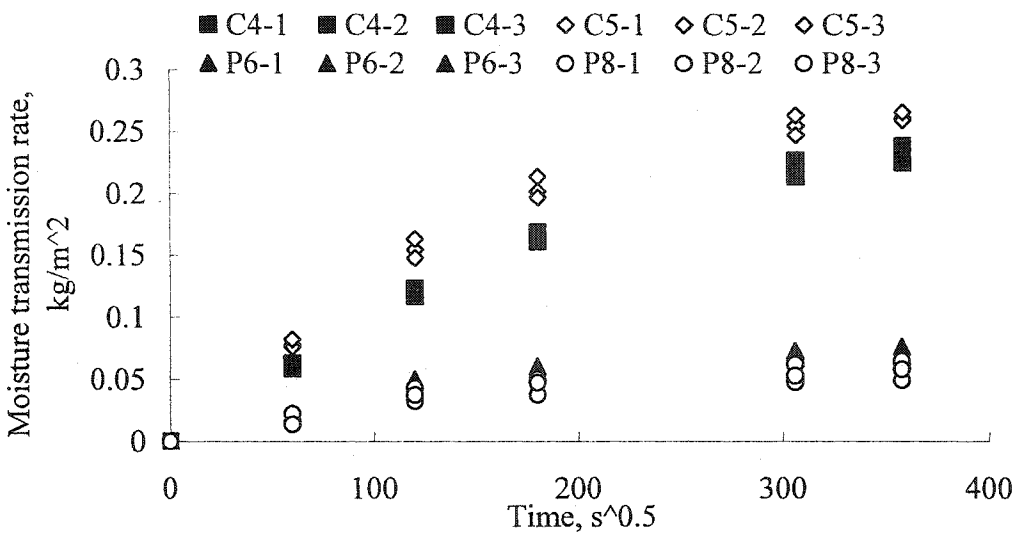

Figure G-3 Water absorption test on the stretched WRB

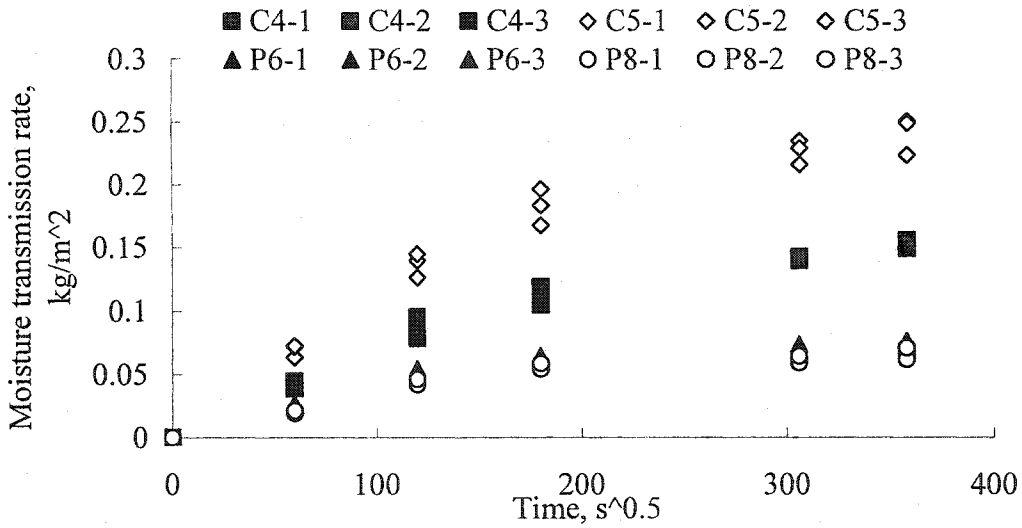

Figure G-4 Water absorption test on the outdoor weathered WRB

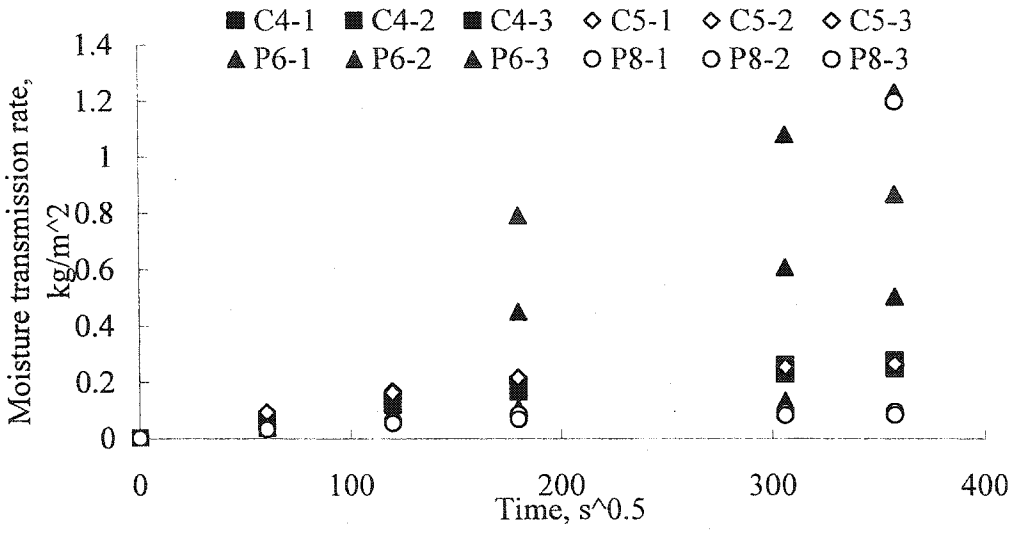

Figure G-5 Water absorption test on the WRB with the wood extract deposition

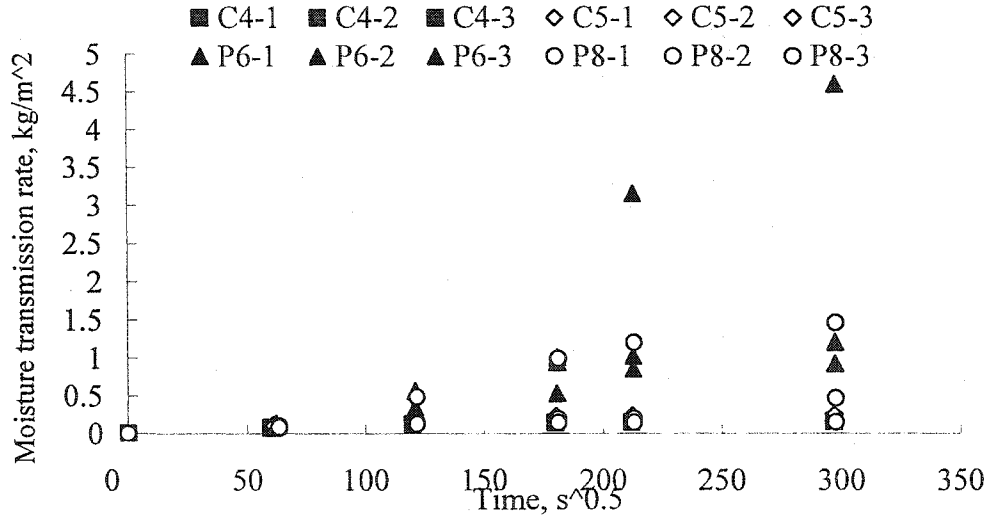

Figure G-6 Water absorption test on the interactively weathered WRB (with 5-cycle wood extract and bentonite deposition)

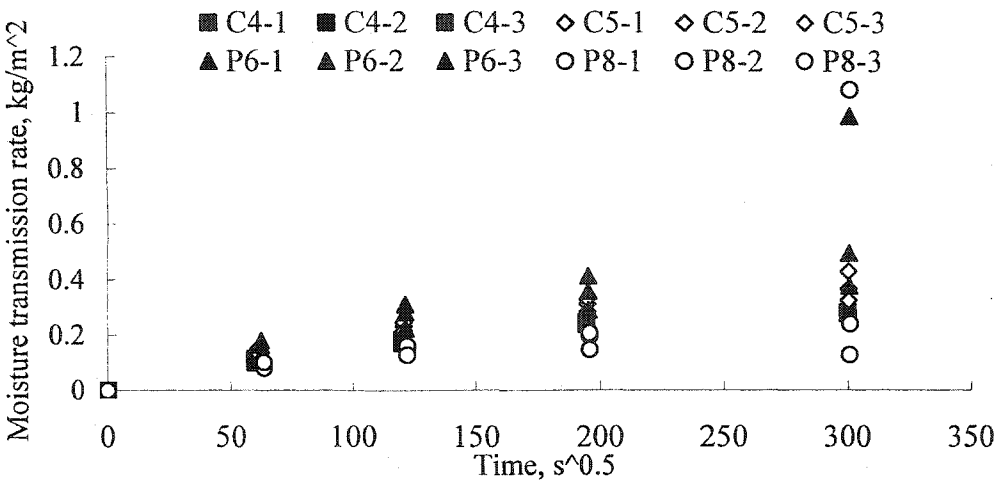

Figure G-7 Water absorption test on the interactively weathered WRB (with 10-cycle wood extract and bentonite deposition)

APPENDIX H: DETAILED RESULTS OF THE AIR PERMEANCE TESTS

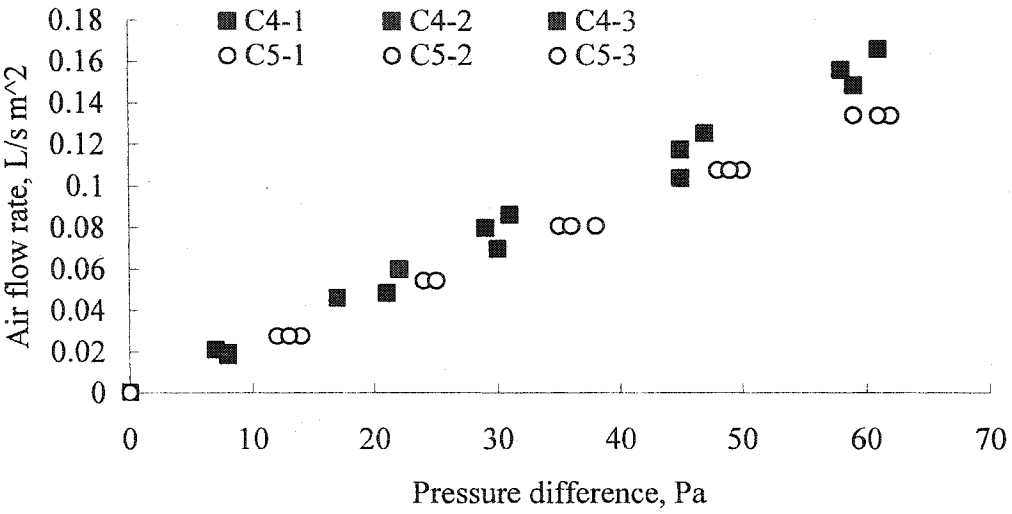

Figure H-1 Air permeance test on the fresh WRB (C4 and C5)

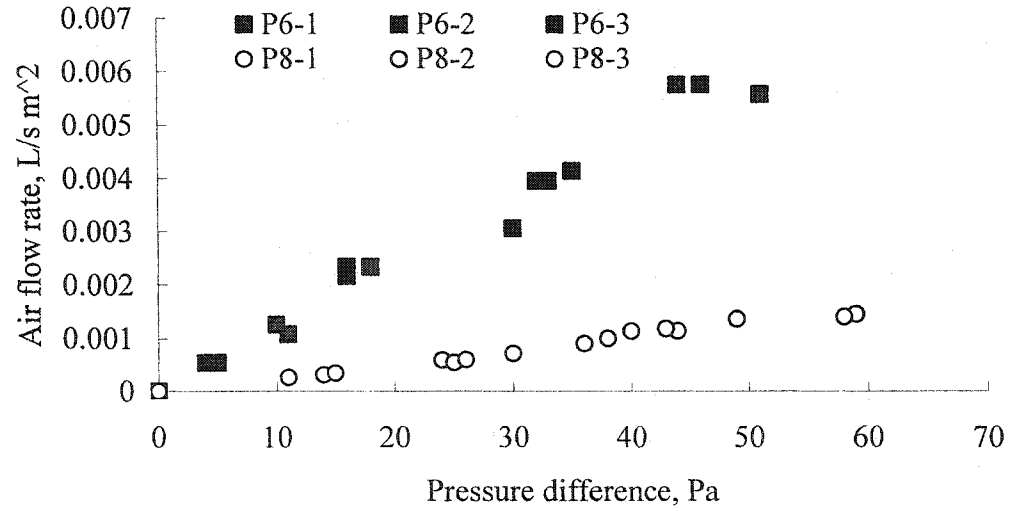

Figure H-2 Air permeance test on the fresh WRB (P6 and P8)

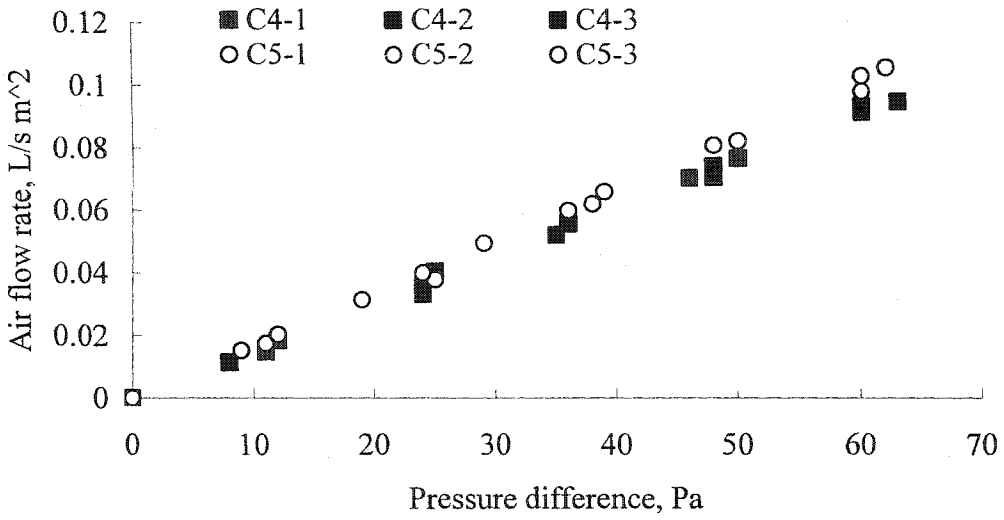

Figure H-3 Air permeance test on the stretched WRB (C4 and C5)

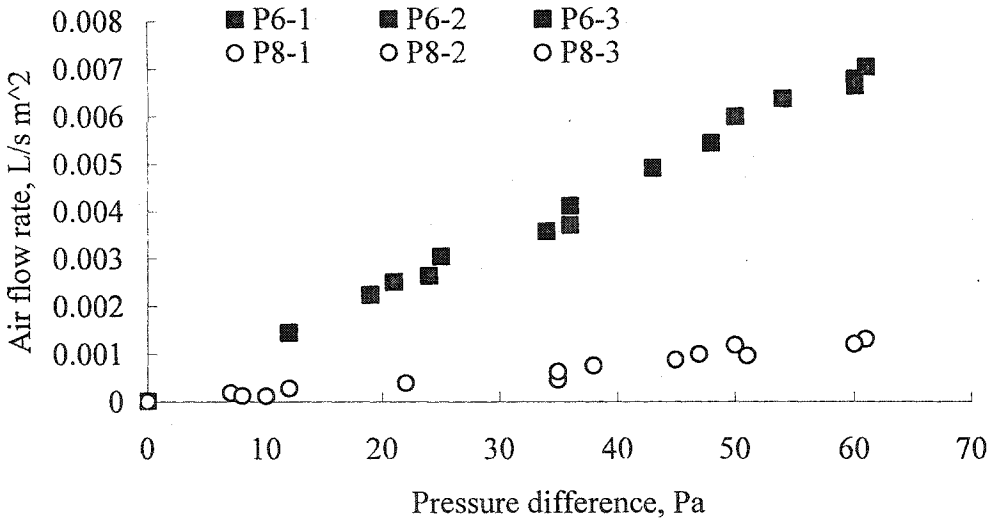

Figure H-4 Air permeance test on the stretched WRB (P6 and P8)

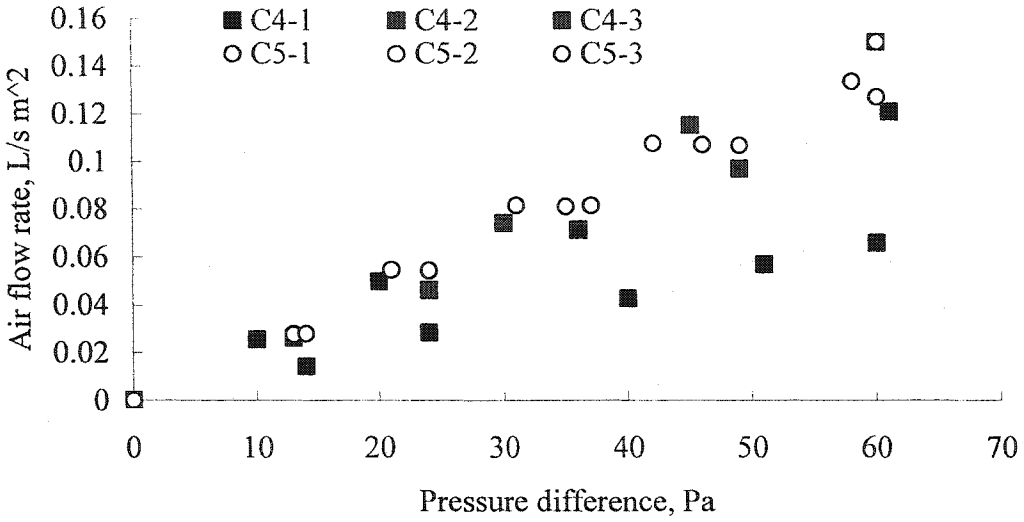

Figure H-5 Air permeance test on the outdoor weathered WRB (C4 and C5)

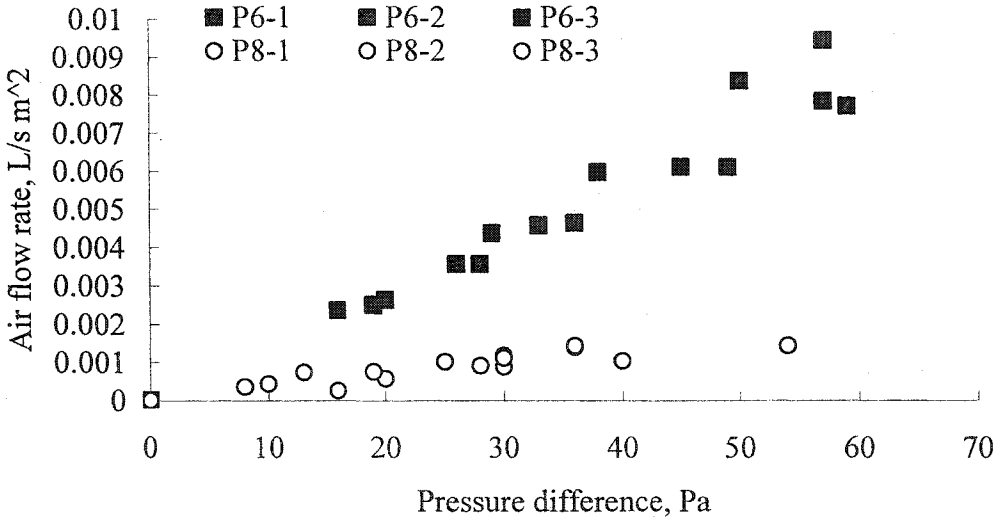

Figure H-6 Air permeance test on the outdoor weathered WRB (P6 and P8)

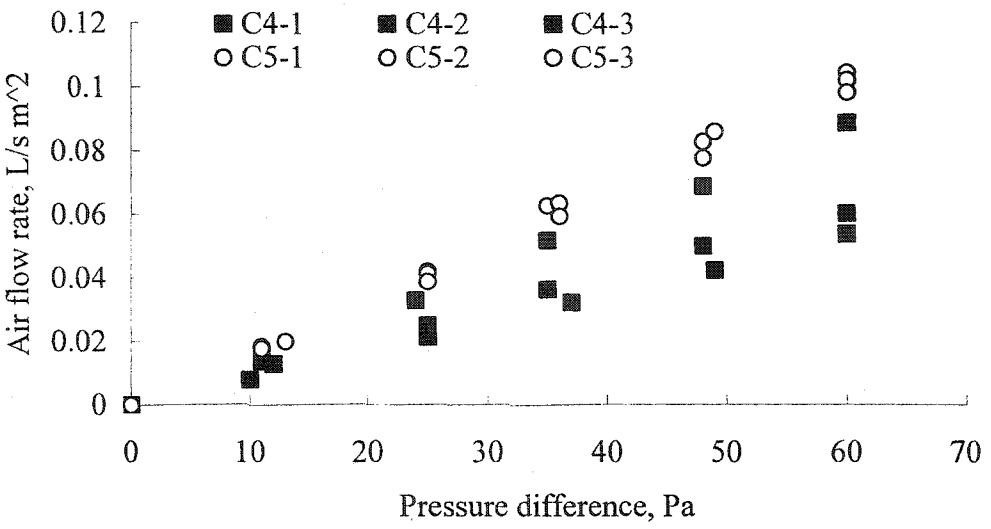

Figure H-7 Air permeance test on the WRB with wood extract deposition (C4 and C5)

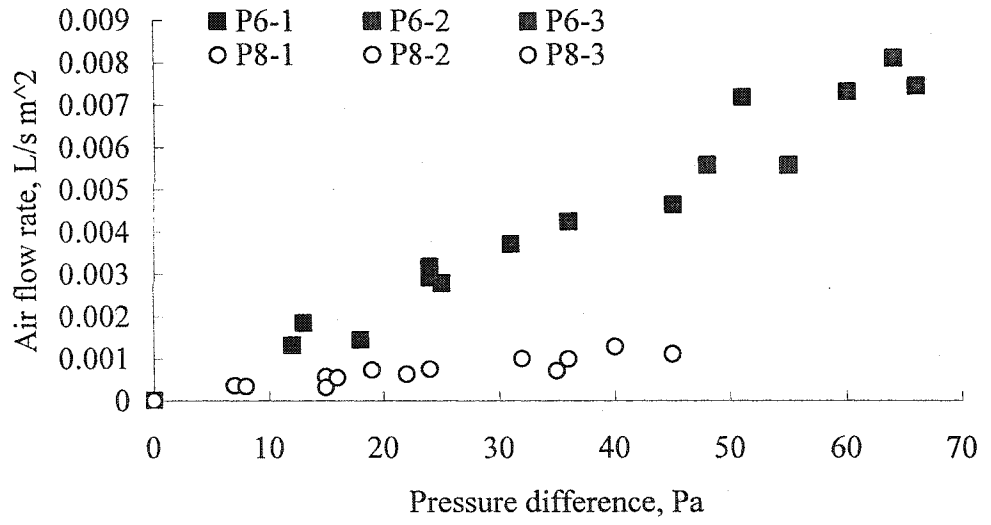

Figure H-8 Air permeance test on the WRB with wood extract deposition (P6 and P8)

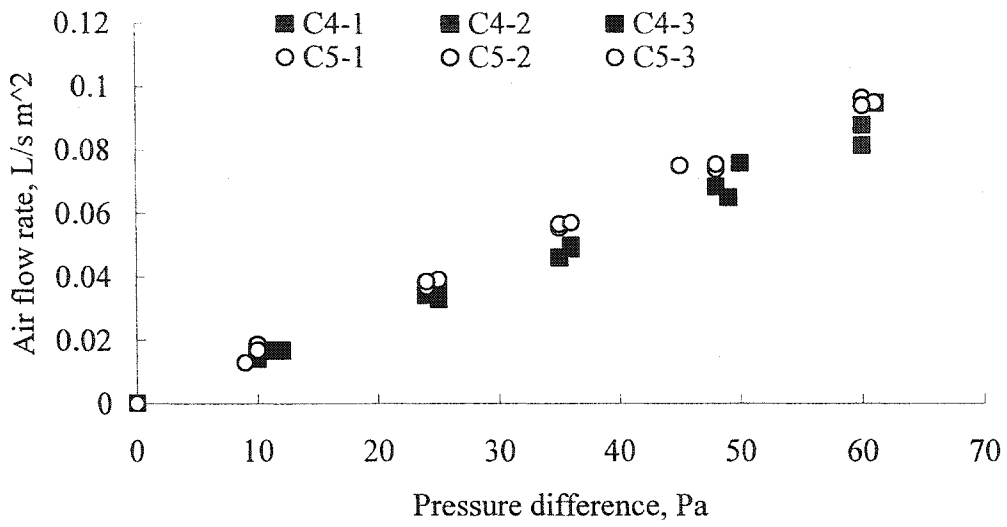

Figure H-9 Air permeance test on the interactive weathered C4 and C5 WRB (with wood extract and bentonite deposition)

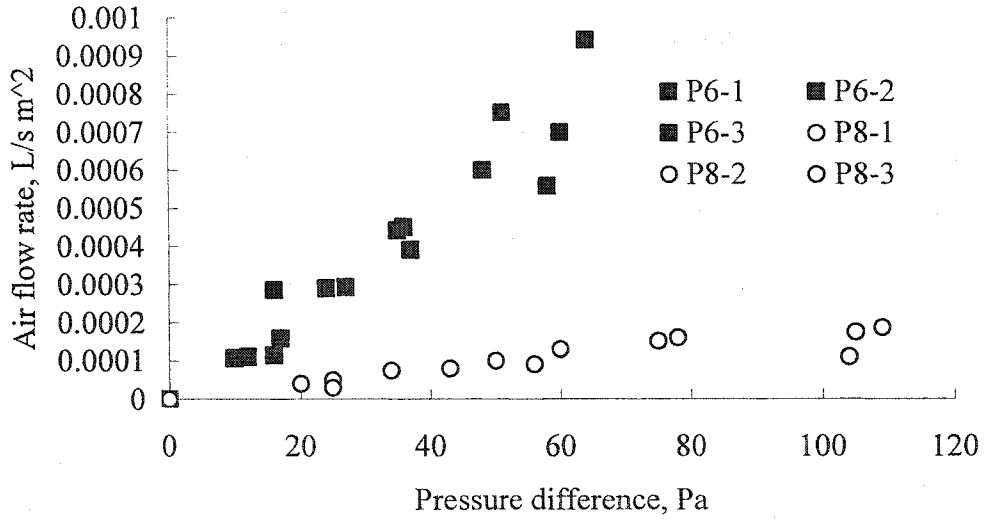

Figure H-10 Air permeance test on the interactive weathered P6 and P8 WRB (with wood extract and bentonite deposition)

APPENDIX I: EXPERIMENTAL SET-UP FOR LIQUID PENETRATION RESISTANCE (LPR) TEST[3]

The experimental set-up included a sealed plastic (acrylic) container with 100 mm inside diameter. A plastic grid (mesh) was inserted at the bottom of the container to, support the WRB membrane. At the side of the container an opening was drilled and a stainless steel capillary outflow fitting was inserted. The bottom of the fitting was located 25 mm above the top surface of WRB. The orifice of the fitting with 0.79 mm inside diameter. A polyimide capillary outflow tubing with 0.25 mm inside diameter was attached to the fitting. A 10 cc syringe was used to extract the liquid that filtrated through the WRB following the onset of continuous liquid flow. A brass fitting with a 4 mm opening was installed in the cover of the container, and provided air pressure equalization at the onset of a liquid flow. The WRB membrane was sealed to the bottom edges of the container by brushing mixture of wax and rosin. As shown in Figure I-1 the specimen's upper surface was subjected to a hydrostatic pressure created by a 25 mm thick layer of distilled water. The sealed set-up was then placed in a wide tank and water was added slowly until a 25 ± 1 mm difference between water levels inside the container and inside the tank was reached. The 25 ± 1 mm difference in water levels represented an overpressure of 250 ± 10 Pa acting on the lower surface of the WRB. The test was conducted in a glass tank measuring 920 mm by 300 mm by 460 mm, and was large enough to provide constant water head during the second stage of the test, that is during the measurement of

[3] The description of the LPR test method is quoted from Pazera (2003).

the filtration rate. A total of 12 specimens were tested in two series with 4 types of WRB, and 3 replicas. During the experiment the tank was covered with a polyethylene sheet to reduce water evaporation. The water level was monitored twice a day, and water was added accordingly to maintain the 250 ± 10 Pa over-pressure acting on the WRB.

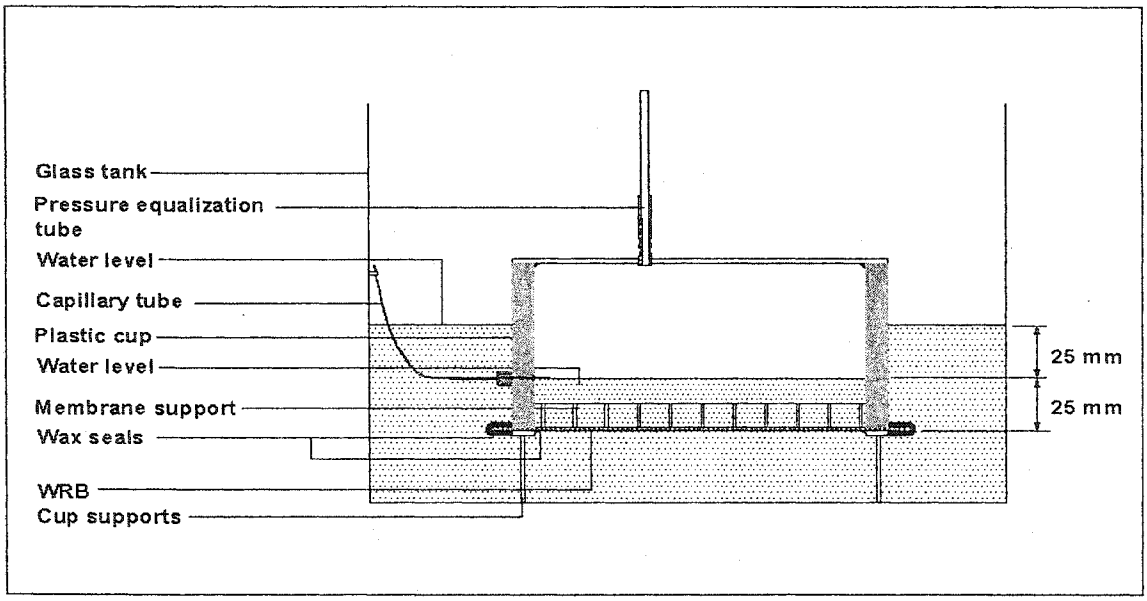

Figure I-1 Set-up for a liquid penetration resistance test.

The test procedure included (1) establishing the period to the onset of the liquid flow (the time in days for a visible increase in water level inside the container), and (2) the rate of liquid filtration subsequent to the onset of continuous liquid flow. For types C, and P, the readings were collected twice a day.